AN INVESTIGATION OF THE NATURE OF THE RADIO-FREQUENCY DIELECTRIC RESPONSE IN CEREAL GRAINS AND OILSEEDS WITH ENGINEERING IMPLICATIONS FOR GRAIN MOISTURE METERS

David B. Funk, Chief
Inspection Systems Engineering Branch
Technical Services Division
USDA-GIPSA

ABSTRACT

The goals for this research were: (1) improving the understanding of the dielectric relaxation processes that influence radio-frequency measurements of the dielectric characteristics of cereal grains and oilseeds, and (2) creating a more effective grain moisture measurement algorithm based on deeper understanding of those physical processes.

The significance of moisture content in cereal grains and oilseeds, the methods used for grain moisture measurement, and the need for improvements in the radio-frequency dielectric moisture method are reviewed. Background information is presented on dielectric characteristics, with emphasis on dielectric relaxation effects and grain moisture measurement.

The grain samples used in this study were obtained in the course of the Annual Moisture Calibration Survey conducted by the USDA-Grain Inspection, Packers and Stockyards Administration during 1998, 1999, and 2000. These grain samples represented

all growing regions for the fifteen most economically significant cereal grain and oilseed crops in the United States and constituted the most extensive set of such samples ever subjected to dielectric characterization.

Dielectric characteristics were measured with three separate instrumentation systems to acquire data covering the frequency range from 100 Hz to 501 MHz. All three instrumentation systems were designed to measure the complex dielectric constant of grain samples and yielded results that were comparable in the overlapping frequency ranges.

Mathematical simulations of dielectric characteristics comparing measured dielectric results with theoretical dielectric relaxation behavior are described. The relative contributions of free and bound water and conductivity effects in the audio-frequency and radio-frequency ranges are quantified. An alternative explanation for the physical mechanism of conductivity in grains is proposed and its plausibility is justified.

The effectiveness of a particular dielectric mixture equation for normalizing the density of grain samples is evaluated and confirmed. An improved moisture measurement algorithm based on an optimum combination of measurement frequency, dielectric parameters, density correction, and temperature correction is proposed.

A unified calibration method for fifteen grain types is described, and its performance is shown to be significantly superior to that of current commercial instrumentation. Implications for the future of grain moisture measurement by the radio-frequency dielectric method are discussed.

CONTENTS

ILLUSTRATIONS

Figure

TABLES

Table

ACKNOWLEDGMENTS

Moisture Group Leader, organized and supervised the Annual Moisture Survey project and allocated resources to successfully accomplish the high-frequency dielectric tests in addition to his group's existing responsibilities. Mr. Larry Freese participated in many valuable discussions regarding statistical techniques and facilitated the data analysis by creating programs to expeditiously merge data from thousands of separate data files.

Mr. Steven N. Tanner, Director, Technical Services Division, consistently supported the research and the author's vision for its potential benefits for the Official Inspection System and the United States grain industry.

CHAPTER 1

INTRODUCTION

Moisture content is one of the most critical grain quality measurements because of the direct economic significance of the fraction of the total product weight that is water and because moisture content largely determines the rate at which the grain will degrade during handling and storage. Grain is bought and sold on the basis of weight. The actual value of the grain is in the dry material, and accurate moisture determinations serve as the basis for appropriate price adjustments. Since grain deterioration due to microbial activity and insects is highly dependent upon moisture content and temperature, maximum moisture guidelines have been set for handling and storing grain. If the moisture content is above the level that ensures safe storage, the grain must be dried to a suitable level. The energy and handling costs associated with drying grain and the reduction in weight of the grain during drying result in substantially reduced prices for high-moisture grain.

Although the value of grain would appear to increase for grain dried below the safe storage level, higher prices are not normally paid for over-dry grain. This asymmetric pricing structure is partially justified by the increased susceptibility to breakage during handling for drier grain. The direct discounts assessed for moist grain and the indirect penalty (giving away dry matter) for dry grain are powerful inducements to deliver grain with a moisture content that is very close to the established safe storage level.

Because of its significance, moisture content is determined virtually every time grain is bought and sold. The vast majority of these measurements are performed by commercial grain handlers. There are an estimated 12,000 grain moisture meters in commercial use in the United States. Grain producers also depend on grain moisture meters to determine when to harvest and how to dry grain to optimize their profit.

The U.S. Grain Standards Act of 1916, as amended, established an official grain inspection service, which is administered by the Grain Inspection, Packers and Stockyards Administration (GIPSA), the author's employer. GIPSA, an agency within the United Stated Department of Agriculture, conducts grain quality inspections at export service points and domestic Field Offices. The agency also oversees a network of nonfederal designated official inspection agencies. The total number of moisture meters in use in the official inspection service is about five hundred.

The designated agencies, some of which are privately owned and some of which are State owned, are authorized to perform official inspections on GIPSA's behalf for grain that is traded domestically. Some State agencies are delegated the responsibility for conducting export grain inspections as well. No private agencies are authorized to perform official export grain inspections. Most exported grain must, by law, be officially inspected, but official inspection is optional for grain that is traded domestically.

Approximately 2.5 million official inspections, representing about 170 million metric tons of grain, are performed each year in the United States. Each official inspection includes moisture determination by the instrument designated by GIPSA as the official moisture device, currently the Model GAC-2100, manufactured by Dickey-john

2

Corporation. Commercial grain handlers are not required to use the same moisture measuring instrument or procedures used for official inspection services, but the desire for moisture measurements that agree as closely as possible with official inspection results causes many commercial operations to use the same grain moisture instrument as is used by the official inspection service.

Overview of Grain Moisture Measurement Technology

The air oven method is the most common reference method for grain moisture determinations. Air oven methods vary widely in procedures and results[1], but all are based on heating the sample for a prescribed period of time at a prescribed temperature and measuring the loss of mass. The amount of mass lost is assumed to be the amount of water that was present in the sample. Unfortunately, the method is not that simple. Water is not the only constituent that is driven off by heating. The heating times and temperatures are set so that the amount of nonaqueous material driven off is approximately equal to the amount of water that remains after drying. Those parameters are determined by comparing the air oven method to other more basic (and difficult) methods such as the phosphorous pentoxide (P_2O_5) method[2] or the Karl Fischer titration method.[3] Most air oven methods require hours or days to complete. Clearly, grain producers, handlers, and processors need much more rapid methods to assess moisture content.

Rapid Indirect Methods

Many different technologies have been tried for rapid grain moisture measurement. Rapid indirect methods all measure some physical parameters (by electrical or optical sensing) and predict moisture content with calibration equations or charts. Invariably, other sample constituents or sample geometry interfere with the signal caused by water. Temperature usually affects both the water signal and the interfering signals. Therefore, calibration equations attempt to achieve a best (but imperfect) fit between the measured parameters and the moisture content as defined by an accepted moisture reference method. Accurate grain moisture measurements depend upon successfully overcoming the effects of the most important interfering factors, such as density, temperature, chemical composition, and impurities.

Near-Infrared Method

Near-infrared spectroscopy instruments sense the absorption of near-infrared radiation by water. The water absorption bands that are used for moisture determinations are at about 1.0, 1.4, and 1.9 micrometer wavelengths. Whole-grain near-infrared (NIR) instruments that are used for moisture determinations generally use one of the lower wavelength regions. Other grain constituents such as protein, oil, and starch have absorption bands that overlap the water absorption bands. Furthermore, differences in grain physical condition caused by growing conditions and grain handling strongly affect NIR instrument measurements. These interferences demand separate calibration equations for different grain types. Multivariate statistical methods such as multiple linear

4

regression, principal components regression, partial least squares regression, and neural networks are used to develop NIR moisture calibrations that achieve excellent accuracy in spite of these strong interferences. NIR instruments are a small but growing segment of the grain moisture meter market in the United States, where their capabilities to simultaneously quantitate levels of moisture and other grain constituents such as protein, oil, and starch justify their relatively high purchase costs and complex calibration development procedures.

Conductivity Method

The conductivity method for measuring grain moisture is based on the approximately linear relationship between grain moisture content and the logarithm of direct-current conductivity of grain kernels.[4] Conductivity-type instruments generally use a small sample size and depend upon compressing, crushing, or grinding the grain to achieve consistent moisture measurement results. Conductivity-type moisture meters are usually the lowest-cost alternative for moisture measurement because of their electronic simplicity. In the United States, conductivity-type grain moisture meters are less popular for on-farm use than RF dielectric types and are rarely, if ever, used for commercial transactions. Conductivity-type moisture meters are quite inaccurate for measuring grain with nonuniform moisture distributions within the kernel, which can result from drying or rewetting the grain.[5]

Microwave Method

Water absorbs microwave energy strongly—a fact routinely exploited to cook moist foods in microwave ovens. Microwave moisture systems direct a beam of microwave radiation through the grain sample and measure signal parameters related to the attenuation and/or the phase shift of the signal caused by the sample's presence (as compared to air). Calibration equations can be established to relate these measured parameters (along with sample type, density, and temperature) to moisture content as determined by routine reference methods. The microwave method is a particularly attractive technology for online measurements of flowing grain (in transit through a pipe or on a moving belt) because the microwave beam can sense the average dielectric properties of a fairly large cross-section of grain. Sample temperature measurements are fairly easily achieved in flowing grain, but simultaneous density determinations are more difficult. Microwave systems that ignore density are unlikely to yield adequate accuracy for intended purposes. Simultaneous measurement of attenuation and phase shift provide enough data to calculate the complex dielectric constant of the sample. The real and imaginary parts of the complex dielectric constant are both functions of sample density. Several different density-independent functions of the complex dielectric constant have been tested and shown to yield good moisture measurement accuracy without explicit sample density measurements.[6,7] Some of these functions also provide an estimate of the sample density.[8,9] That work has also suggested an algorithm for unifying calibration equations for different grain types.[10] This present research demonstrates similar potential

for unifying calibration equations for moisture measurements based on the radio-frequency dielectric method.

Proponents of the microwave method cite its relative immunity to sample conductivity effects as a major advantage over conductivity methods or RF dielectric methods.[11,12] The primary limitation of the microwave method has been the relatively high cost and complexity of microwave-based moisture measurement systems.

Radio-Frequency Dielectric Method

The radio-frequency (RF) dielectric method measures moisture content in grain by sensing the dielectric constant of grain samples. The dielectric constant is a measure of a material's ability to store electrical charge when placed in an electric field. Because of its molecular structure, water has a very high dielectric constant (approximately 80) compared to other grain constituents (2 to 3). This wide difference in dielectric constants between water and other grain constituents should make the RF dielectric method quite insensitive to sample composition. However, the RF dielectric method is influenced significantly by grain kernel structure and composition and moisture distribution within kernels, necessitating individual calibration equations for different grain types and limiting measurement accuracy. Also, the RF dielectric method is expected to be more sensitive to grain conductivity (presumably ionic conductivity) than the higher frequency microwave methods. Despite these limitations, the RF dielectric method presents an attractive combination of good accuracy, close matching (standardization) among instruments within a model, relatively simple calibration development, and moderate manufacturing cost.

Because of these advantages, grain moisture instruments based on the RF dielectric method are used for all official and almost all commercial (unofficial) grain moisture measurements in the United States. Some portable models are very popular for on-farm use.

Motivation for Research on the RF Dielectric Method

The RF dielectric method has been used widely for moisture measurement for over sixty years.[13] However, the method has been burdened by the need for continual calibration equation development and checking. Its reputation has been sullied by significant inconsistencies and inaccuracies among moisture meters.[14] Despite decades of excellent research on the dielectric characteristics of grain by the United States Department of Agriculture and others, moisture measurement algorithms in commercial moisture meters have not changed appreciably in the last twenty-five years.

Calibration development has been the greatest impediment to introducing new moisture measurement algorithms. Grain moisture meter users expect meter manufacturers to provide calibration equations that give accurate results for all grains they need to test—for the life of the moisture meter. Since the relationships between measured parameters and moisture (as determined by air oven methods) are not very stable over time, calibration equations must be routinely evaluated and adjusted to maintain accuracy. The calibration development cost over the life of the model can be several times the cost of the initial design of the instrument. If a manufacturer has developed an extensive set of calibration equations for one technology, there is an overwhelming incentive to preserve the existing

sensing technology (with all its weaknesses) when introducing a new model with updated styling and a better user interface. As a result, some moisture meter models that have been introduced in the last five years still use vacuum tubes in the sensing circuitry. Attempts to improve sensor technology while maintaining backwards compatibility with older technology have met with only limited success.[15]

Different moisture meter manufacturers use different sensing technologies (many of which are patented or trade secrets) in their moisture meters. This prevents spreading the cost of calibration development over several instrument models and ensures inconsistencies in moisture measurement results among models.

The primary goals of this research were to achieve a broader and deeper understanding of the physical processes involved in the dielectric response of cereal grains and oilseeds and, based on that understanding, to create a new algorithm that would warrant a new generation of moisture meters. Better understanding of the physical processes could contribute to significantly improved moisture measurement accuracy, unification of moisture calibrations for different grain types, and more stable grain moisture calibration equations. Such improvements should be an adequate incentive for moisture meter manufacturers to change to newer moisture sensing technology. A public moisture measurement algorithm that is significantly superior to current practice could be the basis for a new generation of calibration-compatible grain moisture meters that would give better consistency across the grain industry.

Questions Addressed by the Research

The goal of developing a more effective grain moisture measurement algorithm raised several important questions. What causes the observed instability in grain moisture meter calibrations? What measurement frequency or combination of frequencies within the RF range is the optimum for moisture measurements? What dielectric parameter is most advantageous for predicting moisture content? What is the optimum function for minimizing the effects of density differences? What type of test cell filling process should be used? How should temperature corrections be implemented in the algorithm? Finally, can optimization of these parameters yield improvements that are significant enough to warrant development of a new generation of grain moisture meters? This research has substantially answered each of these questions.

CHAPTER 2

BACKGROUND

This chapter provides an overview of dielectric characteristics and the techniques used to sense the dielectric constant. The goal is to provide essential background for dielectric moisture measurement, not to delve deeply into the details, which are readily available in the literature.

Complex Dielectric Constant

The complex dielectric constant is a measure of the polarizability of a material in response to the application of an electric field.[16] It is normally expressed as $\varepsilon^* = \varepsilon_0(\varepsilon_r^{'} - j\varepsilon_r^{''})$ where ε_0 is the permittivity of free space, ε'_r (hereafter called dielectric constant) is the real part of the relative dielectric constant, ε''_r (hereafter called dielectric loss) is the imaginary part of the relative dielectric constant, and j is the imaginary operator.

The ratio of the imaginary to the real part of the complex dielectric constant is called the loss tangent (*tan δ*). The loss tangent is the inverse of the Q (quality) factor that is common in electrical engineering. The Q factor provides a useful physical interpretation of the relative magnitudes of the dielectric constant and dielectric loss. The Q factor is the ratio of the magnitude of the reactive current density (out of phase with the driving field)

to the magnitude of the dissipative current density (in phase with the driving field). This

can be expressed as $Q = \dfrac{\omega \varepsilon_0 \varepsilon_r^{'}}{\sigma + \omega \varepsilon_0 \varepsilon_r^{''}}$ where ω is the angular frequency of the driving field

and σ is the conductivity of the medium. This shows that the current due to the

conductivity of a material and the polarization current in phase with the driving field are

closely connected. In fact the two effects are often inseparable and the combination of

dielectric loss and conductivity can be expressed equally well as apparent conductivity

($\sigma_a = \sigma + \omega \varepsilon_0 \varepsilon_r^{''}$) or apparent dielectric loss ($\varepsilon_{ra}^{''} = \dfrac{\sigma}{\omega \varepsilon_0} + \varepsilon_r^{''}$). Harrington further related

the Q factor to the ratio of the peak density of the electric energy stored in the dielectric

(each cycle) divided by the density of energy dissipated in the dielectric in one cycle. This

implies that the dielectric constant is a measure of the peak stored energy density (during

each cycle) and that the apparent dielectric loss (including both conductivity and

polarization loss) is a measure of the energy dissipated in one cycle. These relationships

have proven helpful for formulating density-independent functions for measuring moisture

content in the microwave region.[17]

The polarizability of materials includes permanent polarization (electrets),

deformation polarization (electronic), and reorientation (rotational) polarization. In

measuring the dielectric constant of grain, we are particularly interested in the rotational

polarization attributable to the reorientation of water molecules. The water molecule has a

large dipole moment (1.84 Debye) due to the bond angle (104.5°) between the two

hydrogen atoms and the unequal sharing of the covalently bonded electrons between the

hydrogen and oxygen atoms.[18]

Frequency Dependence of the
Complex Dielectric Constant

The value of the complex dielectric constant of a material varies with frequency

from its low frequency (static) value (ε_s) to its very high frequency value ε_∞. For a

material with a single relaxation mechanism, Debye[19] expressed the frequency

dependence of the complex dielectric constant as

$$\varepsilon^* = \varepsilon_\infty + \frac{\varepsilon_s - \varepsilon_\infty}{1 + j\omega\tau} \tag{1}$$

where ω is the angular frequency of the driving field and τ is the relaxation time.

Separating the real and imaginary parts of the above equation yields expressions for the

frequency dependence of the dielectric constant and dielectric loss. (The static and very

high frequency dielectric constants are both assumed to be real.)

$$\varepsilon_r^{'} = \varepsilon_\infty + \frac{\varepsilon_s - \varepsilon_\infty}{1 + \omega^2\tau^2} \tag{2}$$

$$\varepsilon_r^{''} = \frac{(\varepsilon_s - \varepsilon_\infty)\omega\tau}{1 + \omega^2\tau^2} \tag{3}$$

Figure 1 shows the shapes of the dielectric relaxation curves for free water based

on Debye parameters (ε_s, ε_∞, and τ) given by Hasted.[18] Examining the curves and the

limiting conditions for the above equations provides some insight into the general behavior

of dielectric relaxations. The real part of the dielectric constant decreases monotonically

with frequency from its maximum (static) value (where the second term in the denominator of equation 2 goes to zero) to its very high frequency value (where the second term of the denominator becomes infinite).

The dielectric loss starts out at zero for $\omega = 0$ and increases proportionally to ω while $\omega\tau$ is much less than one. When $\omega\tau$ is equal to one, that is, when the measurement frequency is equal to the relaxation frequency, the dielectric loss reaches its maximum value—which is exactly half the difference between the static value of the dielectric constant and the very high frequency value ε_∞. As $\omega\tau$ becomes large with respect to the one (1) in the denominator of equation 3, the dielectric loss decreases as ω^{-1}.

It is instructive to note the relationship between the slope of the dielectric constant versus the logarithm of frequency and the magnitude of the dielectric loss. It is not a simple relationship, but the slope of the dielectric constant will always be highest where the dielectric loss is maximum. Conversely, if the dielectric loss is zero in a frequency region, the slope of the dielectric constant should be zero. Put in simplest terms, the presence of dielectric loss at a given frequency "starves" the dielectric constant by limiting the polarization current per cycle—which causes the dielectric constant to decrease at higher frequencies. Kramers-Kr★nig relationships provide the exact mathematical transformation between the real and imaginary parts of the dielectric constant.[18]
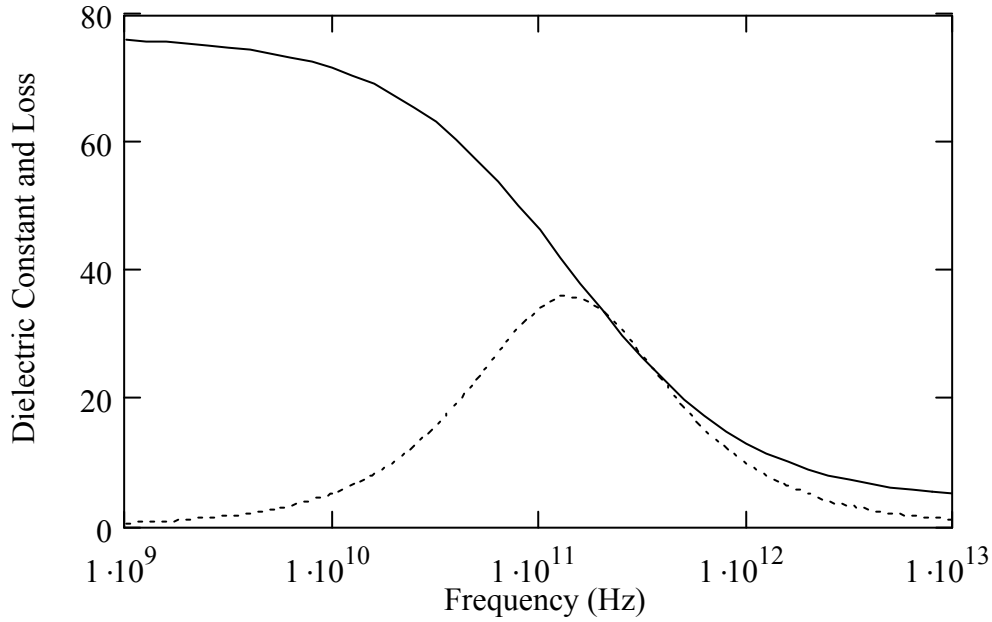
Figure 1. Dielectric constant (solid) and loss (dot) for liquid water at 30 °C.

Circuit Analog of Dielectric Relaxation

The mathematics of dielectric relaxation are exactly the same as the mathematics of

relaxation in resistor-capacitor (RC) circuits.[20,21] For a series combination of a resistor

R_s and a capacitor C_s, the voltage V impressed on the capacitor at time t after applying

voltage V_0 to the series combination is $V = V_0(1 - e^{-\frac{t}{R_s C_s}})$, and the value of the product

$R_s C_s$ is defined as the time constant of the RC circuit. For sinusoidal excitation, the

relaxation frequency (the frequency where the dissipated energy is maximized) is

$F_r = (2\pi R_s C_s)^{-1}$. Given a parallel-plate capacitive test cell with a known empty-cell (air)

capacitance C_0, a desired dielectric decrement (ε_s - ε_∞), and a desired relaxation frequency

15

F_r, the series resistance necessary to simulate the relaxation is $R_s = (2\pi C_0 F_r (\varepsilon_s - \varepsilon_\infty))^{-1}$.

This relationship was useful during the course of this research for simulating dielectric relaxations. Complicated series-parallel RC networks can be synthesized to simulate the dielectric properties of materials with multiple relaxation frequencies attributable to heterogeneity and conductivity.

Bound and Free Water

The literature is replete with discussions of "free" and "bound" water in grain.[1,5,22] Definitions given for free and bound water vary considerably from author to author. Water that is directly hydrogen-bonded to polar sites on protein, carbohydrates, and other grain is considered "monolayer" water according to the BET model.[23] Free water is generally defined as that which fills capillary spaces within grain, is capable of acting as a solvent to support ionic conductivity, and undergoes freezing at 0 °C. Authors acknowledge a continuum of hydrogen-binding energy states between bound and free water, with lower energy layers of water piling upon directly-bound higher energy layers as the moisture content increases (or conversely, being extracted layer-by-layer as the grain is desiccated). Energy considerations suggest that sites offering higher activation energies will, at equilibrium, be preferentially filled. The heat of sorption versus moisture content can be estimated from measurements of water activity (equilibrium relative humidity) at different moisture contents.

Hydrogen Bond Energy and Relaxation Frequency

The binding energy involved in hydrogen bonds plays a crucial role in the dielectric behavior of moist materials. Hilhorst[24] developed the relationship between relaxation frequency and the change in Gibbs free energy to break a hydrogen bond. Kinetic rate theory[25] suggests that the relaxation frequency f_r is related to the probability of breaking the restraining hydrogen bond(s) during the time of one period ($\tau = 1/(2\pi f_r)$). Therefore the relaxation frequency for water can be expressed as

$$f_r = \frac{kT}{2\pi h} e^{-\frac{\Delta G}{RT}} \tag{4}$$

where ΔG is the change in molar Gibbs free energy necessary to break a hydrogen bond, h is Planck's constant, k is Boltzmann's constant, T is the Kelvin temperature, and R is the gas constant. Any bond that breaks is almost immediately reformed—possibly with reorientation of the water molecule if another suitable hydrogen-bonding partner is available. The time necessary for molecular reorientation is only about 0.1 ps.[26] Therefore, the relaxation time for pure water is predominantly determined by molecules waiting for thermal activation to overcome the bond energy. This interpretation of dipolar relaxation in water appears to be much more credible than a simple intuitive model based on the supposed "inertia" of the water molecule.[27] In that interpretation, the lower relaxation frequency for bound water is due to its higher inertia.

The change in Gibbs free energy includes the molar activation enthalpy and the molar activation entropy as ($\Delta G = \Delta H - T\Delta S$). Hilhorst reasoned that the molar activation entropy can be neglected, that the relaxation frequency may be rewritten as

$$f_r \approx \frac{kT}{2\pi h} e^{-\frac{\Delta H}{RT}} \qquad (5)$$

and that for water with molar activation enthalpy ΔH, the ratio of the relaxation frequency

to that of pure water can be expressed as

$$\frac{f_r}{f_{r0}} \approx e^{\frac{\Delta H_0 - \Delta H}{RT}} \qquad (6)$$

where the zero subscript refers to the value of the parameter for free water. Writing this as

$$f_r \approx f_{r0} e^{\frac{\Delta H_0 - \Delta H}{RT}} \qquad (7)$$

suggests that the relaxation frequency of a given species of water is related to the

difference in the molar activation enthalpy between that water species and free water.

Kaatze and Uhlendorf estimated the molar activation enthalpy of free water as 20.5 kJ/mol

with a relaxation frequency of 17 GHz.[28] Assuming these values for free water, the

relaxation frequency for any other molar activation energy may be estimated, as shown in

figure 2.

Hasted[29] gave the molar activation energy of ice as 55 kJ/mol. From figure 2, the

estimated relaxation frequency is about 10 kHz, which is consistent with the measurements

he cited. Hasted stated that the dielectric properties of bound water are expected to lie

between those of free water and ice—but six decades of frequency constitutes a very broad

range. The position of grain's bound water relaxation frequencies within that six-decade

range will profoundly influence how water in grain should be measured.

18
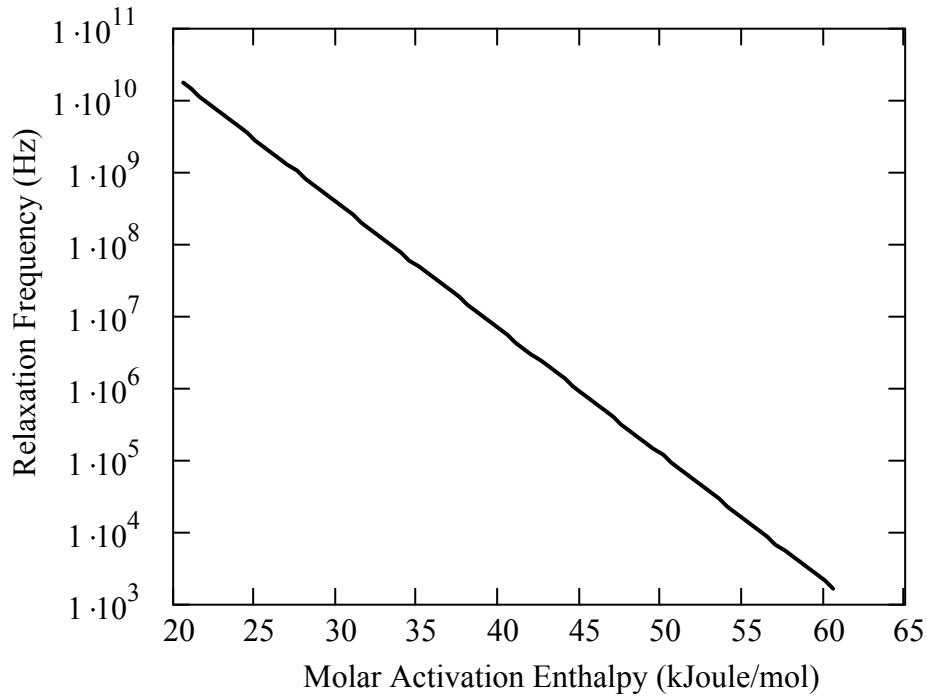
Figure 2. Estimated relaxation frequency of water as a function of the molar enthalpy
for breaking the associated hydrogen bonding to permit reorientation.

Conductivity Effects

Nelson and Stetson[30] pointed out that the measured dielectric constants at low

frequencies are much too high to be caused by dipolar reorientation and stated that they

must be due to conductivity effects. The manifestations of conductivity in the dielectric

spectra of grain are much more complex than would be immediately apparent because

grain is heterogeneous, both macroscopically and microscopically. Hasted,[31] von

Hippel,[32] and Hilhorst [24] described conductivity effects in heterogeneous materials in

detail. The two major types of conductivity effects in grain are electrode polarization

effects and Maxwell-Wagner effects.

A qualitative explanation provides insight into these two effects. Let a test cell

designed as a parallel-plate capacitor be filled with a homogeneous slightly conductive

dielectric material. A sinusoidal voltage is impressed upon the electrodes to set up a time-

varying electric field in the dielectric material. If the contact resistance between the

dielectric material and the capacitor plates (electrodes) is negligible compared to the

resistance (inverse of conductance) through the dielectric material, the conductance of the

material should not affect the apparent capacitance of the test cell at any measurement

frequency.

Now let the contact resistance between the dielectric material and the electrodes be

much higher than the resistance through the material. Charge carriers that reach the

electrodes during one cycle of the driving electric field will tend to "pile up" there until the

field reverses—at which time they will traverse the material and pile up on the opposing

electrode. A "space charge" region appears at each electrode. This charge storage at the

electrodes "looks" like capacitance. At very high frequencies, few charge carriers have

time to reach the electrodes, so the capacitance is small. At very low frequencies,

however, the time to establish the space charge regions at the electrodes may be short

relative to the period of the driving field. The measurement circuitry connected to the

capacitive test cell "sees" a very large capacitance value that is determined by the area of

the electrodes and the thickness of the space charge region—and is virtually unrelated to

the capacitance value that would be measured at high frequencies. This effect is called electrode polarization.

The Maxwell-Wagner effect is conceptually similar. This effect is caused by conducting inclusions within a dielectric matrix that has much lower conductivity (higher resistivity). Charge carriers that manage to traverse a conducting inclusion during a half-cycle of the driving field pile up at the interface and establish a space charge region within the conducting inclusion. This, too, appears to the measurement circuitry as additional capacitance.

The frequency dependence of the added Maxwell-Wagner capacitance depends on the dimensions of the inclusions, the effective width of the gaps between inclusions, and the conductivity of the inclusions. At low frequencies (relative to the Maxwell-Wagner relaxation frequency), the time for charge carriers to traverse the inclusion is short relative to the period of the driving field. The space charge region at the inclusion boundary is fully developed and the apparent capacitance does not change for further reductions in frequency. At high frequencies (relative to the Maxwell-Wagner relaxation frequency) few charge carriers reach the boundaries of the inclusion within one half-cycle of the driving field. No space charge region is established at the boundary, and the external measurement circuitry senses no anomalous capacitance due to the conducting inclusions. Between the low and high frequency limits, the capacitance added by the presence of conducting inclusions varies in a sigmoidal pattern. The dielectric loss associated with the Maxwell-Wagner relaxation behaves like any other relaxation phenomenon. It goes to

zero at low and high frequency limits and is maximum at the frequency where the slope of the capacitance versus frequency curve is maximum.

Conductivity effects are particularly confusing because of the possibility of contributions (at a given frequency) from electrode polarization, macroscopic conducting inclusions, and microscopic conducting inclusions. Furthermore, the appearance of conductivity effects changes radically with moisture content as the relative conductivities of the conducting inclusions and the surrounding medium (or barriers between inclusions) change.

Mixture Formulas

When two or more dielectric materials are mixed, the dielectric constant of the mixture is expected to lie somewhere between the highest and the lowest dielectric constants represented in the components. Hasted[31] explained that the dielectric constant of the mixture is very dependent upon the shapes assumed by the mixture components and their orientation. The general problem of computing the dielectric constant of a mixture (or inferring the dielectric constant of a component from measurements of the dielectric constant of a mixture) is intractable because of the mutual interaction of particles through their polarization fields. However, many approximate solutions have been proposed.

Nelson has evaluated the applicability of various mixture formulas for predicting the relationships between dielectric constants of whole and ground grain at various degrees of compaction and for predicting dielectric constants of solid materials from the dielectric

constants of pulverized materials.[33-36] He determined that the two most suitable

equations were the complex refractive index mixture equation

$$\varepsilon^{\frac{1}{2}} = v_1 \varepsilon_1^{\frac{1}{2}} + v_2 \varepsilon_2^{\frac{1}{2}} \tag{8}$$

and the Landau and Lifshitz, Looyenga equation

$$\varepsilon^{\frac{1}{3}} = v_1 \varepsilon_1^{\frac{1}{3}} + v_2 \varepsilon_2^{\frac{1}{3}} \tag{9}$$

where ε, ε_1, and ε_2 are the complex dielectric constants of the mixture and the first and

second components, respectively, and v_1 and v_2 are the volume fractions occupied by

components one and two of the mixture. Nelson stated a preference for equation 9 as

giving somewhat closer agreement between predicted and measured dielectric constant

values. He noted that for an air-particle mixture where $\varepsilon_1 = 1 - j0$, $v_1 = 1 - v_2$, and

$v_2 = \rho/\rho_2$ (ρ and ρ_2 being the densities of the mixture and the solid component,

respectively) the dielectric constant of a mixture at any density ρ_x can be calculated from

the dielectric constant of the mixture at any other density ρ_y as

$$\varepsilon_x = \left[\left(\varepsilon_y^{\frac{1}{3}} - 1 \right) \frac{\rho_x}{\rho_y} + 1 \right]^3 \tag{10}$$

The significance of equation 10 for grain moisture measurement is demonstrated in this

present research.

Temperature Dependence of Dielectric Characteristics

Temperature profoundly affects the dielectric characteristics of materials. Equation 7 (page 18) suggests that the characteristic frequency of a relaxation mechanism will increase with temperature. The increasing disorder in a system at higher temperatures generally causes the static dielectric constant to decrease. These two effects are observed in the temperature dependence of the complex dielectric constant of pure water. Figure 3 shows values of the dielectric constant and loss for pure water at 0 and 50 °C calculated from the Debye parameters cited by Hasted.[18] The figure illustrates the competing nature of these effects. The static dielectric constant decreases significantly as the temperature increases, but the upward shift of the relaxation frequency more than compensates for the static dielectric constant at some measurement frequencies.
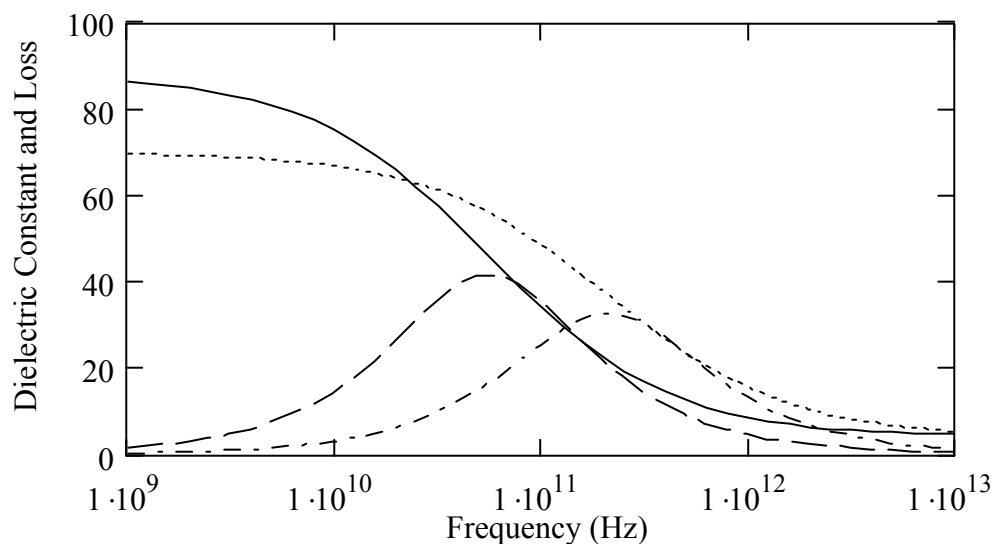
Figure 3. Liquid water dielectric constant at 0 °C (solid) and 50 °C (dot)
and dielectric loss at 0 °C (dash) and 50 °C (dash-dot).

Figure 4 shows the relationships between dielectric characteristics and temperature at 1, 31.6, and 100 GHz. The temperature dependence is determined by whether the measurement frequency is below the relaxation frequency, near the relaxation frequency, or above the relaxation frequency. Generally, the temperature dependence of the dielectric constant is expected to be negative if the measurement frequency is far from a relaxation frequency (dielectric loss is very low) and positive if the measurement frequency is in the vicinity of a relaxation (dielectric loss is significant). The dielectric loss should increase with temperature if the measurement frequency is higher than the relaxation frequency and decrease with temperature if the measurement frequency is lower than the relaxation frequency. Dielectric measurements over very wide frequency ranges are needed to see the temperature effects clearly, but the behavior of the dielectric constant and loss with temperature at a single measurement frequency is good evidence for locating the position (frequency) of a dielectric relaxation mechanism relative to the measurement frequency.
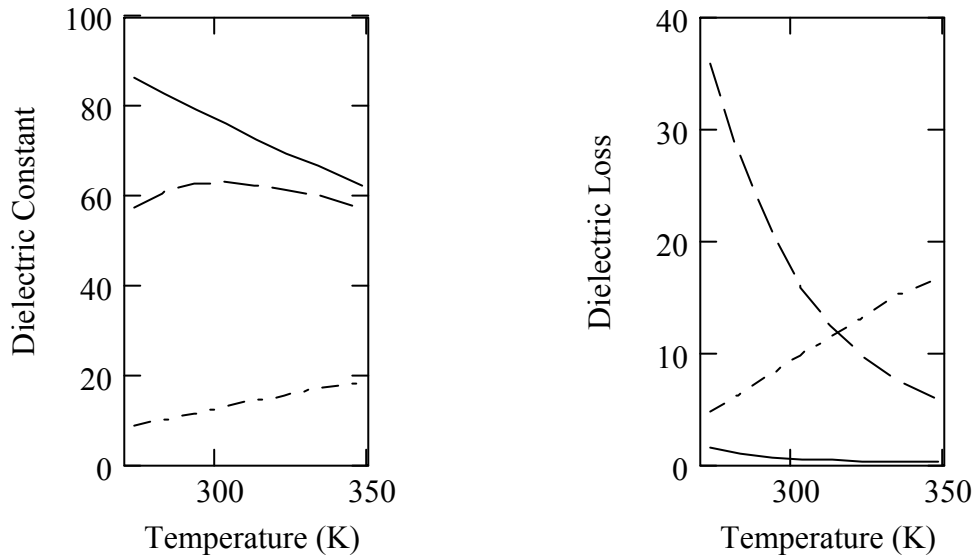
Figure 4. Estimated temperature dependence of dielectric constant and
dielectric loss of liquid water at three frequencies: 1 GHz (solid),
31.6 GHz (dash), and 100 GHz (dash-dot).

Techniques for Sensing Dielectric Characteristics

A considerable body of literature describes techniques for sensing the dielectric

characteristics of grain.[37-45] These methods generally fall into two categories: those

which sense the change in capacitance of a test cell upon the introduction of the grain into

the test cell and those which sense the phase shift, attenuation, or reflection of an

electromagnetic wave propagating through the sample in free space or contained in a

section of transmission line.

The mathematics associated with the former group of measurements are relatively

simple because the test cell is treated using lumped parameter concepts. The complex

dielectric constant is the ratio between the complex capacitance (includes a phase angle

caused by dielectric loss and conductance) of the test cell with the material present and the complex capacitance of the test cell with air separating the electrodes. Any extraneous complex capacitance that is not associated with the space occupied by the dielectric material must be subtracted from both measurements before computing the ratio.

The mathematical treatment of the interaction of an electromagnetic wave with a dielectric material is not nearly so simple. The complex dielectric constant determines the wave propagation constant γ as

$$\gamma = \alpha + j\beta = \gamma_0 \sqrt{\varepsilon^*} = j\frac{2\pi}{\lambda_0}\sqrt{(\varepsilon' - j\varepsilon'')} \tag{11}$$

where α is the attenuation constant, β is the phase constant, λ_0 is the free-space wavelength, γ_0 is the free-space propagation constant, and ε^* is the complex dielectric constant of the material. The transmission coefficient T is related to the propagation constant[8] as $T = e^{-\gamma t}$.

Similarly, the complex reflection coefficient at the interface between the dielectric material and air is determined by the dielectric constant. Modeling the behavior of an electromagnetic wave as it travels from air into the dielectric material and back out requires careful consideration of the multiple reflections that occur at each interface. Signal flow graphs provide a systematic means of modeling such systems to compute complex dielectric constants from complex transmission coefficients or reflection coefficients.[41,46]

Grain Moisture Measurement by the
RF Dielectric Method

Several review articles have provided general information on using the RF dielectric method for sensing grain moisture content.[5,40,47-53] Patents provide some of the most detailed information on the techniques that have been employed in commercial grain moisture meters.[13,15,54-59] Lawrence and Nelson[40] reviewed recent moisture meter patents pertaining to the RF dielectric method. Matthews[60] provided some of the most detailed information available on specific design aspects such as test cell size and shape, temperature correction, and cell filling methods. Jones[61] also shared insights on moisture meter design factors.

Almost all commercial moisture meters employing the RF dielectric method have used the frequency range from 1 to 20 MHz.[53] Some[56] have used lower frequencies to obtain density-independent measurements based on the loss tangent. Others[59] have included audio-frequency measurements to correct for conductivity effects for very moist grain. Recent research [41-43,62,63] has used complex transmission and reflection coefficients at multiple frequencies in the 1 to 400 MHz frequency range.

All sources agree that successful grain moisture measurements require corrections for interfering factors such as density and temperature and careful calibration equation development as well as reliable sensing of dielectric characteristics.

CHAPTER 3

MATERIALS AND METHODS

The grain samples tested in the course of this research were obtained from grain

marketing channels throughout the United States as part of the Annual Moisture

Calibration Survey conducted by GIPSA.[64] The primary purpose of this ongoing effort is

to ensure that GIPSA's official moisture measurements are as accurate as possible—that is,

that the official moisture meter's test results agree as closely as possible with GIPSA's

established moisture reference methods.[65]

Each year, the Moisture Group within the Inspection Systems Engineering Branch

solicits samples of specific grain types from all growing regions of the country. GIPSA's

Field Offices are responsible for collecting and shipping the samples to Kansas City,

Missouri, where the Moisture Group conducts the tests. The sample request is designed to

create sample sets that include the full commercial range of moisture for each grain type

and proportionately represent all growing areas for each grain type. The Moisture Group

receives and tests approximately 1300 samples representing about 30 distinct grain types

each year. Each sample is tested on two units of the official moisture meter and is

analyzed in duplicate by the applicable air oven reference method. These data are

submitted to GIPSA's statistician for analysis. The performance for each grain type is

compared to established tolerances.[66]   New calibration coefficients are developed and issued for grain types that fail to meet the tolerances.

Because of the observed variability and instability in the relationships between dielectric parameters and moisture, each grain type is tested for three years before official calibrations are created or updated from the results. GIPSA is responsible for moisture tests for about 60 grains and commodities, so not nearly all grain types can be tested in any given year. Only the fifteen most significant grain types are tested each year. The others are tested according to a cyclical nine-year plan. This moisture meter calibration verification program has been operating for at least fifty years.[47] Obviously, maintaining accurate moisture meter calibrations has been very expensive.

Since 1995 GIPSA has included some commercial (unofficial) moisture meters in its Annual Moisture Calibration Survey as a collaborative project with the National Conference on Weights and Measures and its National Type Evaluation Program (NTEP). Instruments that undergo evaluation and meet the requirements of the Handbook 44 Moisture Code[67,68] are enrolled in the program. These instruments are tested with the same grain samples that are used to test and calibrate the official moisture meter. Instrument manufacturers use these data to develop calibrations that optimally match GIPSA's air oven reference methods. Also, instrument accuracy on these samples determines the moisture range for each grain type over which a manufacturer can claim "NTEP approved."

Grain Samples Studied

The grain samples that are collected and tested through the Annual Moisture

Calibration Survey provide a uniquely extensive, broad, and representative sample set for

research to investigate dielectric properties that affect moisture measurement and to

develop improved moisture measurement algorithms. About half of the samples in the

Survey during 1997 and 1998 were included in this research. Nearly all of the Survey

samples received in 1999 were tested using two different research-grade instruments. All

of the Survey samples from 2000 were tested with one research instrument, some received

additional testing to assess temperature characteristics, and a few were analyzed with a

third instrument. Appendix A shows a summary of the grain types and numbers of

samples tested each year. For purposes of this dissertation, only data for the fifteen most

significant grain types are included in the data analyses. These include yellow-dent corn,

soybeans, sunflower seeds (oil-type), barley (Six-Rowed and Two-Rowed), wheat (Hard

Red Winter, Hard Red Spring, Soft Red Winter, Durum, Soft White, and Hard White), rice

(Long Grain Rough and Medium Grain Rough), oats, and sorghum.

High-Frequency Measurements (1 to 501 MHz)

This research project began in 1995 as a collaboration between GIPSA and the

USDA-Agricultural Research Service. GIPSA established a research contract with

scientists at the Russell Research Center in Athens, Georgia to pursue development of

improved moisture measurement algorithms. Kurt Lawrence and Stuart Nelson designed,

tested, and established calibration models for a parallel-plate transmission line-type test

cell over the design frequency range of 1 to 500 megahertz. This test cell was completed

and delivered to USDA-GIPSA in 1997. Technical staff at the GIPSA laboratory have

been collecting dielectric data with this test cell since 1997.

A Hewlett-Packard Model 4291A RF Impedance/Material Analyzer (HP-4291A)

was used to measure complex reflection coefficient data at 2 MHz intervals from 1 to 501

MHz. GIPSA technical staff collected data for about 3,700 grain samples from the 1997,

1998, 1999, and 2000 crops with this instrumentation.

<div align="center">Instrumentation and Procedures</div>

The HP-4291A (figure 5) is a single-port RF instrument designed to measure and

record complex reflection coefficients with high precision from 1 to 1800 MHz. It

includes software to calculate correction parameters to calibrate the instrument with

standard networks (open, short, and 50-ohm load) at the instrument's test port and to

extend that calibration to other reference planes as described below. The instrument has

the capability to store data to a floppy disk or send it to an external computer through the

GPIB interface. It also can be programmed in HP-BASIC to serve as a controller for a

system of instruments. In this application, data were simply stored to floppy disks that

were copied to another computer for further processing.

Figure 5. Hewlett-Packard Model 4291A RF Impedance/Material Analyzer

The HP-4291A uses the "RF I-V Technique."[69] Figure 6 shows a simplified diagram of the RF I-V measurement system. A computer-controlled signal generator applies a signal to the device under test through a current-sensing transformer. A vector voltmeter measures the magnitude and phase of the voltage at the device under test (DUT) (in this case, the grain test cell). A current-to-voltage converter produces a voltage proportional to the current delivered to the device. A second vector voltmeter measures the magnitude and phase of this voltage. If the voltage applied to a device and the resulting current through the device are known, the complex impedance of the device is readily calculated by using Ohm's law ($Z = V / I$). Other parameters of interest, such as equivalent parallel capacitance and conductance and reflection coefficient (for a 50-ohm system) can be calculated if the complex impedance is known.
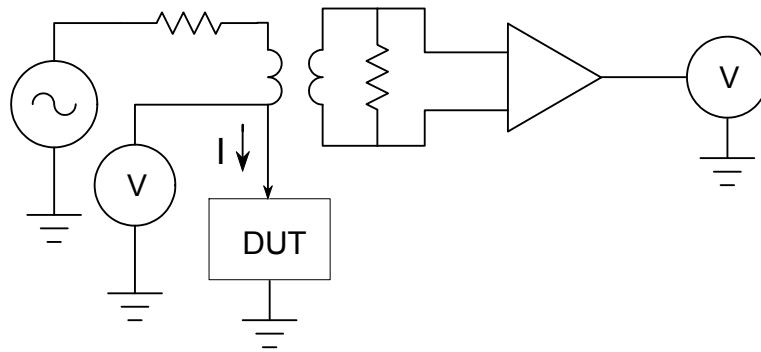
Figure 6. Block diagram of the radio-frequency current-voltage technique
employed by the HP-4291A RF Impedance Analyzer.
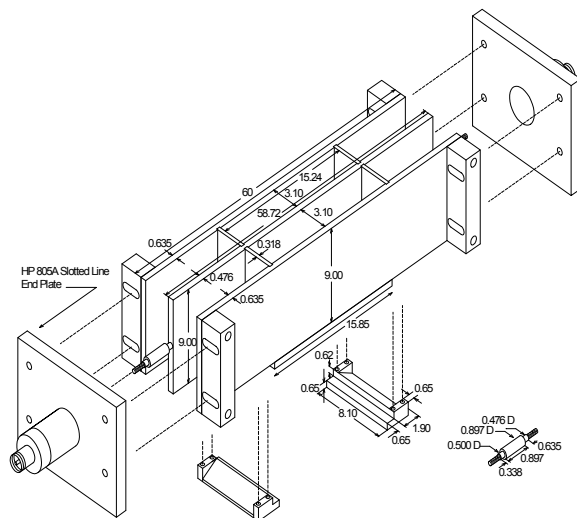
Figure 7. Exploded view of test cell used for high-frequency dielectric measurements.
(Figure provided by Lawrence)

The test cell (figure 7) was constructed as a 50-ohm transmission line. It consists

of three parallel aluminum plates. The ends of the plates are connected to endplates from a

Hewlett-Packard 805A Slotted Line. Each endplate contains a machined 50-ohm transition

from a Type-N coaxial connector to a threaded stud that is connected directly to the center plate. The test cell was designed to permit transmission coefficient measurements as well as reflectance coefficient measurements to permit thorough cell characterization with a vector network analyzer (Hewlett-Packard Model 8753C). Lawrence adjusted the spacing between the plates to 0.0310m to achieve a characteristic impedance as close as possible to 50 ohms and made other mechanical adjustments to minimize the reflection coefficient for the empty test cell.[42]

Lawrence developed a mathematical model for the test cell using signal flow graphs.[46,70] His process was similar to that used for characterizing an earlier coaxial test cell for grain.[41] Lawrence measured S-parameters[46] for the test cell filled with air, methanol, propanol, n-butanol, n-pentanol, n-hexanol, and n-decanol with the HP-8753C vector network analyzer. He calculated the complex dielectric constants at each frequency for each material from the complex transmission coefficients. He iteratively adjusted the assumed length of the air-filled sections on each side of the sample section to optimize agreement with complex dielectric constant values computed from recognized Debye parameters for each alcohol.[41] He provided the S-parameter data for each alcohol and the calculated theoretical complex dielectric constants for each alcohol so that the model could be further refined during the present research.

In the current work, a program (appendix B) was written in Mathcad[71] to solve for the complex dielectric constant of a sample from the measured complex reflection coefficient. Another program used that algorithm to optimize Lawrence's mathematical

test cell model for relating reflectance coefficient measurements to complex dielectric constant values. The agreement between measured dielectric characteristics and predicted (Debye) characteristics for several types of alcohol is shown in appendix C. Adjusting the assumed electrical length of the air-filled sections from 0.345 m in Lawrence's original model to 0.332 m substantially reduced errors on alcohol measurements at high frequencies. Also, the current work improved upon Lawrence's model by explaining the 1.31 multiplier (on the complex dielectric constant) originally proposed by Lawrence as a correction.[70] The need for the correction is probably due to a hybrid transverse magnetic/transverse electric (TM-TE) wave mode instead of a pure TEM mode in the test cell.[72] This could be caused by the exposed edges of the sample-filled section. Changing the form of Lawrence's correction improved the accuracy of the calculated complex dielectric constant values for air and very dry materials.

The sample test area was a 0.1524 m section in the center portion of the parallel plates. The volume of the sample section of the test cell was 850 cm^3. Thin polystyrene spacers between the plates contained the grain in that center section. A sliding PVC gate under the center section was supported by two PVC rails attached to the aluminum plates with machine screws. The sliding gate permitted loading and unloading grain samples without moving the test cell. The gate and its supports contributed a small discontinuity to the test cell and increased the empty cell reflection coefficients. Figure 8 shows the complex reflection coefficients measured with the gate present and removed. Removing the gate reduced the magnitude of the reflection coefficients by nearly one half. The test

cell design might be improved by reducing the amount of dielectric material in the gate and supports.
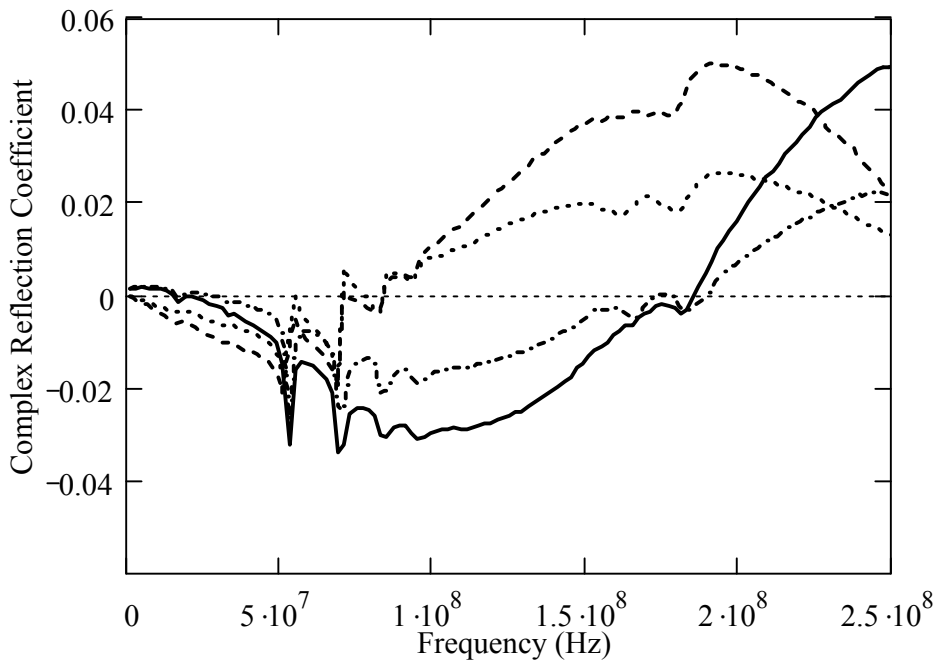
Figure 8. Real and imaginary parts of empty-cell complex reflection coefficients measured with test cell gate present (solid and dash) and removed (dash-dot and dot).

A funnel apparatus (Seedburo Filling Hopper and Stand, Model #151) centered over the center section was used to fill the test cell repeatably. A digital thermometer (Shore Sales Digital Thermometer Model LT-207) for room temperature tests and alcohol-in-glass thermometers for extreme-temperature tests were used to determine sample temperature immediately before pouring the sample into the loading funnel. After the funnel was emptied into the test cell, it was swung away from the filling position and the

37

sample volume was struck off with a straightedge to achieve a constant sample volume. All stray kernels were removed from the test cell area before the instrument scan was triggered. After the test, all grain in the test cell was removed by opening the sliding gate. The grain was collected and weighed with a electronic scale (Mettler Model PM-4000). Grain identification number, sample weight, and sample temperature were recorded in a log book for subsequent data entry.

At the beginning of each day's tests, the instrument was warmed up for at least one hour. The current "state" file was recalled from floppy disk to set the instrument to its standard configuration. The instrument was calibrated with short, open, and 50-ohm load fixtures at the instrument test port (Type APC-7 connector) according to the manufacturer's instructions.[73] An APC-7 to Type N coaxial adapter and a 15-cm long 50-ohm coaxial cable were used to extend the test port to the connector on the test cell. Before attaching the coaxial cable to the test cell, a calibration was performed with open (no connector), short (HP 11511A Type-N Short), and 50-ohm load (HP 909C 50-ohm Termination) standards.

The test cell was connected to the coaxial cable and the 50-ohm standard load was attached to the other end of the test cell. (Figure 9 shows the entire measurement system.) A scan of the empty cell reflection coefficients was recorded and evaluated. If the magnitude of the reflection coefficient exceeded 0.06 at any frequency between 1 and 501 MHz, the calibration procedure was repeated. Problems with excessively high empty cell reflection coefficients were usually resolved by tightening all coaxial connectors more

carefully. After the empty cell test passed, a "Daily Check" sample was tested before any other samples. This sample served as a check on the instrument's long-term stability.
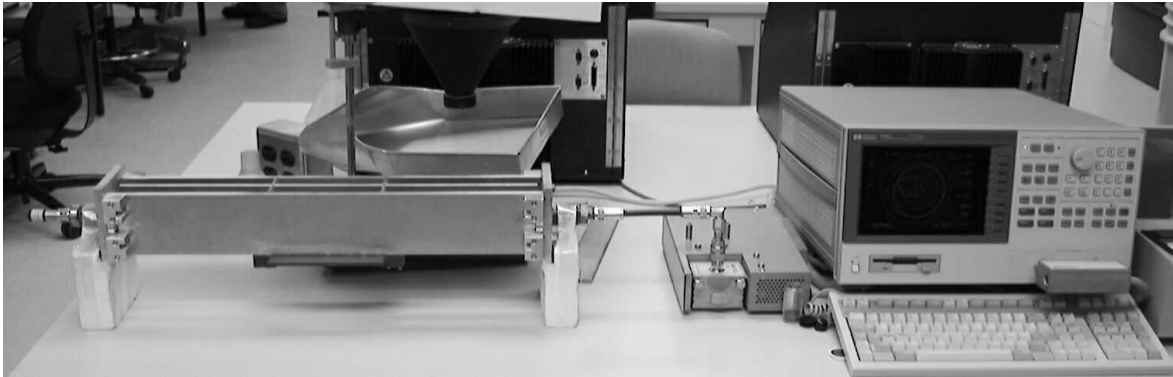
Figure 9. System for high-frequency grain dielectric measurements.

Except for samples chosen for temperature tests, all samples were removed from refrigerated storage (4 °C) and equilibrated overnight to room temperature (22 °C +/- 1 °C) before testing. Temperature test samples were placed in a temperature-controlled chamber in sealed containers and equilibrated until stable (approximately four hours) as determined by a thermometer inserted in the sample through a rubber stopper. Temperature test samples and room temperature samples were tested by the same procedure except for taking care to complete the testing very quickly for temperature test samples to minimize sample temperature ambiguity. The moisture content was determined for each sample by the applicable air oven method.

Medium-Frequency Measurements (0.1 to 18.5 MHz)

The medium-frequency range from 0.1 to 20 MHz has traditionally been used most extensively for grain moisture measurement. With very few exceptions, grain moisture meters used for commercial transactions in the United States operate in this frequency range. Gaining a better understanding of dielectric behavior in this frequency region was an important goal for this dissertation research. A test cell from a commercial grain moisture meter (Dickey-john Corporation Model GAC-2100) was adapted to make dielectric measurements with a research-grade impedance analyzer. A Hewlett-Packard Model 4285A Precision LCR Meter was used to measure capacitance and conductance at ten frequencies (0.1, 0.2, 0.3, 0.5, 1, 2, 3, 5, 12, and 18.5 MHz). The data from this system overlapped the frequency range provide by the HP-4291A, but this system was better suited for measurements below 20 MHz than the HP-4291A. Data were collected for about 1400 grain samples from the 1999 crop with this system.

Instrumentation and Procedures

The HP-4285A uses a four-terminal pair measurement with an "auto-balancing bridge technique".[74] Figure 10 shows a simplified diagram of the measurement technique. The four terminals are: high current (HC), high potential (HP), low potential (LP), and low current (LC). The HC lead supplies the drive signal to the high side of the test cell. The HP lead is used to sense the voltage magnitude and phase at the high side of the test cell. The LP lead senses the voltage magnitude and phase at the low side of the test cell and drives an auto-balancing bridge (essentially an operational amplifier) to cause the LC lead

40

to sink current to maintain the low side of the test cell at virtual ground. That is, the low

side of the test cell is held at ground potential by the action of the LC lead, but it is not

electrically grounded. The system uses the measured voltage magnitude and phase at the

high side of the test cell and the measured current magnitude and phase at the low side of

the test cell to calculate the complex impedance (magnitude and phase) of the test cell.

Many different derived parameters such as capacitance, inductance, conductance,

resistance, Q, D, etc. can be readily calculated from the complex impedance. The HP-

4285A offers direct computation of many such values. For ease of interpretation, the data

were recorded as parallel capacitance and conductance.
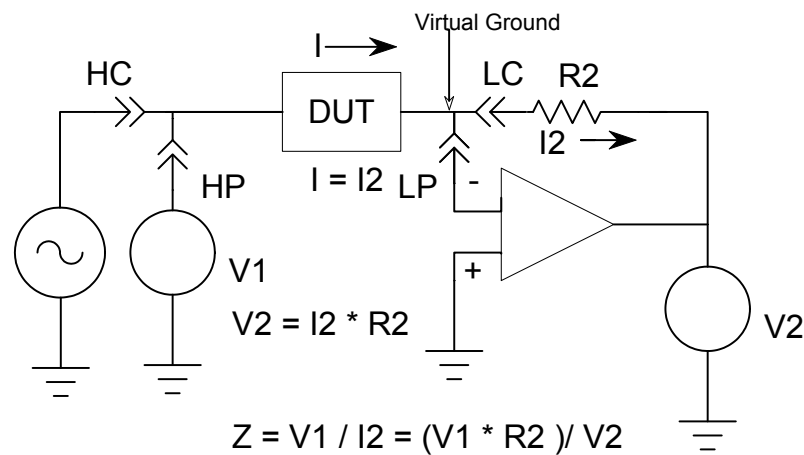
Figure 10. Block diagram of the auto-balancing bridge technique
employed in the HP-4285A Precision LCR Meter and
the AT-4294A Precision Impedance Meter.

The HP-4285A has no built-in mass-storage capabilities. Programs were written in

BASIC to control the instrument through the GPIB interface and collect data on an

external computer. The program also controlled a programmable multimeter (Hewlett-

Packard Model 3457A) that measured the voltage across two temperature sensing diodes in

the test cell. The program created two data files for each set of measurements. One file

contained text information such as notes on sample condition and test modifications. The

other file contained only ASCII numeric entries to permit access by Mathcad file-handling

statements.[71]

As mentioned above, the test cell (figure 11) was a modified GAC-2100 moisture

meter test cell. The test cell consisted of two outer aluminum plates, a double-sided

epoxy-glass circuit board with measurement circuitry around the periphery and gold-plated

electrodes in the center, and two plastic parts that served as shrouds for the circuitry and

spacers between the outer and center electrodes. The two outer electrodes were

electrically connected through five long machine screws and two gold-plated pins and

sockets on each side of the center circuit board. The pins were swaged into the aluminum

plates and the sockets were soldered to ground traces on the circuit board.
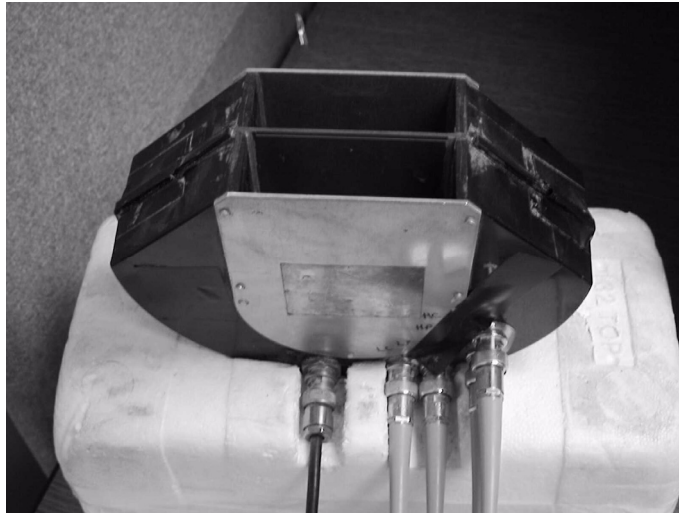
Figure11. Test cell used for medium-frequency and wide-frequency range
grain dielectric measurements.

The modification to the circuit board consisted of removing all of the circuitry that

was connected to the center electrode, installing miniature gold-plated sockets to connect

the LCR meter to the center and outer electrodes, adding wire braid to reduce the

inductance between the new socket and the existing sockets for the outer electrodes, and

installing sockets to connect the temperature sensor diodes to a BNC-type jack. The

plastic parts were modified by mounting the BNC-type jack for the temperature sensor and

four BNC-type jacks for the four-terminal connection to the LCR meter. Copper foil tape

was placed on the plastic part where the latter four BNC-type jacks were attached to

provide reliable low-inductance connections between the shield terminals on the jacks.

The outer electrodes were unmodified except for covering three screw holes with copper

foil tape. When measurements were taken, the test cell was always supported on thick

expanded polystyrene blocks to minimize capacitance to surrounding surfaces.

43

The area of the outer electrodes was 67.93 cm^2 and the spacing between the inner

and outer electrodes (d) was 2.54 cm, giving a cell volume of 345.7 cm^3. The "active"

inner electrode active area ($A = 58.55$ cm^2) was less than the outer electrode area because

of a cutout section for the temperature sensor diodes. Inserting these values in the parallel

plate capacitor formula ($C = \varepsilon_0 A / d$) yielded an estimated cell capacitance of 4.082 pF,

which is very close to values obtained through test cell characterization tests with

deionized water. For purposes of computing dielectric constants from capacitance

measurements, the empty (air) cell capacitance was assumed to be 4.00 pF.

Sample temperature was sensed by measuring the voltage across two silicon diodes

forward-biased with a current of 1.0 milliamp. A simple regulated supply was constructed

to provide a constant current to the temperature sensor. The temperature sensor slope

coefficient was -0.0042 volt/°C and the sensor voltage at 25 °C was 1.2267 volts. The

slope coefficient was supplied by Dickey-john Corporation, and the sensor voltage at 25

°C was determined during test cell characterization tests with deionized water. Sample

temperature (Celsius) was calculated from these coefficients and the measured sensor

voltage V as:

$$T = \frac{1.2267 - V}{0.0042} + 25 \qquad\qquad (12)$$

The HP-4285A and 1-m cable assembly HP-16048A were calibrated according to

the manufacturer's instructions. This included cable corrections and open/short

corrections at the pin-plugs mounted in the test cell.[75] This process was repeated only

when empty cell measurements showed significant differences from previous readings.

Figure 12. System used for medium-frequency grain dielectric measurements.

The HP-4285A was warmed up for at least 30 minutes before each day's tests. The

measurement system is shown in figure 12. Each sample was tested twice on the HP-

4285A system using two different cell filling techniques to cause different packing

densities. For a fast fill, the sample was poured into the "dump cell" for a Motomco

Model 919 Moisture Meter (right side in figure 12).[54] This mechanism is a 76.2 mm

diameter aluminum cylinder with two semicircular plates mounted on a shaft half-way

along the length of the cylinder. In the filling position, the two plates were held horizontal

(perpendicular to the axis of the cylinder) resting on two spring-loaded pins that protrude

through the walls of the cylinder. Pressing a button caused the pins to retract and the

leaves to fall together dropping the grain out the bottom of the cylinder and into the test

cell manually positioned just under the cylinder. After thus filling the test cell, the drop

cylinder was removed and the excess grain was struck off with a metal straightedge to achieve a constant sample volume.

The second filling method attempted to achieve a significantly denser fill. In this method, the sample was poured slowly into the test cell while the test cell was shaken horizontally (parallel to plane of the electrodes) with a displacement of about 1 cm and a period of about 0.5 second. After the sample overflowed the top of the test cell, the test cell was shaken vigorously (period of about 0.2 second) for about 4 seconds (again, horizontally and parallel to the electrodes) and the surface was struck off with a metal straightedge to achieve a constant volume.

After filling, the test cell was placed on an expanded polystyrene block. The measurement was triggered by command from the computer keyboard. The HP-4285A automatically performed measurements at the ten specified frequencies and transmitted the data to the computer. The computer triggered the HP-3457A multimeter to measure and transmit the temperature sensor voltage. When the computer received the data, it requested manual entry of sample weight. The operator emptied the test cell into a weighing pan, weighed the sample with an electronic scale (Mettler Model PE 1600), and typed the weight. The computer assembled and stored the data files. Reference moisture values were determined for each sample by the applicable air oven method. Empty-cell readings were recorded each day before the first grain test and after the last grain test. These empty cell test were used during subsequent data processing to minimize the effects of cable movement or temperature differences.

Special software was written to collect measurements of sample characteristics over a temperature range. The software automatically measured the temperature of the grain in the test cell every thirty seconds and triggered a new set of dielectric measurements whenever the temperature changed by at least 0.5 °C. The temperature and dielectric results were automatically logged to a data file so that the system could run unattended.

The temperature tests involved the following steps. (1) Fill the cell with the slow filling procedure described above. (2) Seal the top of the cell with a wide strip of clear adhesive-backed packing tape to avoid moisture exchange with the atmosphere. (3) Perform an initial set of dielectric measurements on the filled test cell. (4). Disconnect the test cell from the HP-16048A test cables and place the sealed test cell in a freezer at approximately -15 °C to equilibrate overnight. (5) Remove the cold test cell from the freezer and place it in a well-insulated container for transport to the testing location. (6) Connect the HP-16048A test cables to the test cell (still in the insulated container). (7) Start the measurement program. (8) Check on the rate of warming about every thirty minutes during the test and gradually open the lid on the insulated container further to maintain an acceptable warming rate (less than 0.5 °C in four minutes). (9) Terminate the test when the sample temperature essentially reaches room temperature (about four hours). (10) Remove the sealing tape, pour out the sample and weigh it with the electronic scale. (11) Remove a 25-gram portion of the sample for analysis by the applicable air oven reference method.

Wide Frequency Range Measurements
(100 Hz to 100 MHz)

The data obtained with the two systems described above had a low-frequency limit

of 0.1 MHz. As these data were analyzed, it became apparent that data over a much wider

frequency range were needed to correctly interpret the physical basis for the dielectric

characteristics observed above 0.1 MHz.—the frequency range normally used for grain

moisture measurements. Late in this research project a third instrument (Agilent

Technologies Model 4294A Precision Impedance Analyzer) was obtained to supplement

the data obtained thus far for this research. The instrument will also be valuable for

ongoing research for characterizing grain samples. Data for only thirteen samples were

included in this research, but these data yielded disproportionately rich insights.

Instrumentation and Procedures

The AT-4294A offers high-precision complex impedance measurement from 40 Hz

to 110 MHz. It can record data for up to 801 frequencies in a single scan. The operating

principle is similar to that of the HP-4285A, but it is designed for accurate measurements

over a much wider frequency range. The AT-4294A, like the HP-4285A, uses a four-

terminal pair measurement with an auto-balancing bridge, but its operating system is more

similar to that of the HP-4291A. Results can be saved to internal nonvolatile memory or

floppy disk or exported to a computer through the GPIP interface or a LAN connection.

For these tests, data were recorded at 201 logarithmically spaced points from 100 Hz to

100 MHz and saved to floppy disks. The AT-4294A's "native" measurement mode is

complex impedance, but results were converted to equivalent parallel capacitance and conductance for ease of interpretation and compatibility with other data.

The four terminal measurement technique made the AT-4294A compatible with the test cell that had been previously modified for use with the HP-4285A. A 1-m cable set (Agilent Technologies Model 16048G) was used to connect the instrument to the test cell. The instrument and cable set were calibrated according to the manufacturer's instructions[76] with the supplied 100-ohm reference fixture. "Open" and "short" compensations were performed at the test cell by disconnecting the pin-plugs from the test cell completely and shorting the two pin-plugs together, respectively. The instrument automatically saved the results of each of these tests and calculated correction parameters for the full range of test frequencies. The correction parameters were saved in nonvolatile memory and automatically recalled prior to each set of grain tests.

The same HP-3457A multimeter and current source that were used with the HP-4285A system were used to measure sample temperature with the AT-4294A system. For these tests, the temperature sensor cable was disconnected except during the actual temperature measurement because it affected the measured capacitance and conductance values slightly. The same electronic scale (Mettler Model PE-1600) was used to determine sample weight.

Prior to each day's tests, the AT-4294A was allowed to warm up for at least 30 minutes. The test cell, connected to the AT-4294A through the AT-16048 test cable, was placed on an expanded polystyrene block to minimize capacitance to other surfaces. An

49

empty-cell test was recorded by triggering the instrument manually and saving the dielectric data to a floppy disk.

Most of the samples tested were subjected to temperature tests as follows. Samples were equilibrated for at least 12 hours in a cooler at about 8 °C. They were removed one at a time and transported to the measurement laboratory in an insulated container. The sample container was opened and sufficient sample for one test was poured into the Model 919 dump cell, loaded into the test cell, and struck off as described previously as the "fast fill" method for the HP-4285A system. The dielectric measurement was manually triggered and saved to a floppy disk after assigning a unique file name. The temperature sensor cable was connected, the voltage was read and recorded, and the temperature cable was removed. The sample was poured into a weighing pan and weighed. The sample, along with any excess grain struck off in the filling process, was placed in a one-gallon zip-closure polyethylene storage bag. After smoothing the bag to eliminate excess air and spreading the sample to a thin layer in the bag, the bag was closed to minimize moisture loss during warming. A fan was directed at the bag to warm it to room temperature within a few minutes. While the first sample was warming, a second portion of the same sample was tested using the same procedure. After the samples warmed to room temperature, each of the portions was tested again with the same procedure. The tested portions were recombined and a 25-gram portion was removed for reference moisture testing by the applicable air oven method.

CHAPTER 4

RESULTS AND DISCUSSION

At the conclusion of chapter 1, several questions to be addressed during this research were posed. In this chapter, several related aspects of the dielectric response in grain will be examined and will yield significant answers.

The Nature of the Dielectric Response in Grain

The goal of grain moisture measurement is to yield results that agree as closely as possible with the values obtained by air oven moisture analyses. The measurement technique may be "blind" to some portion of the water that the air oven method finds in the sample. If the amount of water the measurement misses is constant for all grain samples (at least for a given grain type), a mathematical offset can restore the missed moisture fraction during moisture content prediction. However, if the amount of water missed by the measurement varies from sample to sample, this could contribute significantly to moisture meter inaccuracy. If the amount missed varies from grain type to grain type this could be a major factor in determining whether a single moisture measurement calibration equation could be applied to many grain types instead of only one. Also, if the measurement is insensitive to moisture below a certain moisture content, it cannot provide valid moisture results for very dry grain.

Sensing nothing but the water in the grain is just as important as sensing all of the water in the grain. If the moisture measurement method is "fooled" by interfering effects that masquerade as additional moisture in the sample, accuracy will suffer. As noted in chapter 1, the huge difference in the dielectric constants of water and dry grain should make moisture measurement by the RF dielectric method fairly simple. What is complicating the situation?

Conductivity-type moisture meters are inherently blind to bound water.[5] Stuchly[77] noted a dramatic reduction in sensitivity to water below a threshold value (presumably the upper limit for bound water) for the microwave absorption method. The RF dielectric method seems to have an inherent advantage over the conductivity and microwave methods because of its sensitivity to all of the water in grain—both bound and free.[47] Changing the measurement frequency within the RF range could sacrifice that advantage. A better understanding of the RF dielectric method's sensitivity to bound water in grain is crucial to optimizing its performance for grain moisture measurement.

<center>Optimum Frequency for Grain Moisture Measurement</center>

Nelson's research[30,78-80] on dielectric characteristics of grain showed large decreases in the dielectric constant and significant loss peaks in the audio-frequency and low megahertz frequency ranges. Are these all due to bound water relaxation? Are any of them due to bound water relaxation? If bound water is relaxing in the kilohertz or low megahertz regions, measurements at higher frequencies could be blind to that water. On

the other hand, if these features are not due to dipolar motion, they may be making grain's

dielectric characteristics much more complex without adding useful information.

Grain Dielectric Simulations

If the water that is directly hydrogen-bonded to grain constituents has a single

relaxation frequency or a reasonably narrow band of relaxation frequencies in the kilohertz

or low-megahertz range, dielectric measurements that span that range of frequencies

should show a dramatic flattening of the dielectric constant versus moisture curve in the

region corresponding to the moisture involved in that bonding. Figure 13 shows a

simulation of dielectric response versus moisture content with a single bound water

relaxation frequency at 6.5 MHz (with other water relaxing at a much higher frequency).

Bound water, free water, and dry material were simulated as parallel-connected RC

circuits. For this simulation, it was assumed that the material contained bound water sites

equivalent to ten percent water by weight. Because of the higher binding energy

associated with those sites, they should be preferentially filled before less tightly bound

sites in the water-grain matrix.

According to this simulation, the dielectric response is linear with moisture content

at measurement frequencies significantly below the relaxation frequency. For

measurements at the relaxation frequency, a significant slope change appears at the bound

water to "other" water breakpoint. As the measurement frequency is increased beyond the

relaxation frequency, the contribution of the bound water to the measured dielectric

constant becomes progressively less until a limit is reached where the measurement is

completely insensitive to moisture below the bound water limit (except to the extent that

the electronic polarizability of water is greater than that of the dry grain). If low-frequency

bound water is present, for higher measurement frequencies the linear part of the dielectric

constant versus moisture curve should extrapolate to an intercept less than the expected

dielectric constant for completely dry grain (as can be seen from figure 13). Therefore, the

shape of the dielectric constant versus moisture curve and the extrapolated intercept value

should indicate the presence or absence of significant bound water relaxations within or

below the measurement frequency range.
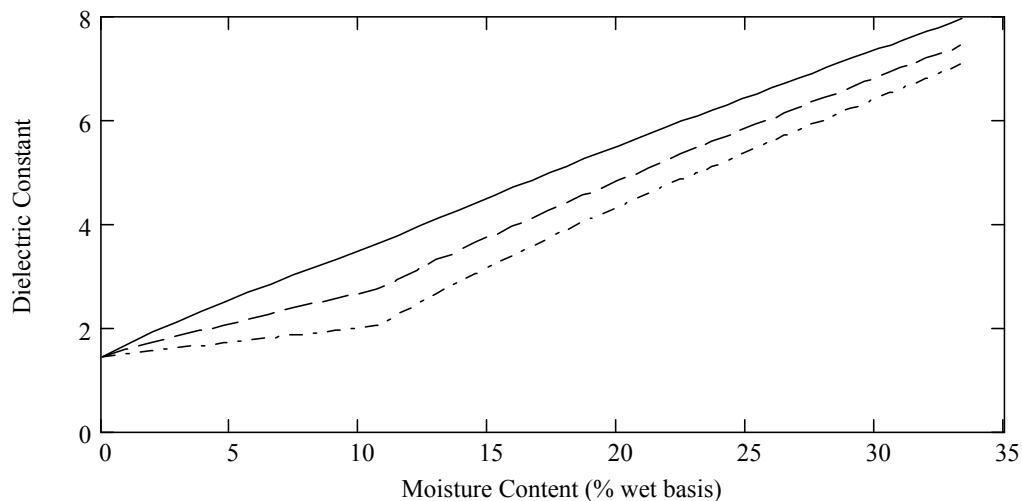
Figure 13. Simulated effects of 10 percent "bound" water sites in a grain sample with a
relaxation frequency of 6.5 MHz. Measurements of dielectric constant at
3 MHz (solid), 7 MHz (dash), and 13 MHz (dash-dot).

Figure 14 shows a much more detailed simulation (based on equation 16, page 88)

of the expected dielectric response of yellow-dent corn superimposed upon actual data

(217 yellow-dent corn samples from the 1999 crop) measured at 1, 15, and 149 MHz with

the HP-4291A system. (Similar simulations were performed with other grain types with similar results.) This simulation assumes all of the water in the grain to be contributing to the dielectric constant of the mixture as if its dielectric constant were that of pure water (static dielectric constant of 78.5 and relaxation frequency of about 17 GHz).   The shape of the curves for the high frequency results (15 and 149 MHz) show good qualitative agreement with the simulation. There appears to be an offset between the 15 and 149 MHz curves, but the two curves are essentially parallel. The 1 MHz and 15 MHz curves converge at the low moisture end, but the 1 MHz curve has an upward bend at about 13 % moisture.

    Since the 1 MHz and 15 MHz curves are superimposed at the low-moisture end, there can be no appreciable dielectric relaxation occurring in that frequency range for corn below 13 % moisture. (Dielectric relaxation between those two frequencies would cause an offset and/or slope difference between the curves at the low moisture end.) On the other hand, the offset between the essentially parallel 15 MHz and 149 MHz curves suggests that there is dielectric relaxation occurring in this frequency region—but that the relaxation is not specific to the tightly bound water assumed to constitute the low-moisture fraction. The dielectric constant curves certainly do not behave as if there were a well-defined relaxation associated with a specific "bound" water fraction. The relatively close agreement between the simulation and the measured dielectric constants at the two higher frequencies suggests that the dielectric constant of all of the water in grain is close to that of bulk (pure) water.

From figure 14, it is apparent that a moisture meter operating at 1 MHz would see a much higher sensitivity to moisture (change in dielectric constant per % moisture) than one operating at either of the higher frequencies. This higher sensitivity and the fact that electronic design and manufacturing are much easier at lower frequencies would seem to make low frequencies preferable for grain moisture meters. However, figure 14 provides a caution about using low frequencies for moisture measurement. The rapid rise in dielectric constant (shown in figure 14) above 13 % moisture at 1 MHz cannot be due to reorientation of water molecules because the simulation establishes an upper bound on the polarization contribution from water dipoles. Something else is causing that increased sensitivity.
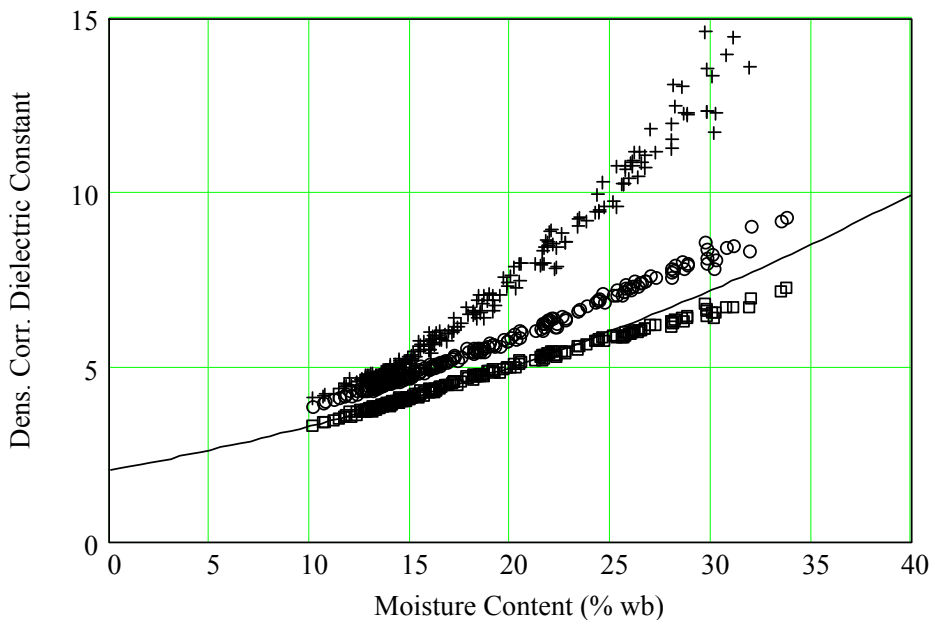
Figure 14. Density-corrected dielectric constant for yellow-dent corn at 1 MHz (+), 15 MHz (o), and 149 MHz (Î) compared to mathematical simulation based on mixture formulas (solid line).

**Grain Dielectric Behavior in the
Kilohertz to Low-Megahertz Range**

The wide frequency range data available from the AT-4294A system provided

further insight into the dielectric behavior in the low megahertz region by simultaneously

showing how the dielectric constant behaves at much lower frequencies as well. Figure

15 shows the dielectric constant for four Durum wheat samples of different moisture

contents. Figure 16 shows dielectric loss values for the same four samples. The spacing of

the dielectric constant curves at different frequencies in figure 15 shows that the

relationship between dielectric constant and moisture content is more nearly linear at

higher frequencies.
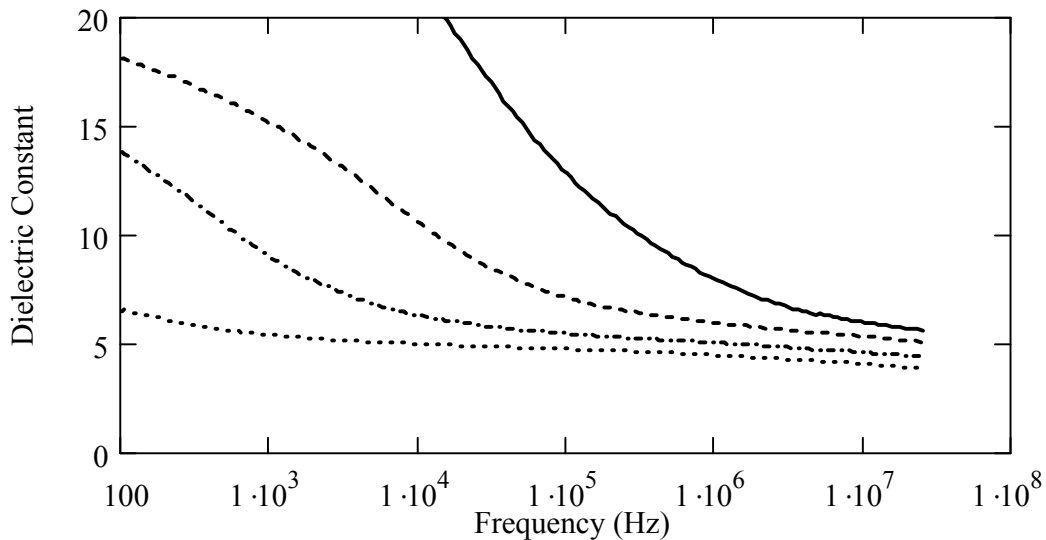
Figure 15. Dielectric constant for Durum wheat at four moisture levels:
8.5 % (dot), 12.2 % (dash-dot), 15.5 % (dash), and 20.8 % (solid).
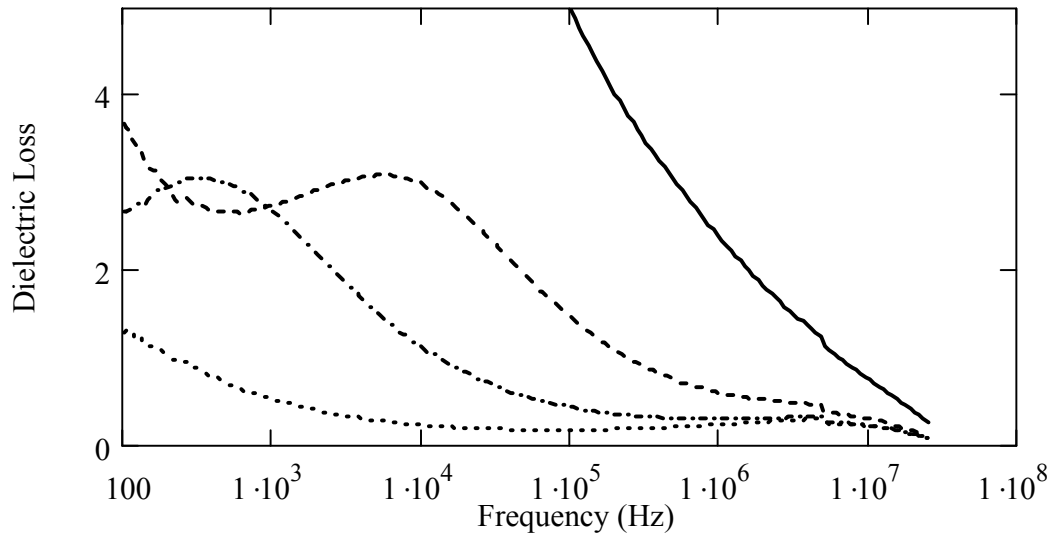
Figure 16. Dielectric loss for Durum wheat at four moisture levels:
8.5 % (dot), 12.2 % (dash-dot), 15.5 % (dash), and 20.8 % (solid).

Figure 16 shows a huge loss peak that moves to higher frequencies but does not

change appreciably in amplitude as the moisture content increases from 12.2 % to 15.5 %

moisture. A comparison of figures 15 and 16 reveals that the frequency of the loss peak

corresponds to the frequency where the slope of the corresponding dielectric constant

curve is most negative (as is expected for a relaxation mechanism). This large loss peak

and the attendant enhancement of the dielectric constant appear to be due to a Maxwell-

Wagner (conducting inclusion) relaxation mechanism because of the moisture dependence

of the relaxation frequency.[11] The conductivity of the inclusion would be expected to

increase with moisture content and to thereby shorten the (equivalent resistor-capacitor)

time constant of the relaxation.

The dielectric loss curve for the 15.5 % moisture sample in figure 16 has a "shoulder" between 100 Hz and 1 kHz that could be due to either a second Maxwell-Wagner relaxation or electrode polarization. The dielectric loss curve for the 20.8% sample continues upward monotonically (off scale) to a value of 170 at 100 Hz. The dielectric constant for the highest moisture sample also soars at low frequencies (to 86 at 100 Hz). This is certainly due to electrode polarization. There is no hint of a shoulder in the loss curve for the 20.8 % sample. Apparently the increased conductivity of the barriers between the conducting inclusions has "shorted out" the space charge regions in the conducting inclusions.

Figure 17 displays similar dielectric loss curves for low, medium, and high-moisture sunflower seed samples. Again, Maxwell-Wagner and electrode polarization effects are evident. In this case, the electrode polarization effect has not completely overwhelmed the Maxwell-Wagner effect for the high-moisture sample, so a shoulder is visible on the curve. The elevated loss due to the electrode polarization effect is evident well above 10 MHz.
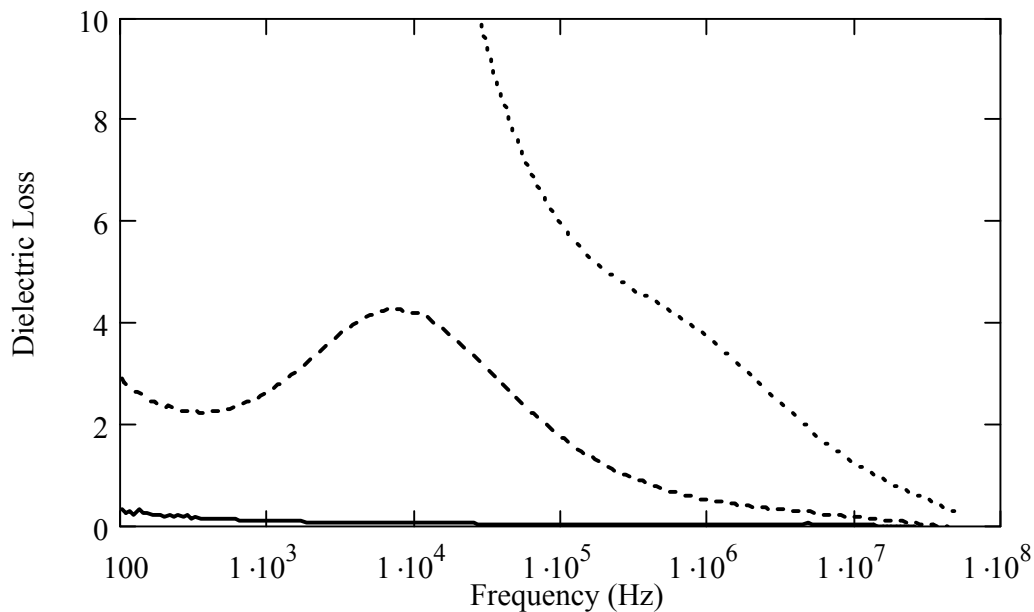
Figure 17. Dielectric loss for sunflower seeds at three moisture levels:
4 % (solid), 9 % (dash), and 14 % (dot).

Figures 18 and 19 show dielectric constants and loss for 14 % moisture sunflower seeds over the range of 100 Hz to 250 MHz. These data were collected with three different systems. Agreement between the systems is good—especially for the dielectric constant. The electrode polarization effect and the shoulder caused by the Maxwell-Wagner effects are visible. Both decrease to very low levels by about 80 MHz. The dielectric constant decreases slowly above 10 MHz.
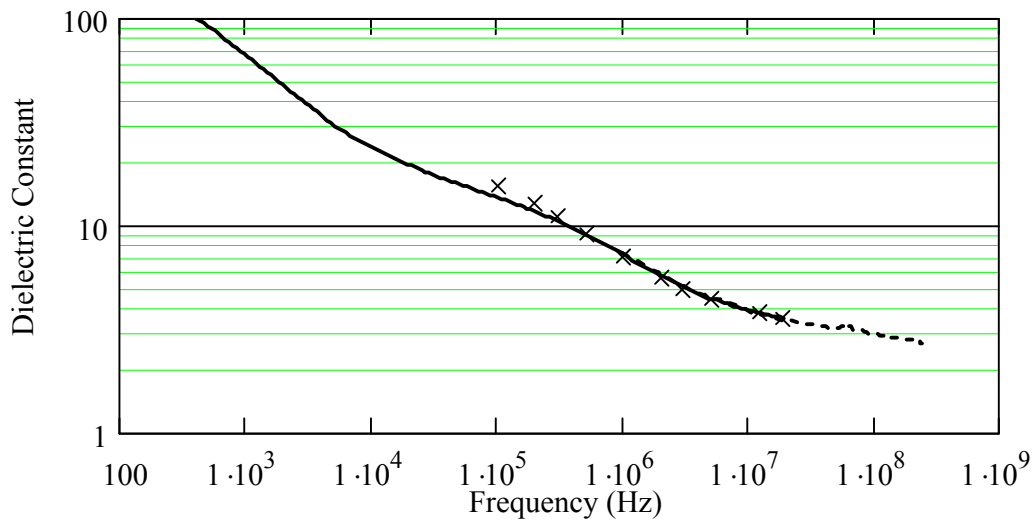
Figure 18. Dielectric constant for sunflower seeds at 14 % moisture measured with three instruments: HP-4294 (solid), HP-4291A (dash), and HP-4285A (X).
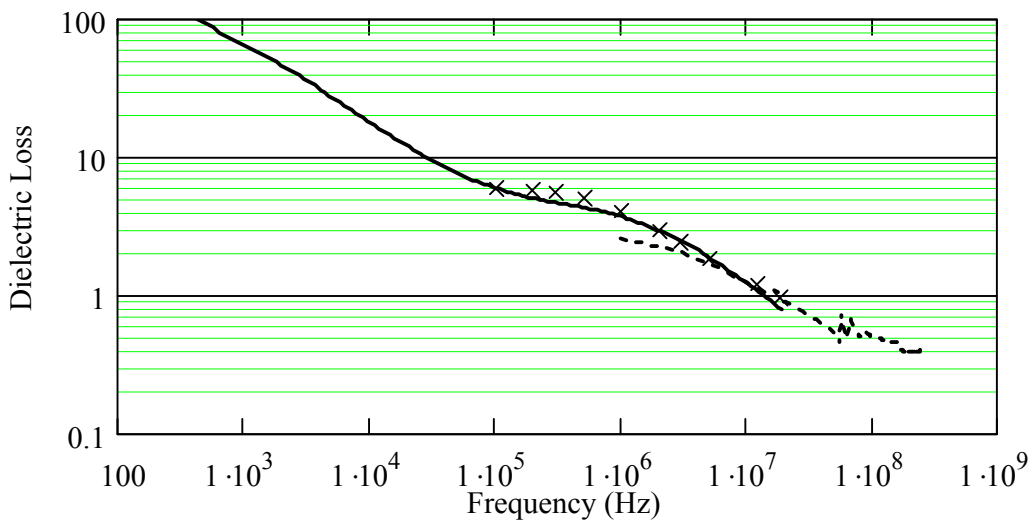
Figure 19. Dielectric loss for sunflower seeds at 14% moisture measured with three instruments: HP-4294 (solid), HP-4291A (dash), and HP-4285A (X).

Figure 20 shows the dielectric constant (upper plot) and dielectric loss (lower plot) for 19.6 % moisture soybeans, 37 % moisture yellow-dent corn, and 21 % and 35 % moisture sunflower seeds. These were some of the highest moisture samples tested during this four-year project.

From a moisture meter design standpoint, the loss tangent (the ratio of the dielectric loss to the dielectric constant) is particularly important. Sensing circuits based on resonant LC circuits (with a capacitive test cell as part of the tank circuit) need high circuit Q (inverse of loss tangent) to yield precise results. The resonant frequency of an LCR circuit is affected by the resistance (loss) component. Also, if the loss tangent is low, the magnitude of the complex dielectric constant is essentially equal to the real part (dielectric constant) alone. This would permit circuitry that is sensitive to the magnitude of the complex dielectric constant (sensitive to admittance, for instance) to yield virtually the same results as circuitry that could sense the dielectric constant independent of the dielectric loss. Thus, making dielectric measurements in a frequency range where the loss tangent is low should allow more flexibility in the sensing technology.

Figure 21 shows the loss tangent for the same four high-moisture samples whose dielectric constants and loss are shown in figure 20. This plot shows that dielectric measurements at frequencies above 100 MHz offer much lower loss tangent values than measurements made between 1 and 20 MHz—the region used by commercial grain moisture meters.
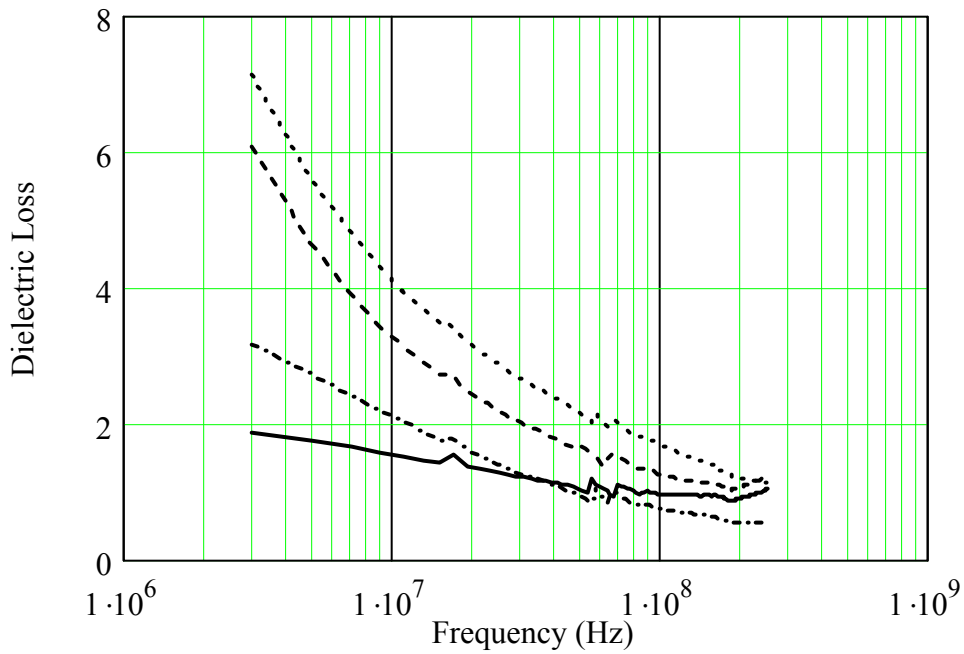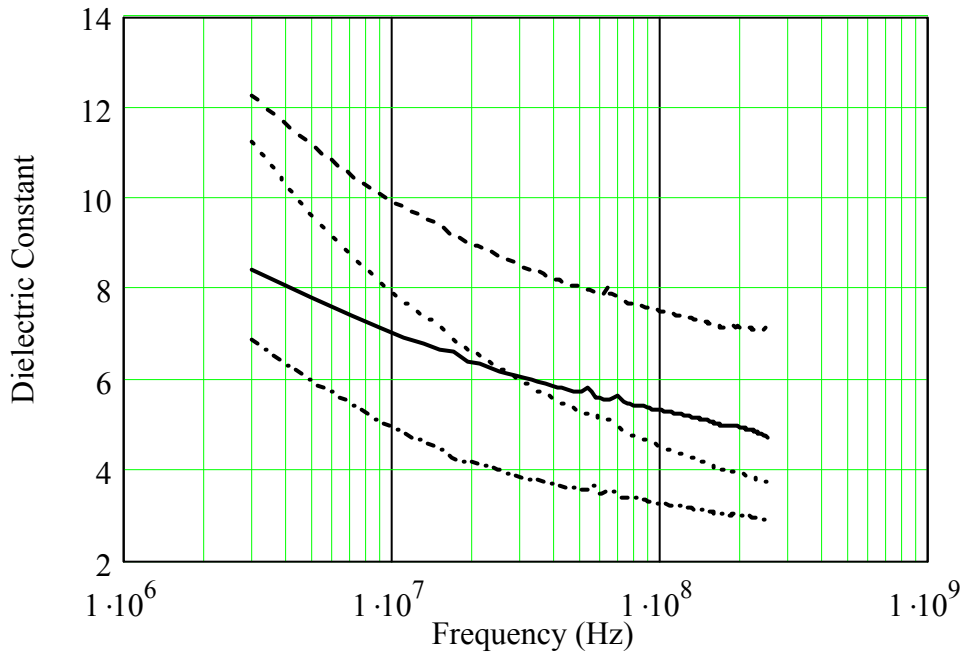
Figure 20. Dielectric constants and loss for high-moisture samples: 19.4 % soybeans
(solid), 37 % yellow-dent corn (dash), 21 % sunflower seeds (dash-dot),
and 35 % sunflower seeds (dot).
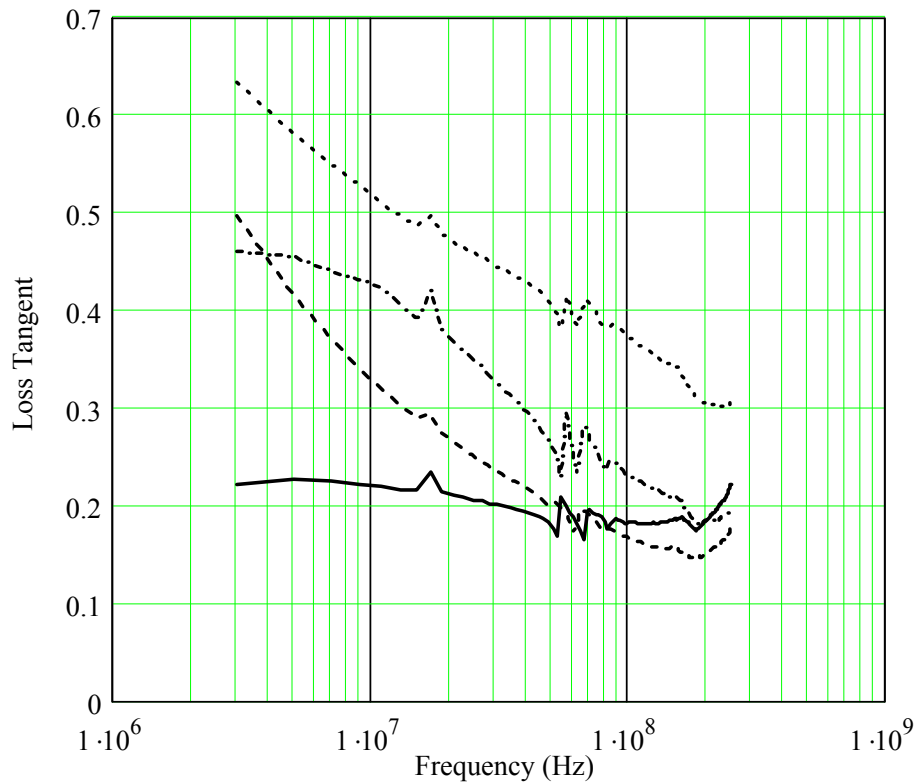
Figure 21. Loss tangent values for high-moisture samples: 19.4 % soybeans (solid),
37 % yellow-dent corn (dash), 21 % sunflower seeds (dash-dot),
and 35 % sunflower seeds (dot).

The high loss tangent values for high-moisture sunflower seeds in the 1 to 20 MHz

region partially explains the great difficulties that moisture measurement specialists have

experienced in testing high-moisture sunflower seeds accurately. The distribution of

moisture within the individual sunflower seeds is another part of the problem, as shown

below.

Moisture Rebound

Grain moisture meters are calibrated to agree (on the average) with the results for the air oven method for grain samples that are at moisture equilibrium—that have been in sealed containers for hours or days prior to the test and have achieved a stable moisture distribution within the kernels. When moist grain undergoes rapid partial drying, moisture gradients are established in the kernels. Modeling a test cell full of grain as a massively interconnected network of lossy capacitors would suggest that drying the outside of the kernel (essentially introducing a capacitance-limiting series capacitor in the model) would necessarily reduce the overall capacitance (or measured dielectric constant). It would also be expected that when a uniform moisture distribution is restored at the new lower moisture content, the capacitance would increase slightly as compared to the nonuniform condition.

If the dielectric constant of the grain in its "normal" state includes a significant contribution from electrode polarization or Maxwell-Wagner effects, disturbing the distribution of water in the grain can cause much more dramatic effects. Figures 17-21 show that both electrode polarization and Maxwell-Wagner relaxations contribute to the measured dielectric constant of high-moisture sunflower seeds in the 1 to 20 MHz frequency range.

Figure 22 shows the results of an experiment that was performed to assess the magnitude and frequency dependence of "moisture rebound" effects in high-moisture sunflower seeds. The dielectric characteristics of a high-moisture sunflower seed sample

(28.0 % moisture) were measured at the start of the test. The sample was then spread out in an open pan in the laboratory and a fan was directed at it for half an hour. The sample was tested again immediately after the drying period. After this test, the sample was sealed and stored for 24 hours under refrigeration (to prevent spoilage). Then the sample was removed from cold storage, allowed to warm to room temperature, and retested. The actual moisture was reduced by 3.6 % moisture during the half hour of room-temperature drying (as determined by air oven measurements). A commercial dielectric moisture meter included in the experiment read 30.3 % before drying, 19.2 % immediately after drying, and 26.8 % after re-equilibration. This "moisture rebound" effect makes existing grain moisture meters useless for high-moisture sunflower seeds. The effect is not as extreme, but still significant, at lower moisture levels.
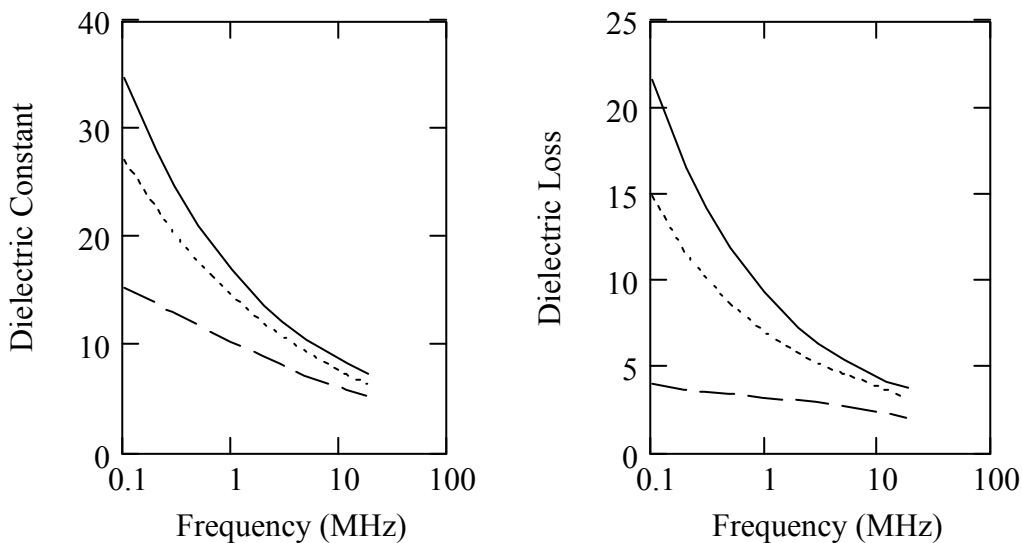
Figure 22. Moisture rebound effect in high-moisture sunflower seeds. Dielectric constant and loss before drying (solid), after one-half hour room temperature forced-air drying (dash), and after 24 hours equilibration (dot).

Figure 22 shows why the moisture rebound was so extreme. The dielectric loss curve provides the critical clue. The original sample exhibited large electrode polarization effects (as evidenced by the steep sloping loss curve). After drying, the dielectric loss curve is almost level. The Maxwell-Wagner relaxation (similar to that in figure 17) is still contributing to the dielectric characteristics, but the electrode polarization effects have been shifted to far lower frequencies by decreasing the conductivity of the sunflower hulls. After the sample re-equilibrated, the electrode polarization effects reappeared. At higher frequencies (where the electrode polarization effects were less significant) the moisture rebound effect on the dielectric constant measurement was reduced. A similar study of moisture rebound in soybeans showed that the use of higher frequencies also reduces such errors in soybean moisture measurements.

These results reinforce statements in the literature that the distribution of water in the grain kernels can be a major cause of calibration instability.[47] This research adds to the current understanding by showing that the moisture rebound effect is as large as it is because of the disruption of the "normal" Maxwell-Wagner and electrode polarization effects that are present when grain is at equilibrium. Furthermore, this research shows that moisture rebound effects should be dramatically reduced if the dielectric measurements were made at frequencies above 100 MHz where the electrode polarization and Maxwell-Wagner effects are minimal.

Sample Origin Effects

Analysis of data for Medium Grain Rough rice (MGRR) revealed another way in which conductivity effects contribute to calibration instability. Moisture meter calibrations for rough (unmilled) rice have required frequent adjustments to keep predicted results agreeing (on the average) with the air oven method. At times, significant differences have been observed for rice grown in different areas of the United States. During the 1999 crop year, a large difference was observed between MGRR grown in California and that grown in Arkansas. For MGRR above about 12 % moisture, moisture results for a commercial RF dielectric moisture meter were nearly 1 % moisture higher than the air oven for California samples and nearly 1 % lower than the air oven for Arkansas samples.

There were no apparent physical differences between the samples, although the samples were known to be of different varieties. Measurement of the oil contents of the samples did not reveal a location difference. Unusual growing conditions in California during rice harvest in 1999 might have contributed somehow to differences in dielectric characteristics.

Analysis of dielectric characteristics from 0.1 to 18.5 MHz revealed the cause of the problem. Figures 23-25 are plots of density-corrected (see pages 83-88) dielectric constant and loss for MGRR at 0.1 MHz, 2 MHz, and 18.5 MHz, respectively. At each frequency, polynomial regression was used to create a moisture prediction calibration. The calibration curves are superimposed on the dielectric constant data. Samples whose dielectric constant values lie above the calibration curve would predict moisture contents

higher than the air oven, and samples whose dielectric constant values lie below the calibration curve would show negative moisture errors.
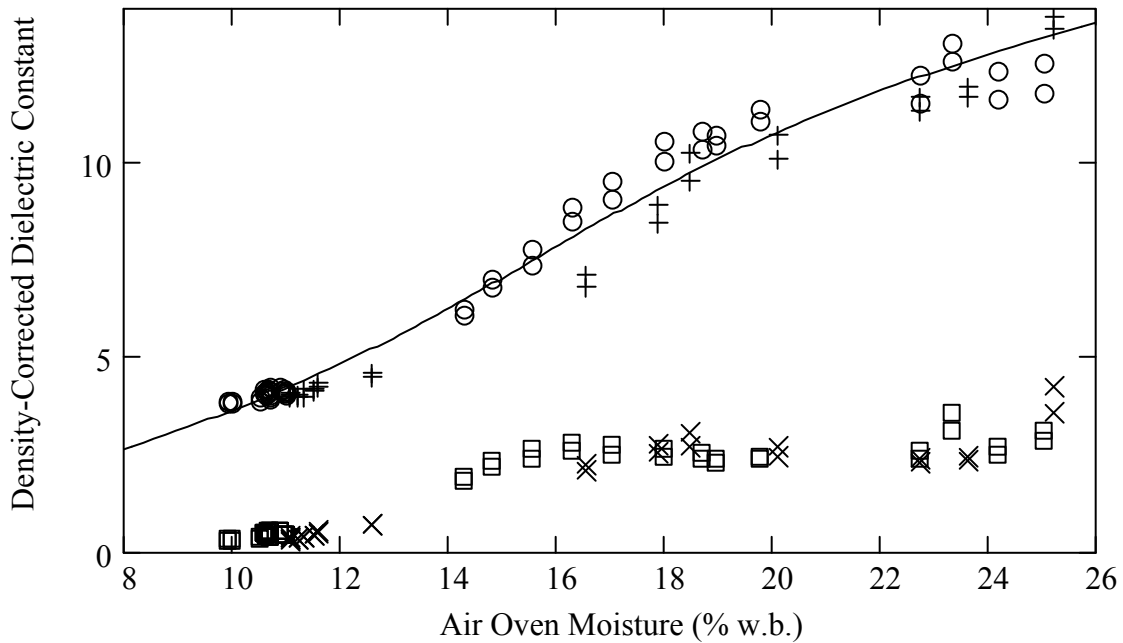
Figure 23. Medium Grain Rough rice density-corrected dielectric constant and loss values at 0.1 MHz for samples from California (o) and (I) and from Arkansas (+) and (x).

The dielectric constant data are lower in magnitude and show considerably less scatter at 18.5 MHz than at 0.1 MHz. The relationship between dielectric constant and moisture at 0.1 MHz seems nearly flat below 13 % moisture. The slope of the dielectric constant versus moisture curve increases above 13 % for all three measurement frequencies—but much less dramatically for the two higher frequencies.
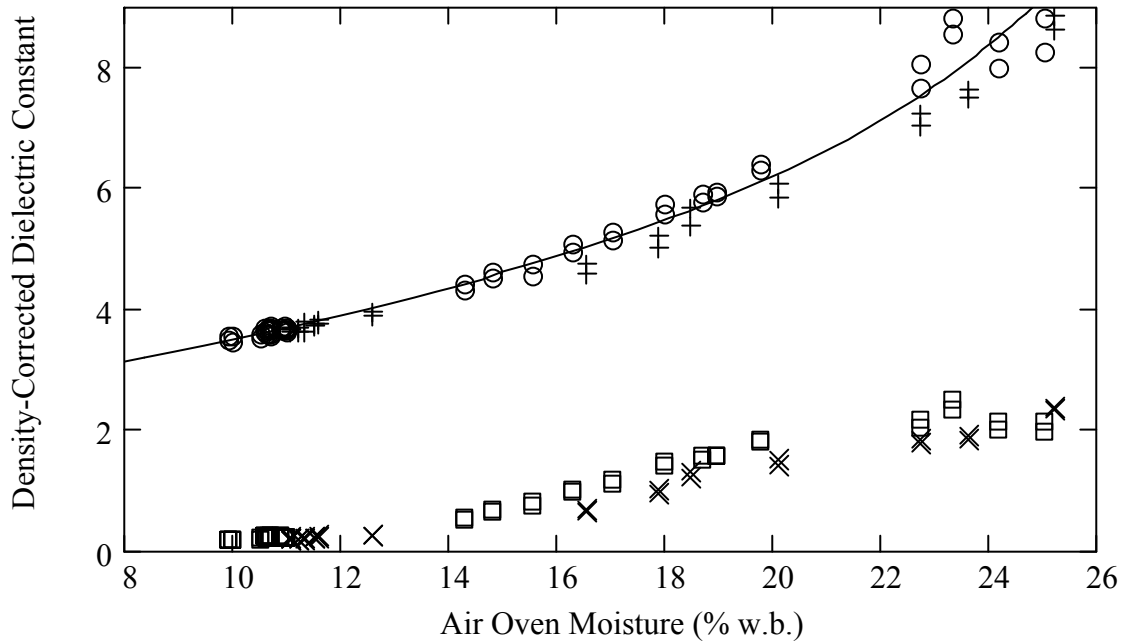
Figure 24. Medium Grain Rough rice density-corrected dielectric constant and loss values at 2 MHz for samples from California (o) and (ĺ) and from Arkansas (+) and (x).

As in the moisture rebound study, the dielectric loss data supplied the critical clue. A distinct Maxwell-Wagner relaxation peak (centered at about 16 % moisture at 0.1 MHz) moved to higher and higher moisture contents at higher measurement frequencies. This was observed when figure 23 was animated by substituting data for different measurement frequencies from 0.1 to 18.5 MHz in sequential frames.

The two different sample populations (those with positive moisture errors and those with negative errors) also showed up in the dielectric loss data. Their behavior with increasing frequency indicated that the difference between the populations was a difference in conductivity associated with the Maxwell-Wagner relaxation.
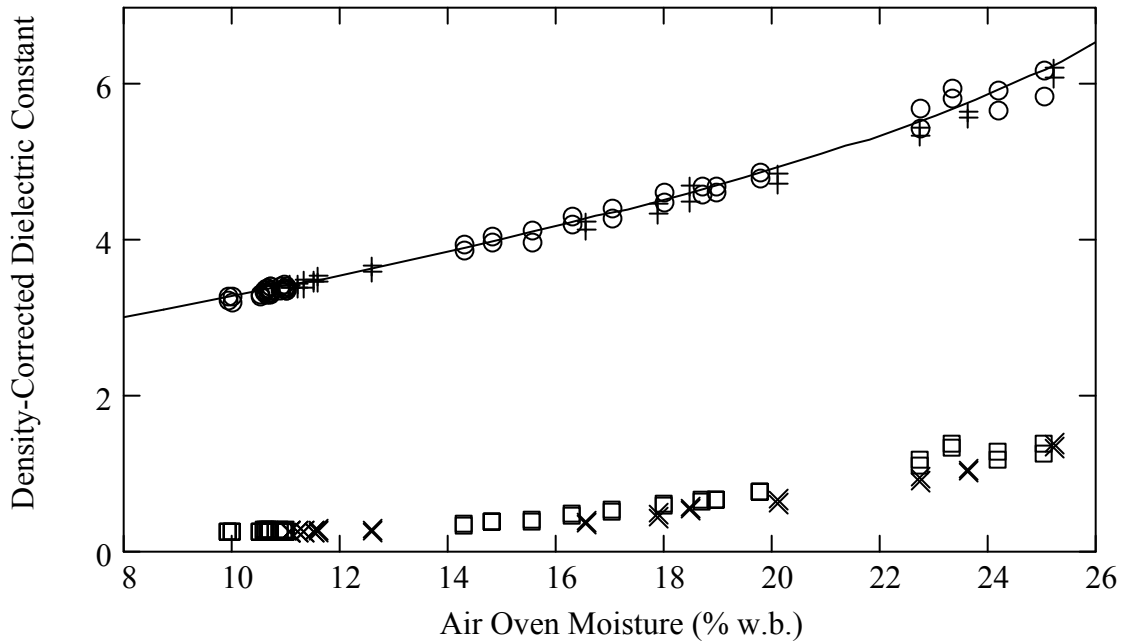
Figure 25. Medium Grain Rough rice density-corrected dielectric constant and loss values at 18.5 MHz for samples from California (o) and (□) and from Arkansas (+) and (x).

The loss peak for the Arkansas samples was offset by about +2 % moisture, so the dielectric loss and dielectric constants for those samples were significantly lower. At 18.5 MHz, the loss peaks for both sample populations had moved above 20 % moisture and the scatter in the dielectric constant and loss values were greatly reduced in the 14 % to 20 % moisture region where the problem was originally observed. However, the difference in the Maxwell-Wagner relaxations still appeared to be causing significant errors for samples above 20 % moisture.

The conclusions drawn from this study complement those from the moisture rebound study. If a moisture meter uses a measurement frequency where Maxwell-Wagner

effects contribute significantly to the dielectric measurements, any differences in grain characteristics that disturb the Maxwell-Wagner relaxation frequencies will cause significant differences in the dielectric measurements that may masquerade as "location," "crop-year," or "variety" effects that make grain moisture meter calibrations appear unstable. This strongly suggests the need to move dielectric moisture measurement to frequencies well above 20 MHz. Conductivity effects (electrode polarization and Maxwell-Wagner) definitely will cause calibration instability in the 1 to 20 MHz range. Figures 20 and 21 suggest that measurements at about 150 MHz should be minimally affected by Maxwell-Wagner and electrode polarization effects at the highest grain moisture levels likely to be encountered. There is no need to move to microwave frequencies to avoid conductivity effects in grain moisture measurement. The question of the relative involvement of bound and free water in RF dielectric measurements is not yet resolved, however.

Bound and Free Water Temperature Characteristics

Hasted[11] suggested that the behavior of the dielectric constant at the freezing point of water is a useful diagnostic for determining whether absorbed water is free or bound. The dielectric constant of free water measured at RF or microwave frequencies undergoes a dramatic fall at 0 °C whereas bound water shows only a monotonic change with temperature. This drop in dielectric constant is caused by the kilohertz relaxation frequency of ice as compared to the gigahertz relaxation frequency of pure water. Figure 26 shows the variation of dielectric constant with temperature for medium and high-

72

moisture corn and soybeans. None of the curves show the step-discontinuity that would be expected if free water were present in significant quantities. For the two medium moisture samples, the dielectric constant versus temperature curve is quite linear through the freezing point. The 27 % moisture soybean sample shows a slight slope change at the freezing point, and the 30 % moisture corn sample has a more dramatic slope change. These curves are typical of the tests performed for several grain types in the 0.1 to 18.5 MHz frequency range. The slope changes at the freezing point for high-moisture samples may be related to the temperature dependence of Maxwell-Wagner and electrode polarization effects.
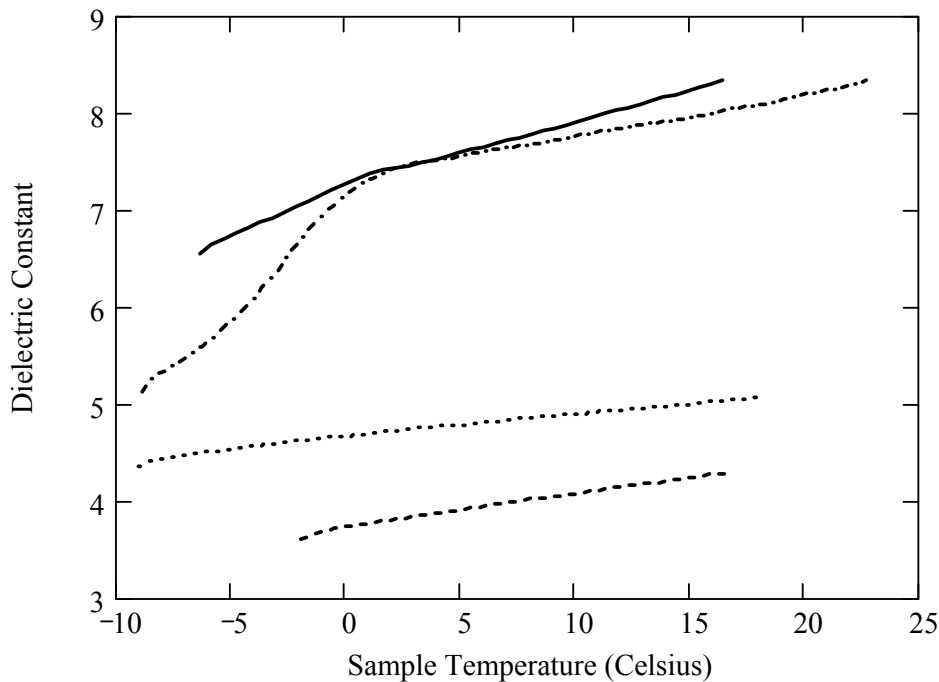
Figure 26. Relationships between dielectric constant at 18.5 MHz and temperature for yellow-dent corn at 30 % moisture (dash-dot) and 17 % moisture (dot) and for soybeans at 27 % moisture (solid) and 13 % moisture (dash).

Figure 27 shows temperature test results for four soybean samples at 149 MHz. These data also indicate a generally linear relationship between dielectric constant and temperature that is continuous at the freezing point. It was concluded from these temperature studies (and from previous unpublished research) that all of the water in grain, at least up to the moisture levels represented in these tests, must be bound water—associated with grain constituents through multiple levels of hydrogen bonds that are energetically advantageous relative to the free (bulk water) state.
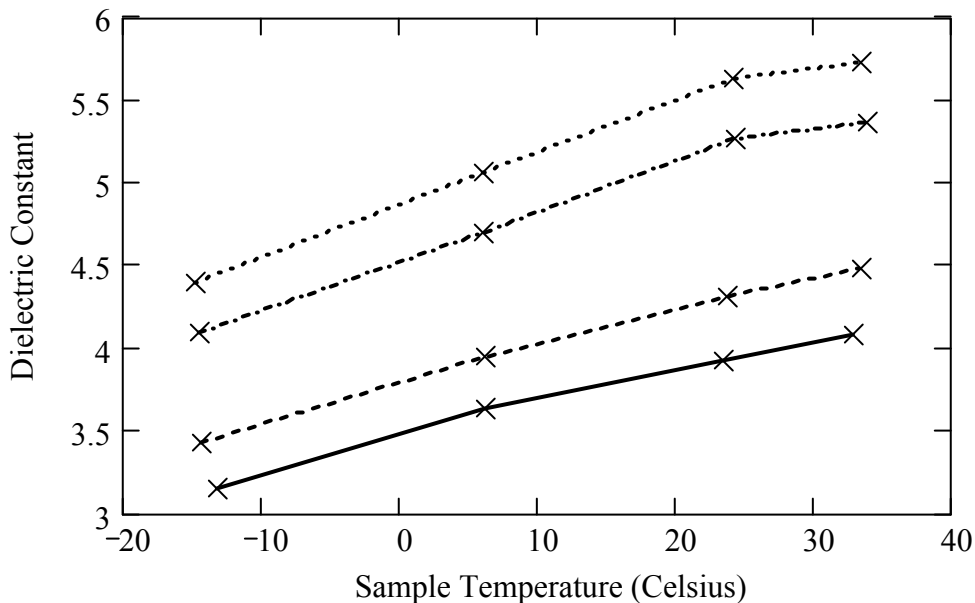
Figure 27. Relationships between dielectric constant at 149 MHz and temperature for soybeans at 12.6 % moisture (solid), 14.3 % moisture (dash), 17.6 % moisture (dash-dot), and 19.4 % moisture (dot).

The observed continuity of the dielectric constant through the freezing point suggests that it is possible to use RF dielectric-type grain moisture meters to test grain below 0 °C—with the possible exception of very moist grain. More research is needed to

74

explore the temperature behavior over the full range of moisture contents and to determine the moisture level at which free water contributes significantly to the dielectric characteristics.

Conductivity in Grain

The apparent absence of free water in grain raises a troubling question. If there is no free water, and if free water is necessary to support ionic conductivity (presumably motion of dissolved salts), what is the conductivity mechanism that causes the problematic Maxwell-Wagner and electrode polarization relaxations? Furthermore, figure 16 shows conductivity effects present in Durum wheat at 8.5 % moisture. Is ionic (salt) conductivity a believable explanation at such moisture levels? Although motion of dissolved salts has been tacitly assumed by many authors, there has apparently never been any research to confirm its role in grain dielectric behavior.[81] In the course of this research, a body of literature was discovered that gives a new interpretation to conductivity in grain—percolating protonic conductivity.

Percolating Protonic Conductivity

Dewey[82] briefly reviewed proton transport around hydrated protein macromolecules as an example of a two-dimensional percolation phenomenon. In a series of papers,[83-85] Careri et al proved the existence of protonic transport along continuous chains of hydrogen-bonded water on the surface of protein macromolecules. Rupley et al[85] used deuterated water to confirm that protons serve as the charge carriers. Fractal

geometry explains the observed relationship between conductivity and hydration level. If the hydration level (dry basis) needed to fully populate the hydrogen bonding sites on a protein molecule is h_m, there is a critical hydration level h_c below which protonic percolation around the molecule through continuous chains of adjacent hydrogen bonds cannot occur. The critical threshold $\theta_c = \dfrac{h_c}{h_m}$ is known from percolation theory to be equal to 0.16 ± 0.02 for three-dimensional networks and equal to 0.45 ± 0.03 for two-dimensional structures. From the known number of binding sites on the proteins in the study and the observed percolation threshold, they determined that the percolating structure was two-dimensional. The behavior of the conductivity $\sigma(h)$ at and near the critical hydration level is expressed as

$$\sigma(h) = \sigma(h_c) + K(h - h_c)^t \tag{13}$$

where $\sigma(h_c)$ is the conductivity at the critical hydration level (due to other mechanisms), K is a constant, and t is the critical exponent for the dc conductivity. The critical exponent was estimated to be 1.23, which is consistent with the theoretical range of 1.1 to 1.3 for surface percolation. Careri et al[84] anticipated that this conductivity mechanism is generally applicable to hydrated protein matrices because of the structural similarities among proteins and the broad applicability of fractal mathematics. Pissis and Anagnostopoulou-Konsta[86] applied the method of thermally stimulated depolarization currents to study relaxation processes in the proteins used for Careri's tests and agreed

with Careri's assessment that percolating protonic conduction was responsible for the observed effects.

Colomban[87] provided theoretical background for proton conduction, including proton transfer processes.[88] He gave an expression for the temperature dependence of ionic conductivity in general as

$$\sigma(T) = \frac{\sigma_0}{T} e^{\frac{-E_a}{kT}} \tag{14}$$

where σ_0 is the conductivity at a reference temperature and E_a is the activation energy for conduction.

The temperature dependence for percolating protonic conductivity may be estimated by setting K in equation 13 equal to $\sigma(T)$ from equation 14 to give

$$\sigma(h,T) = \sigma(h_c) + \frac{\sigma_0}{T} e^{\frac{-E_a}{kT}} (h - h_c)^t \tag{15}$$

Conductivity Simulations

A simulation program (appendix D) was developed with Mathcad[71] to compare the qualitative behavior of this function to actual grain measurements. Figure 28 shows the simulation results for dielectric constant and loss at two measurement frequencies for an h_c of 4.5 % moisture (0.45 times the assumed monolayer moisture limit of 10 % moisture). A threshold is apparent for the lower frequency curves (but not for the upper frequency) for both the dielectric constant and dielectric loss. Figure 28 is qualitatively similar to actual grain measurements shown in figures 14, 23, 24, and 25.
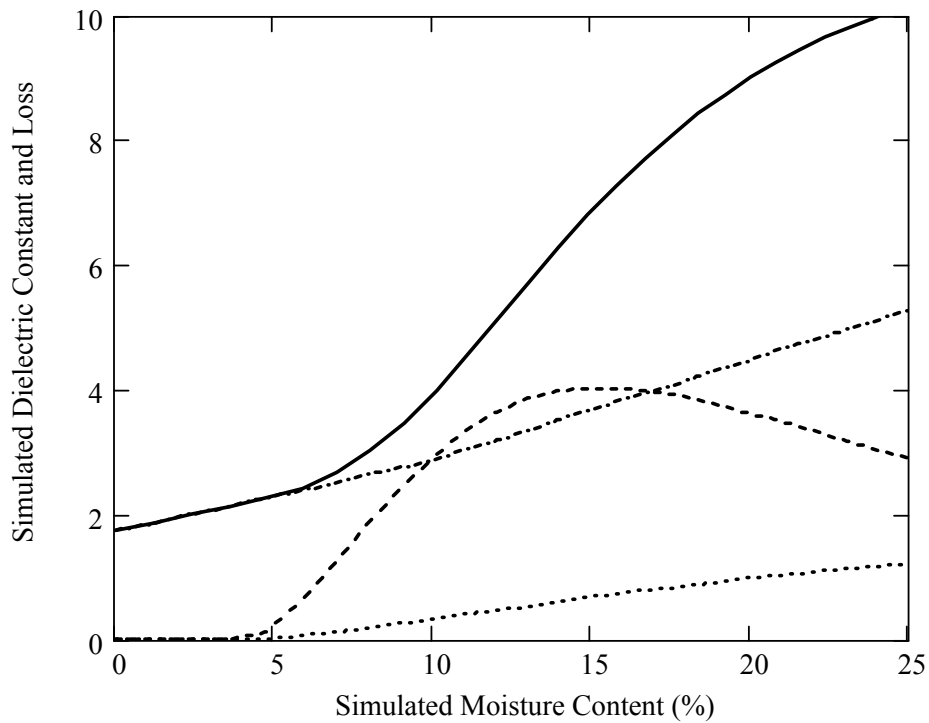
Figure 28. Simulated Maxwell-Wagner, electrode polarization, and monolayer
water threshold effects. Dielectric constant (solid and dash-dot) and
dielectric loss (dash and dot) at 10 kHz and 100 kHz, respectively.

Figure 29 predicts the change in dielectric constant and loss versus frequency for a

change in sample moisture content. There is good qualitative agreement with the

measured data for Durum wheat shown in figures 15 and 16.
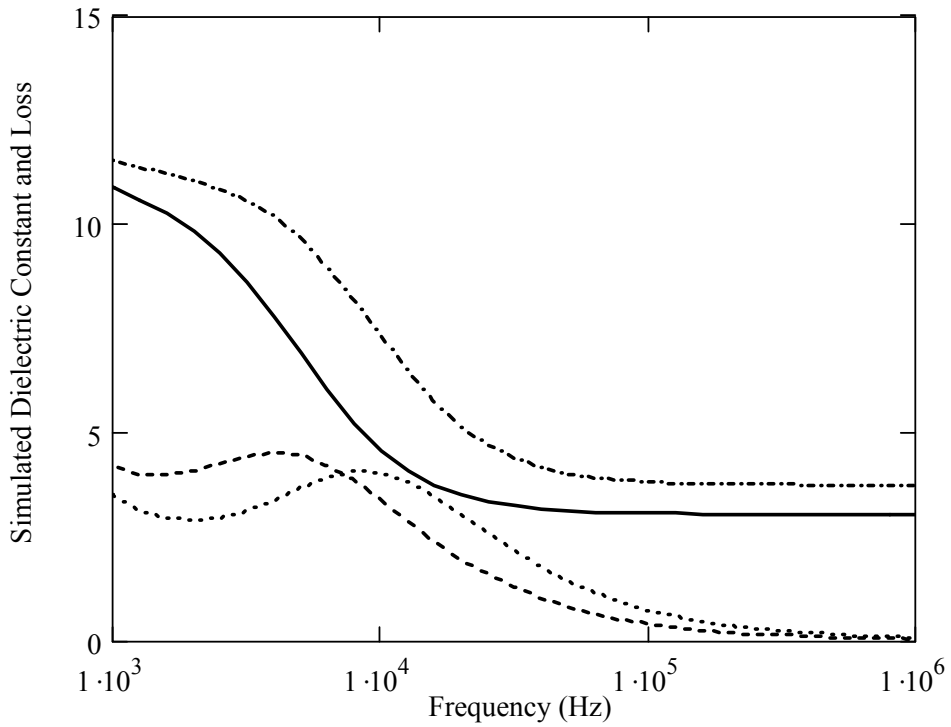
Figure 29. Moisture relationships for simulated Maxwell-Wagner and electrode
polarization effects. Dielectric constant for 10 % (solid) and 15 % (dash-dot)
and dielectric loss for 10 % (dash) and 15 % (dot).

Figure 30 illustrates temperature behavior of Maxwell-Wagner effects in Durum

wheat and figure 31 shows the results of simulations of the temperature behavior of

Maxwell-Wagner effects in grain. Again, the qualitative agreement is encouraging.
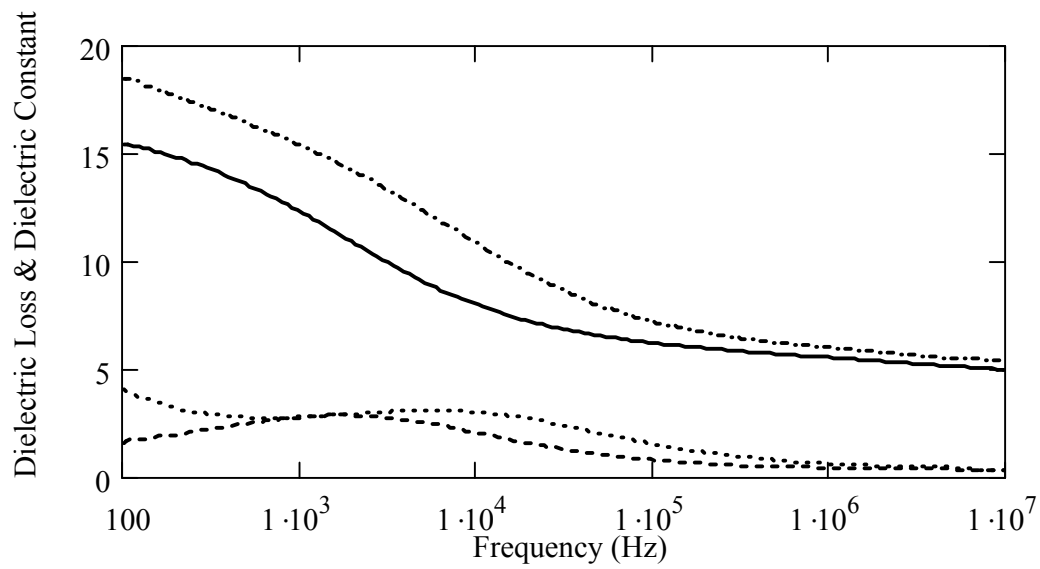
Figure 30. Dielectric constant and loss for 15.5 % moisture Durum wheat
at 8 °C (solid and dash) and 21 °C (dash-dot and dot).
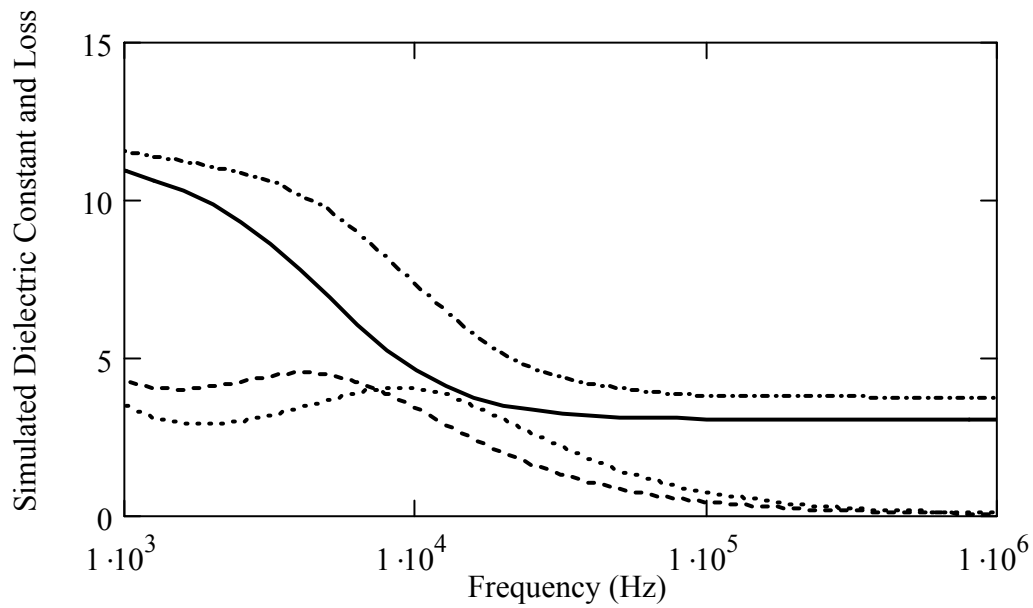
Figure 31. Simulated Maxwell-Wagner and electrode polarization effects.
Dielectric constant at 280 K (solid) and 310 K (dash-dot) and
dielectric loss at 280 K (dash) and 310 K (dot).

Figure 32 shows simulation results for the (logarithm of the) conductivity of grain versus hydration level. The logarithm of the predicted conductivity is approximately linearly related to the simulated moisture content. This is consistent with the reported relationship between conductance and moisture used to measure moisture with conductance-type moisture meters.[89]
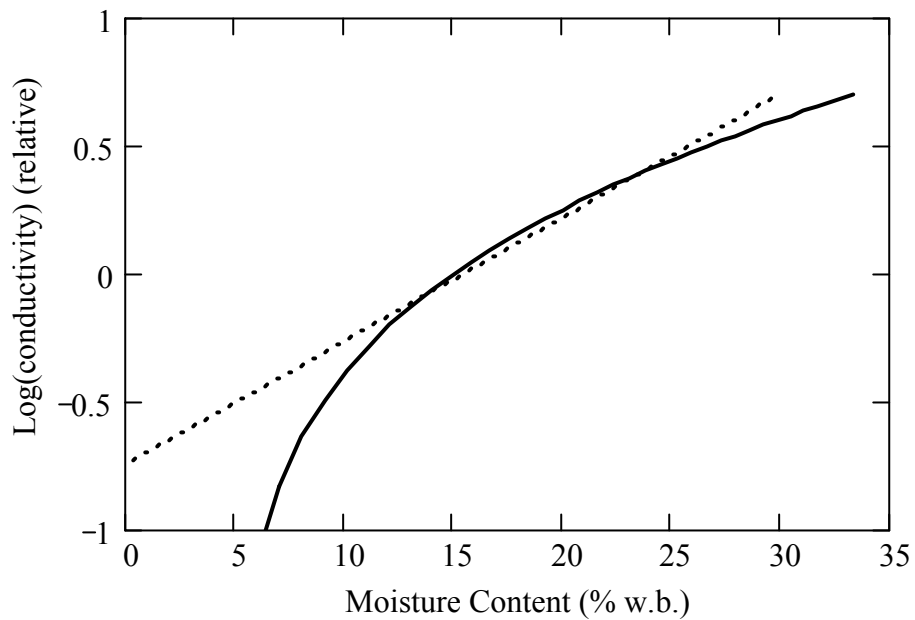
Figure 32. Logarithm of simulated conductivity versus moisture content (solid)
for the percolating protonic conductivity model with linear fit (dot)
over 10 to 25 % moisture range.

These simulations certainly do not prove that conductivity in grain is due to percolating protonic conductivity. Ionic conductivity based on dissolved salts might behave similarly. However, these simulations suggest that the relationships between dielectric characteristics, hydration level, temperature, and frequency that are predicted by

percolating protonic conductivity are qualitatively consistent with actual measurements on grain. This hypothesis deserves further study.

Density Correction

The complex dielectric constant is inherently a volume-based parameter, but grain moisture is expressed as the percent of the total grain mass (water and dry material). Assuming an average bulk density for each grain type causes large moisture measurement errors because the bulk density of grain samples within most grain types varies by more than twenty percent of the nominal value. Across grain types, bulk density varies by more than a factor of three times. Thus some means of density correction must be incorporated in a grain moisture meter to achieve good accuracy. Grain moisture meter manufacturers have employed a range of solutions to the problem with varying degrees of success.[49]

This research confirmed Nelson's assessment that equation 10 (described on page 23) is highly effective for estimating the dielectric constant at a second bulk density from the measured dielectric constant at an original bulk density. Hereafter in this document, equation 10 (a restatement of the Landau and Lifshitz, Looyenga equation) will be referred to as the "cube-root density correction."

$$\varepsilon_x = \left[\left(\varepsilon_y^{\frac{1}{3}} - 1 \right) \frac{\rho_x}{\rho_y} + 1 \right]^3 \tag{10}$$

Application of the Cube-Root Density Correction

The strategy used in this current work for density correction was to apply the cube-root density correction to the measured complex dielectric constant for each grain sample to predict what the measured dielectric constant would have been had the sample been expanded or compacted to a standard nominal bulk density prior to the measurement. This brought the dielectric measurements for all samples within a grain type to a common weight basis—the goal for making grain moisture measurements. Figures 33-35 illustrate the effectiveness of this strategy. Figure 33 shows sample weight (contained in the test cell used for the medium frequency tests) versus moisture content for all 1999-crop yellow-dent corn samples.
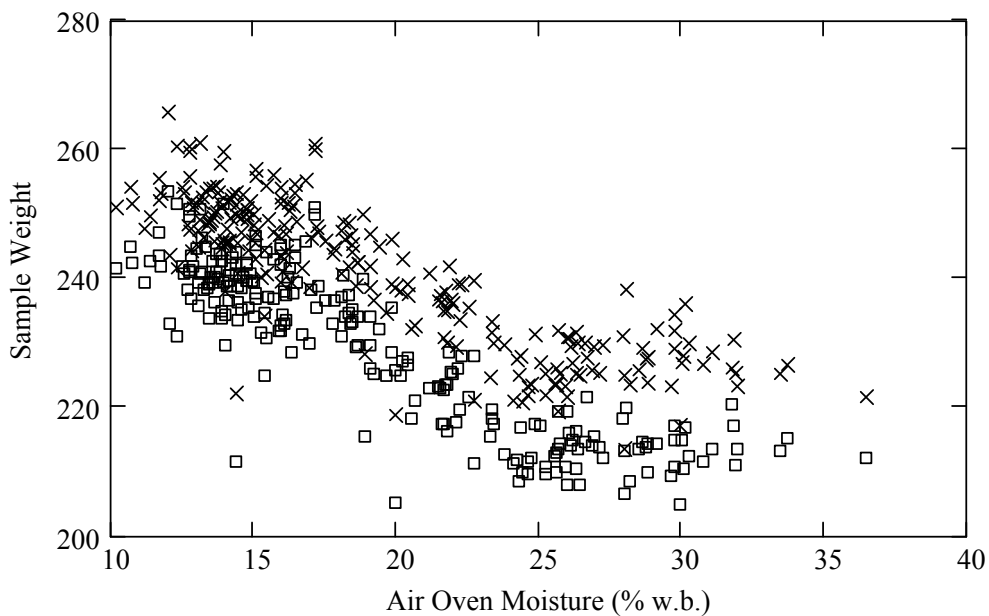
Figure 33. Fixed-volume sample weight versus air oven moisture content for yellow-dent corn with slow (X) and rapid (I) filling techniques.

Three sources of density variations are apparent from the graph. There is a general trend for the density to decrease at higher moistures levels. This is expected because the density of water is less than that of the dry corn kernel. Moisture level contributed a density variation of about twenty percent of the nominal value. For these tests, each sample was measured with two different cell filling methods to enhance the differences in packing density. The filling method caused differences of about five percent of the sample weight. At any given moisture level with either filling method, the density varied by about five percent of the nominal value, presumably due to differences in kernel density and shape.

Figure 34 shows the relationships between dielectric loss (at 18.5 MHz) and moisture content without density correction and with density correction. The difference between the fast and slow filling methods that is readily apparent without density correction virtually disappears (except at very high moisture levels) with density correction. These residual differences are of little concern for moisture measurement because the dielectric loss will be discarded in the moisture measurement algorithm.

Figure 35 shows the effect of the cube-root density correction on dielectric constant measurements for yellow-dent corn. The density correction dramatically reduced the scatter and caused the relationship between dielectric constant and moisture to become almost perfectly linear. Linear regression was used to fit the relationships between moisture content and density-corrected and uncorrected dielectric constants. The magnitude of the improvement achieved is reflected in the standard deviation of differences for the prediction equations. For the uncorrected case, the standard error of

84

calibration was 1.78 % moisture. With density correction, the standard error of calibration

dropped to 0.51 % moisture—an improvement by more than a factor of three.
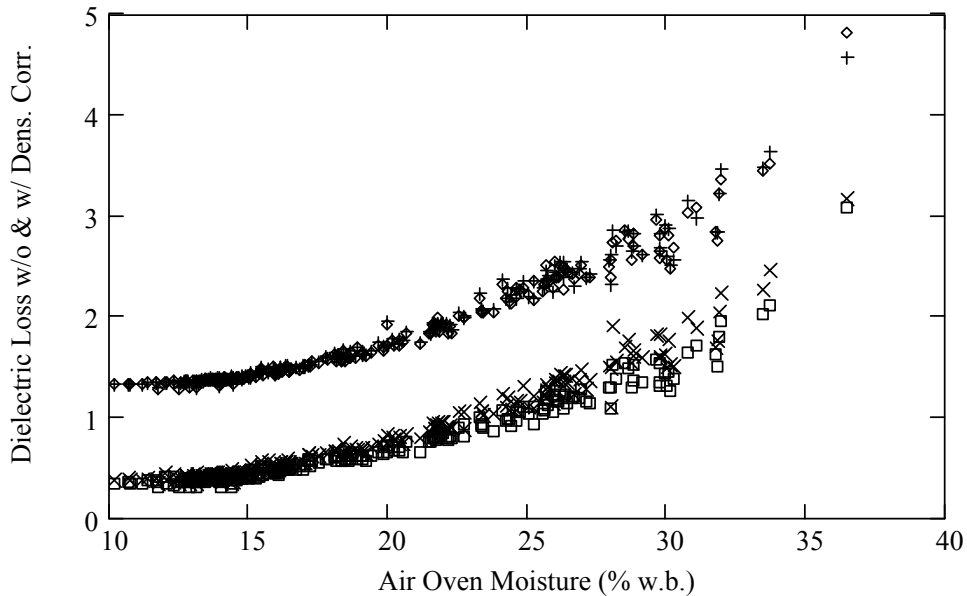
Figure 34. Dielectric loss at 18.5 MHz versus air oven moisture content for yellow-dent
corn. Loss without density correction with slow (x) and fast (í) filling techniques.
Loss with density correction using slow (+) and fast (◊) filling techniques
(offset vertically by one unit for clarity).

The cube-root density correction effectively eliminated errors caused by all three

sources of density variations: moisture level, filling method, and sample-to-sample

variation. The effectiveness demonstrated in figures 33-35 was apparent for each of the

other grain types tested and at all frequencies tested (0.1 to 250 MHz). Other semi-

empirical density correction algorithms were attempted, but those required separate

parameters for each grain type to yield optimum results. Thus, the cube-root density

correction was adopted for development of an improved moisture measurement algorithm.
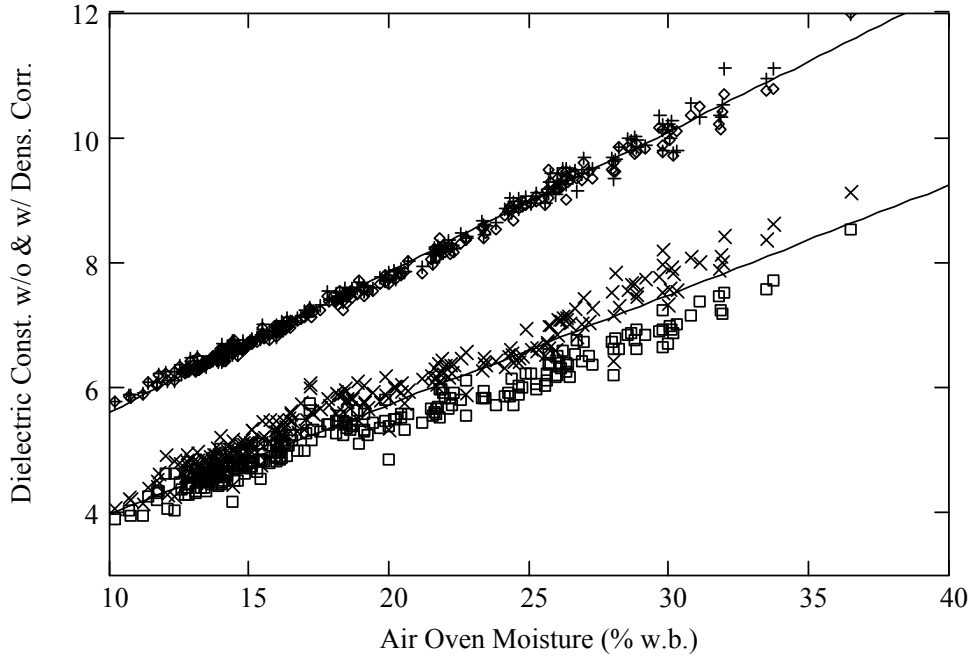
Figure 35. Dielectric constant at 18.5 MHz for yellow-dent corn versus air oven moisture content. Dielectric constant without density correction with slow (×) and fast (|̂) filling techniques. Dielectric constant with density correction with slow (+) and fast (◊) filling techniques (offset vertically by two units for clarity).

The cube-root density correction was used in simulations (such as shown in figure 14) to estimate the dielectric constant of a mixture of moist grain and air. Equation 10 was applied twice to yield equation 16. First, the dielectric constant of the moist solid material was estimated taking pure water and dry solid material as the two components in the mixture. Second, the dielectric constant of the mixture of moist grain and air was calculated to yield

$$\varepsilon_m = \{v_{ms}[\varepsilon_w^{\frac{1}{3}} \frac{M\rho_2}{M(\rho_2-1)+1} + \varepsilon_2^{\frac{1}{3}} \frac{(1-M)}{M(\rho_2-1)+1} - 1] + 1\}^3 \qquad (16)$$

where ε_m, ε_w, and ε_2 are the complex dielectric constants of the mixture of moist grain and air, water, and dry solid kernels, respectively, v_{ms} is the fraction of the mixture volume occupied by the moist solid, M is the moisture content (weight basis) of the mixture, and ρ_2 is the density of the dry solid kernel.

The assumptions inherent in equation 16 are: (1) The volume fraction occupied by the moist material doesn't change with moisture content. (The grain swells but maintains its same shape at higher moisture contents.) (2) The volume of the solid moist material is the sum of the volumes of the dry material and the water. (3) The density of water is 1.000 gram/cc. (4) The dielectric constant of water at the measurement frequencies considered is not affected by its absorption in the solid material. Equation 16, with reasonable values for ε_2, v_{ms}, and ρ_2, achieved good qualitative agreement with measured dielectric characteristics for grain, as shown in figure 14.

<div style="text-align:center">

Summary of Findings on the Nature
of the Dielectric Response
</div>

The work described thus far led to several conclusions regarding the nature of the dielectric response in the kilohertz and low-megahertz regions: (1) The large dielectric loss peaks and steep slopes and the unusually high dielectric constant values observed in the kilohertz region are due to conductivity effects—Maxwell -Wagner relaxations and electrode polarization—and not to bound water. (2) These conductivity effects are probably due to percolating protonic conductivity along chains of hydrogen bonds around the surface of macromolecules, through the interfaces between macromolecules, and through the interfaces between individual kernels of grain. (3) These conductivity effects

are extremely sensitive to the distribution of moisture within kernels and subtle differences in kernel morphology—contributing significantly to moisture meter calibration instability. (4) Moving the measurement frequency for dielectric moisture meters from the 1 to 20 MHz range to about 150 MHz should dramatically reduce the influence of conductivity effects on moisture measurements and improve calibration accuracy and stability. (5) It is not necessary to go to much higher frequencies (the microwave range) to avoid conductivity effects in grain. (6) For grain, the cube-root density correction effectively normalizes grain samples (within a grain type) to a common density—thereby minimizing density-induced errors from test cell filling methods, grain moisture level, and kernel density and shape. (7) The cube-root density correction reduces the achievable moisture measurement error to less than one third of the error observed without density correction. (8) All water in grain (to about 30 % moisture, at least) appears to be "bound" in the sense that it does not freeze at 0 °C, but there is a difference in the dielectric behavior of "tightly-bound" or "monolayer" water and the dielectric response of the rest of the water in grain. (9) The linear relationship between dielectric response and temperature extends through the freezing point for all but very wet samples.

A New Algorithm for RF Dielectric-Type
Grain Moisture Measurement

Based on the insights gained from studying the nature of the dielectric response in grain, a new algorithm for measuring grain moisture with the RF dielectric method was formulated and was applied to the fifteen most significant types of cereal grains and oilseeds in the United States.

Optimum Measurement Frequency

As noted above, the frequency range between 100 and 200 MHz appeared to be advantageous for low-loss dielectric measurements. A question remained as to whether multiple frequencies or a single frequency should be used in the measurement algorithm. Lawrence et al[42,43,63] previously reported moisture measurement results from a portion of this data set based on complex reflection coefficient measurements at about 1, 40, and 140 MHz. Other work by Lawrence et al[62] reported the use of density-independent functions (combining the dielectric constant and loss) at 41, 241, and 341 MHz for measuring moisture.

All of these measurements (including the present research) were acquired with expensive research-grade instruments that were designed for very accurate complex impedance measurements spanning decades of frequency. Prediction models based on multiple frequencies offer no particular problem in the research laboratory. However, duplicating the wide-band performance of a research-grade instrument in a moderately priced grain moisture meter is a difficult design challenge. An instrument based on an

89

algorithm that could achieve excellent moisture measurement performance with a single measurement frequency should be much less expensive to design and manufacture than one requiring multiple widely-spaced frequencies.

Another advantage of an algorithm that uses a single measurement frequency is the simplicity of the calibration process. Chemometric methods such as multiple linear regression, principal components regression, partial least squares regression, and artificial neural networks are powerful tools for extracting useful results that are buried in complex interactions. However, if a calibration parameter that inherently untangles the interactions can be found, powerful chemometric methods are unnecessary and only mask the simplicity of the solution. Such an advantageous calibration parameter has been found in the density-corrected dielectric constant.

The combination of the move to higher measurement frequencies and the application of the cube-root density correction drastically reduced the scatter observed in the (density-corrected) dielectric constant versus moisture relationship. There was little error remaining to be corrected by incorporating data from other frequencies in the model. Figure 36 shows the square of the linear correlation (Pearson's r) between the density-corrected dielectric constants for yellow-dent corn at 149 MHz and those at 1 to 251 MHz. The correlation is higher than 0.94 over the entire frequency range. Above about 70 MHz, the correlation is greater than 0.999. This means that there is virtually no extra information available at any frequency between 70 and 251 MHz for improving upon a single measurement at 149 MHz. The extra "information" available at lower frequencies has been identified as due to conductivity effects, which should be avoided if at all

possible. (The "blips" on the correlation curve at 17, 52, and 61 MHz are believed to be due to residual reflections in the test cell.) Therefore, it was concluded that a single measurement frequency of about 150 MHz may be nearly optimum both for achieving excellent accuracy and simplifying moisture meter design.
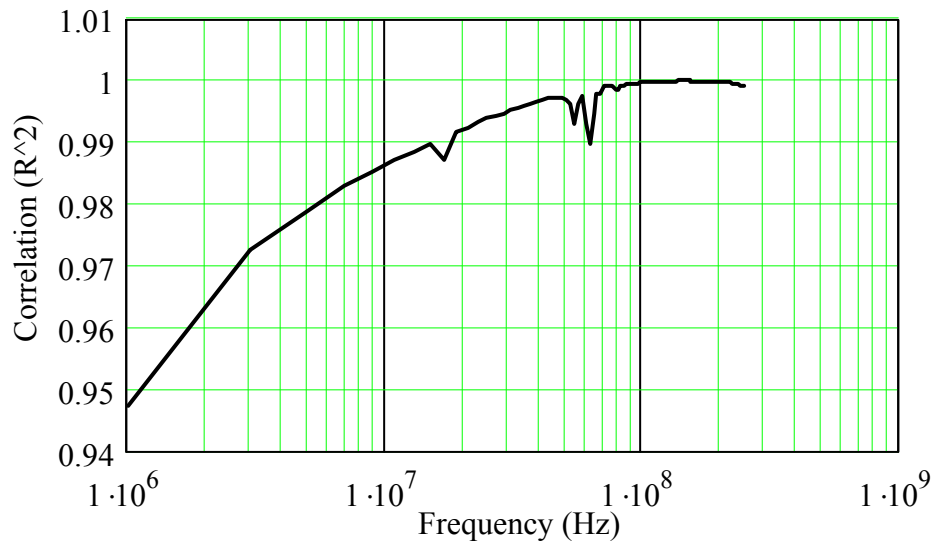
Figure 36. Pearson's *r* correlation coefficient (squared) of yellow-dent corn density-corrected dielectric constant at 149 MHz and at 1 to 251 MHz.

Unified Grain Moisture Calibration Equations

The following series of plots illustrates the calibration development process, which is shown in detail in appendix E. Figure 37 shows the dielectric constant values at 149 MHz for 2,331 samples representing 15 grain types and three crop years. Figure 37 seems to offer little hope of achieving unified calibrations for these grain types.
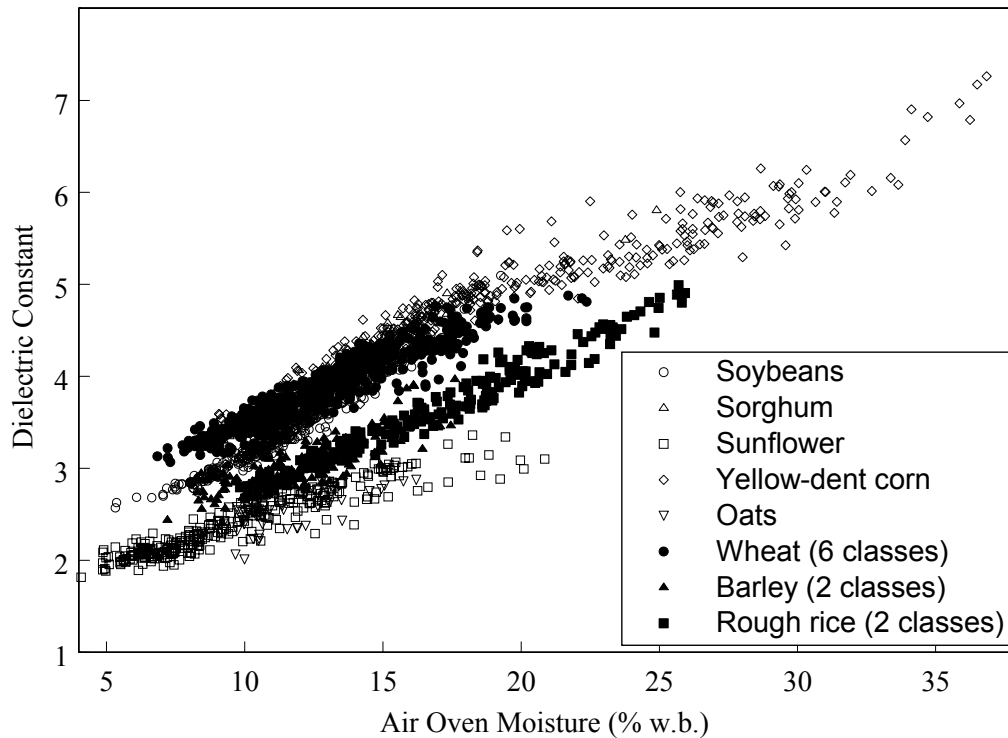
Figure 37. Dielectric constants without density correction
for 15 grain types at 149 MHz.

Figure 38 shows the same data after applying the cube-root density correction to

the dielectric constants. Each sample in each grain group (six classes of wheat in one

group, for instance) was density-corrected to the average sample weight for that group. A

dramatic reduction in scatter (similar to that observed in figure 35) is apparent.
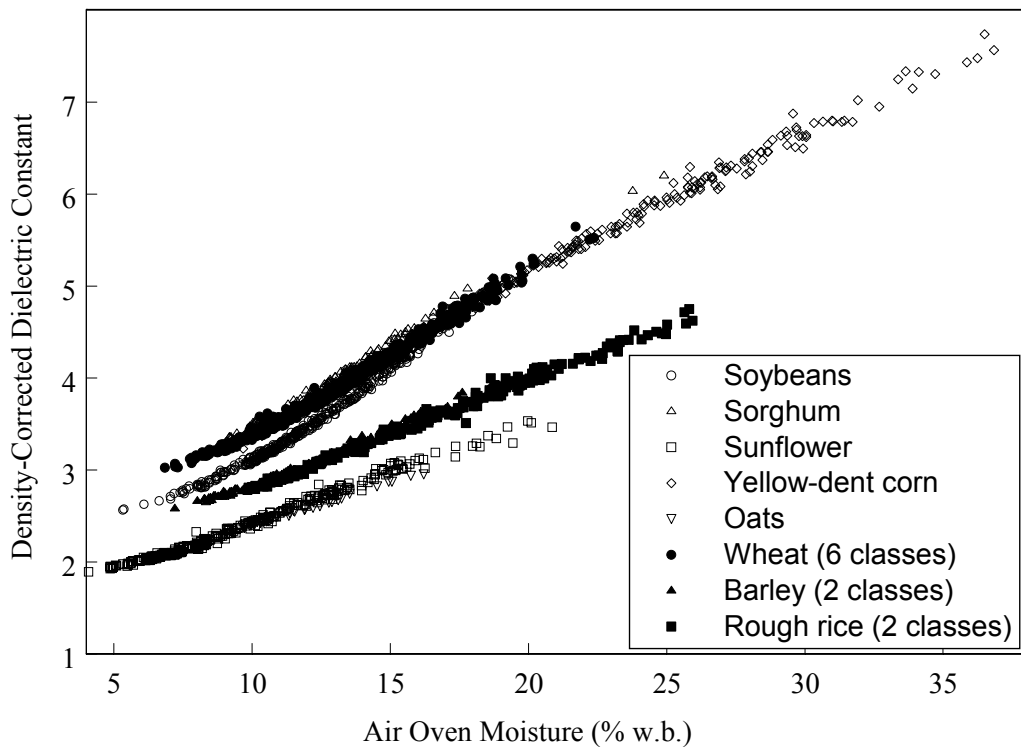
Figure 38. Density-corrected dielectric constants for 15 grain types at 149 MHz. Each grain group density-corrected to the average density for that grain group.

The effects of applying different target sample weights to each grain group were tested. It was found that the error in the linear fit between density-corrected dielectric constant and moisture content was essentially independent of the target sample weight chosen. However, varying the target sample weight adjusted the slope of the linear regression. Therefore, target sample weights were chosen for each grain group to make the linear regression (between density-corrected dielectric constant and moisture content) be exactly 6.000 % moisture per unit of density-corrected dielectric constant. This was

essentially a slope adjustment step. Figure 39 shows the results of this adjustment. All grain types essentially coalesced into two groups—soybeans and sunflower seeds (oilseeds) in one and all other grains (cereal grains) in the other.
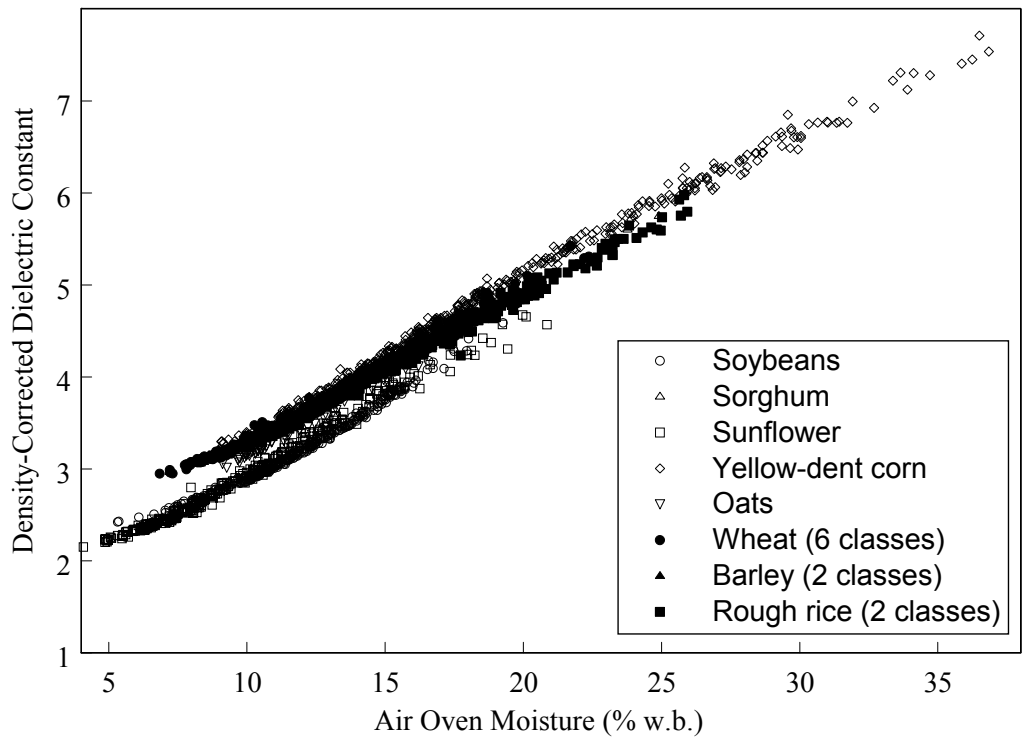
Figure 39. Density-corrected dielectric constants for 15 grain types at 149 MHz.
Each grain group density-corrected to a value selected to yield slope
of linear regression equal to 6.000 % moisture per unit of
density-corrected dielectric constant.

At this point, it appeared that the differences among the groups were essentially offsets along the vertical axis. An offset was applied to the density-corrected dielectric

94

constants in each grain group according to the intercepts of the linear regressions

performed to achieve the common slope of 6.000. The results are shown in Figure 40.
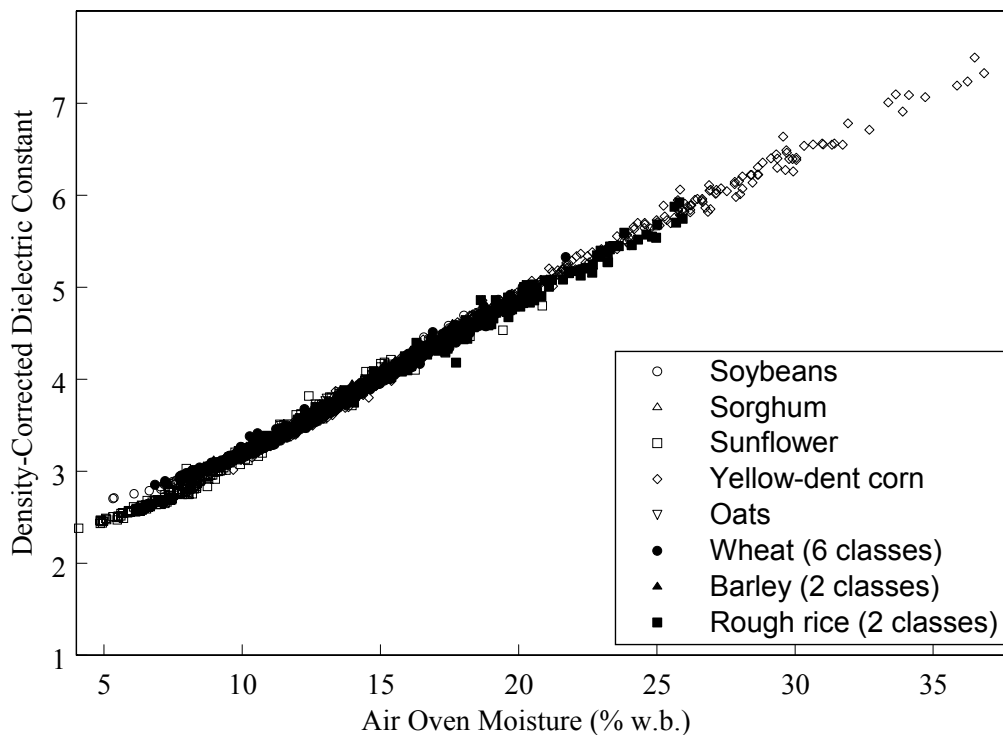
Figure 40. Density-corrected dielectric constants for 15 grain types at 149 MHz. Each grain group density-corrected to give slope of 6.000 (% moisture per unit dielectric constant) and biased according to the intercepts found by linear regression.

After applying the intercept adjustments, the density-corrected dielectric constant

versus moisture curves are very nearly superimposed for all grains. However, some

differences are visible in the very low moisture region. Analysis of this "problem"

yielded further insight into the nature of the dielectric response. Figure 41 shows a detail

view of the low moisture portion of figure 40 with the individual grain groups offset vertically to show the behavior of each one separately. Laying a straightedge on this plot reveals slope changes for each grain group at or below about 10 % moisture. The bend for sunflower seeds occurred at about 7 % moisture, the bend for soybeans was at about 8.5 % moisture, and the bend for the cereal grains was at about 10 % moisture (or slightly higher). It was recognized that these bends were occurring at about the same moisture levels where conductivity caused much more dramatic bends in the dielectric constant versus moisture curves at much lower frequencies. The effects of conductivity seemed to completely disappear well below 150 MHz, however. This change in slope was found to be fairly stable over the range of 100 to 250 MHz.

It was concluded that this slope change is due to two different water phases (monolayer water and higher layers of water) that have different dielectric constants and that both have very broad distributions of relaxation frequencies spanning the range of 10 MHz to well above 250 MHz. The monolayer moisture limit is known to be much lower for oilseeds than for cereal grains.[22] This same monolayer limit that determines the threshold for percolating protonic conductivity seems to show up in high frequency measurements as the breakpoint between two different slopes in the density-corrected dielectric constant versus moisture curve.
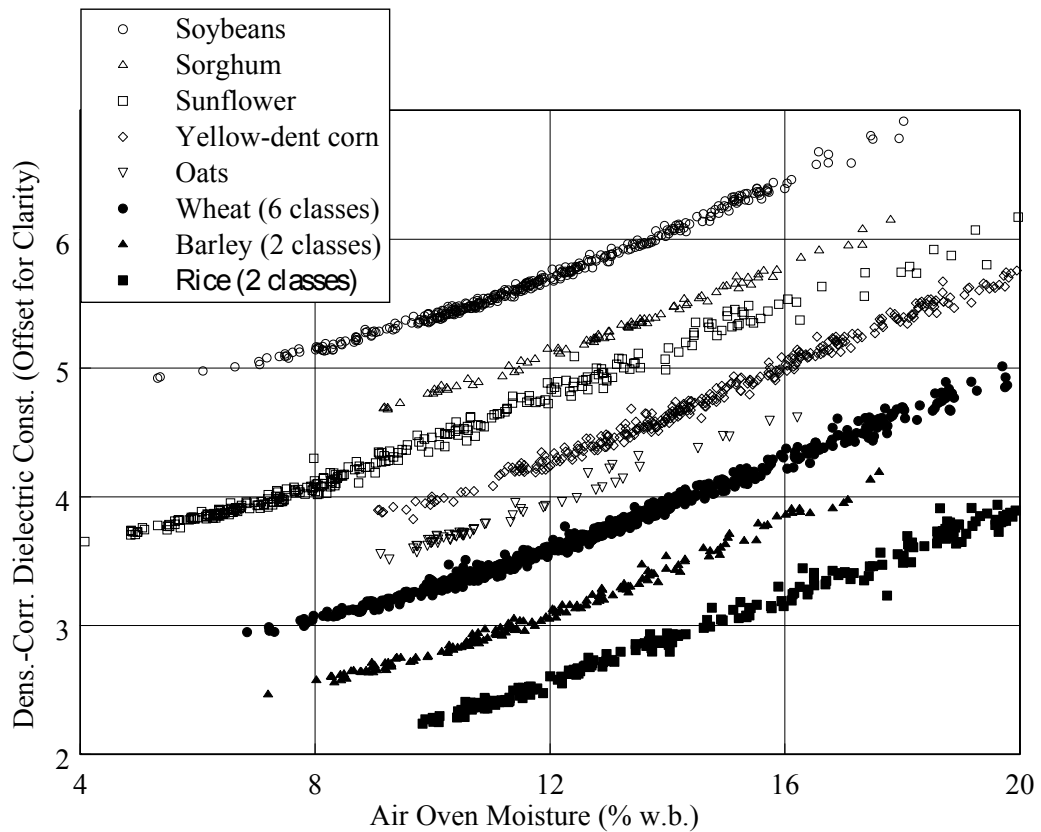
Figure 41. Density-corrected dielectric constants for 15 grains at 149 MHz.
Each grain's target density adjusted to give overall linear slope of 6.000
(% per unit dielectric constant). Curves offset for clarity and
expanded about low moisture range.

For most of the grain types there isn't sufficient data at moisture levels below the

breakpoint to precisely estimate the slope of the lower portion of the curve. However, the

data suggest that the low-end slopes for each grain may be nearly the same value—

approximately 10 % moisture per unit of density-corrected dielectric constant (as opposed

to 6 % moisture per unit of density-corrected dielectric constant for the high end). Further

research is needed to better characterize the low-moisture behavior for most of these grain types.
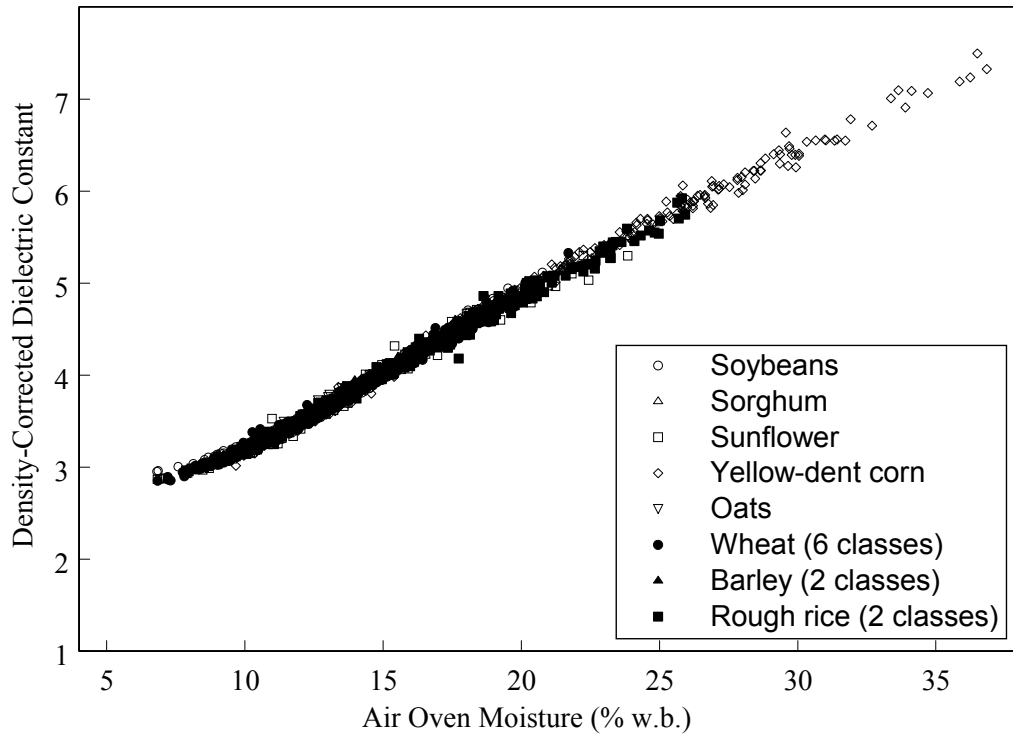
Figure 42. Final dielectric constants for 15 grain types at 149 MHz adjusted according to the proposed grain moisture meter calibration algorithm.

This commonality of slopes in both regions suggested one last correction to bring all grain types together in a single prediction equation. Starting from the condition portrayed in figure 40, the data for soybeans were translated along the common curve by 1.5 % moisture content and $1.5/6.0 = 0.25$ units of dielectric constant, and the data for sunflower seeds were translated by 3.0 % moisture content and $3.0/6.0 = 0.50$ units of

dielectric constant to get the results shown in figure 42. A 4th-order polynomial was fitted

to these data to create a unified calibration equation. Figure 43 shows the predicted

moisture measurement error for this calibration model.   The overall standard deviation of

differences for the calibration was 0.29 % moisture.
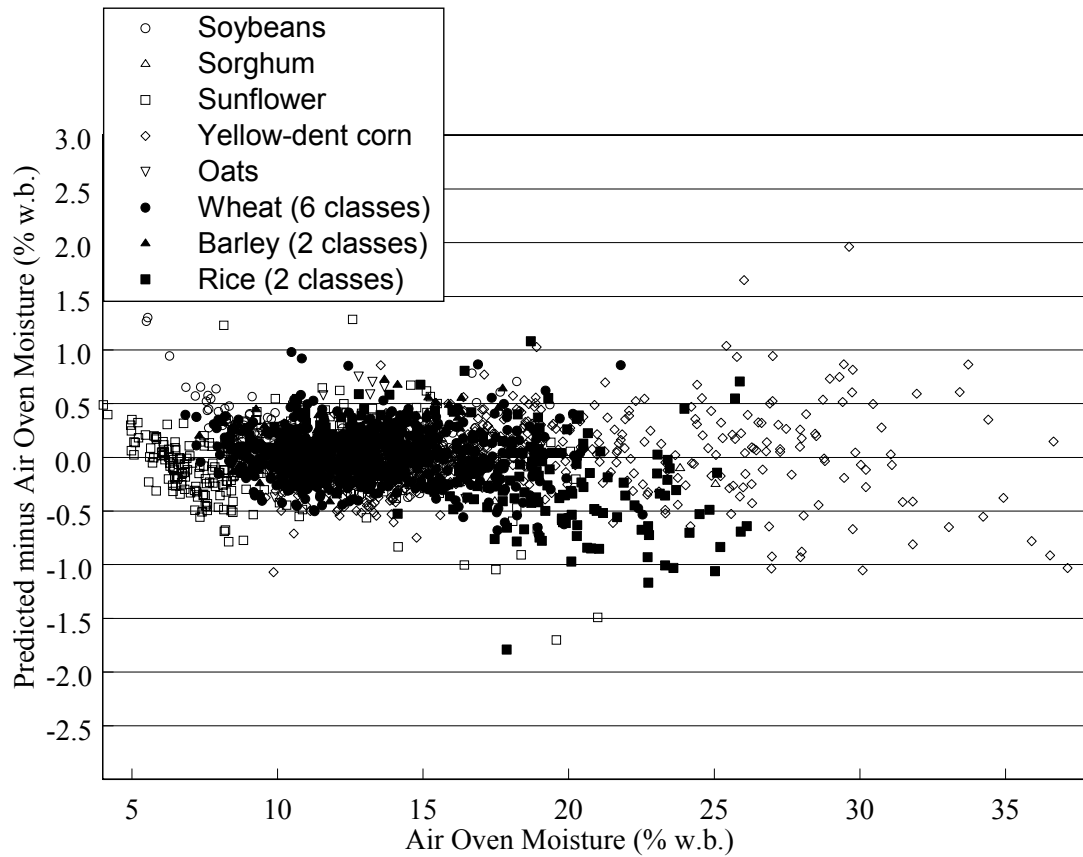
Figure 43. Predicted moisture measurement error for 15 grain types
at 149 MHz with proposed calibration algorithm.

Figure 44 shows the moisture measurement error for the 15 grain types with the

unified calibration as a function of sample weight. The lack of correlation of moisture

error with sample weight within grain types shows the effectiveness of the cube-root density correction function.
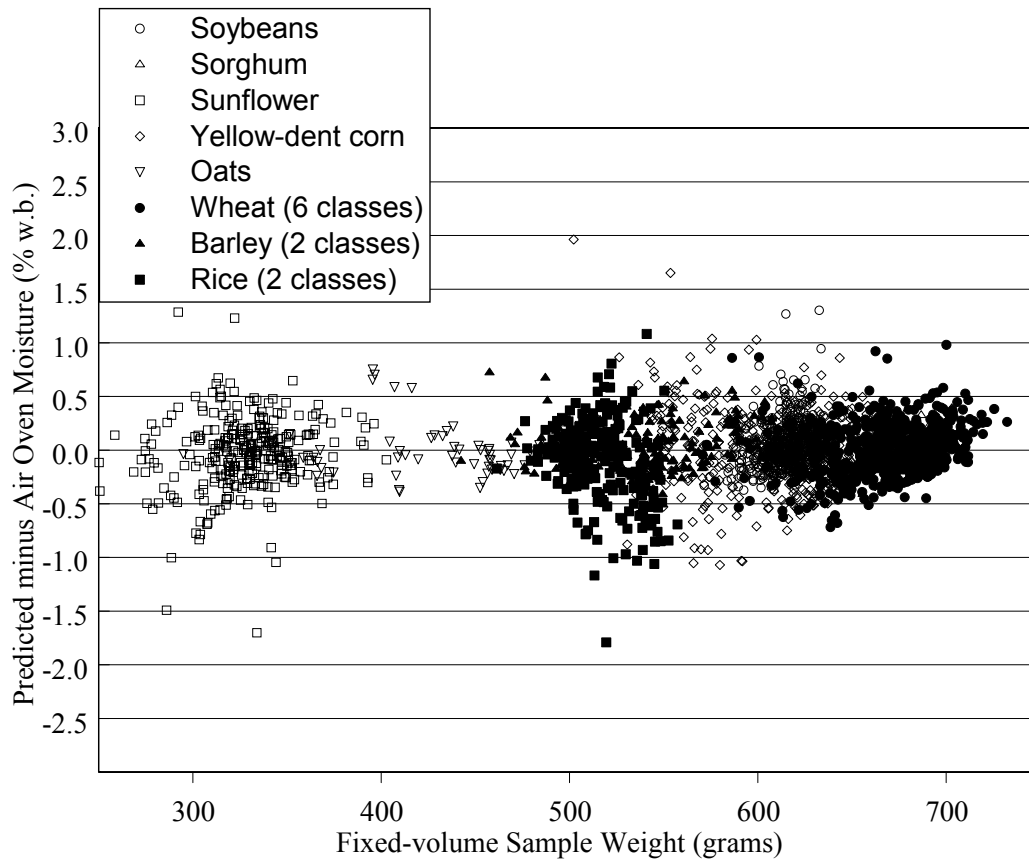
Figure 44. Moisture measurement error across the range of
sample weights for fifteen grain types.

Figure 45 is a plot of the best-fit 4th-order polynomial regression curves for the fifteen grain types (taken together) at 99, 149, 199, and 249 MHz. The small shifts between the curves further confirm the earlier claim that bound water relaxations are small but observable in this frequency range. Also, the parallelism of the curves re-emphasizes

that the main relaxation frequencies for both the monolayer water and the other water must lie above 250 MHz.
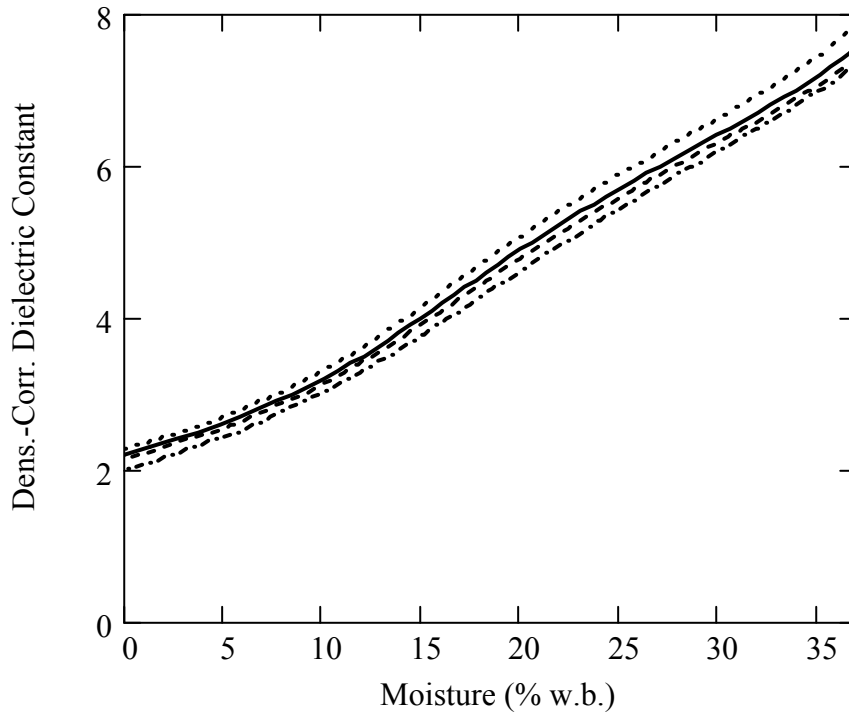
Figure 45. Best-fit 4th-order polynomial regression lines for 99 MHz (dot), 149 MHz (solid), 199 MHz (dash), and 249 MHz (dash-dot).

Figure 46 shows the calibration error as a function of frequency for a 4th-order polynomial regression with 15 grain types. The broad minimum in the error curve from 100 MHz to 200 MHz is particularly striking. The blips in the error curve at 17, 54, 62, and 80 MHz are believed to be due to resonance conditions related to residual reflections within the transmission-line test cell.
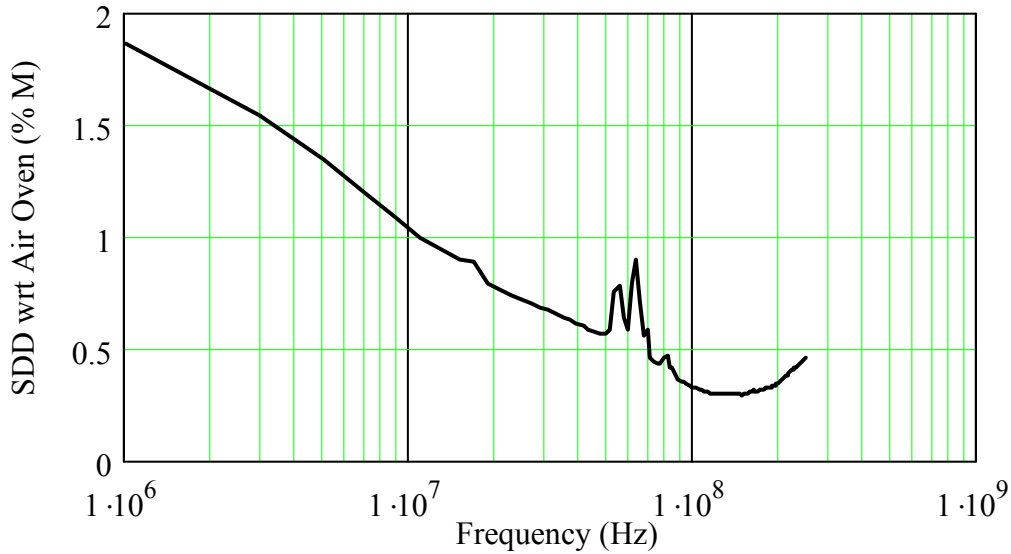
Figure 46. Calibration error versus frequency for 4th-order polynomial regression with 15 grains and 3 crop years.

Temperature Correction for the Moisture Measurement Algorithm

The temperature correction algorithm was developed through an iterative process. Linear regression was used to develop initial calibration equations for each grain group based on the density-corrected dielectric constant data shown in figure 38. Prior to computing the linear regression, an initial temperature correction was used to adjust the air oven moisture value for each sample according to

$$AOM_{TC} = AOM + K_{TC}(T - T_0) \tag{17}$$

where AOM_{TC} is the adjusted air oven moisture, AOM is the unadjusted air oven moisture, K_{TC} is the temperature correction coefficient (% moisture/°C), T is the sample temperature measured at the same time as the dielectric characteristics, and T_0 is the reference

temperature (25 °C). The effect of this adjustment was to apply a reverse temperature correction to the air oven moisture values instead of a forward correction to the dielectric constant values. This simplifies calibration development, especially when multi-term (polynomial or other) equations are used to fit dielectric data to air oven results.

Linear regression yielded initial calibration coefficients for the grain type. Those calibration coefficients and the initial temperature correction coefficient were used to predict moisture values for several samples of the grain type that had been analyzed at three or four different temperatures. Moisture M was predicted according to

$$M = A + B\varepsilon'_{DC} - K_{TC}(T - T_0) \tag{18}$$

where A and B are the intercept and slope values from linear regression and ε'_{DC} is the density-corrected dielectric constant at 149 MHz. The differences between predicted and actual (air oven) moisture values were plotted and the value of the temperature correction coefficient was adjusted interactively to minimize the differences between predicted results for different temperatures. Once a value for K_{TC} was found that minimized moisture prediction differences with sample temperature changes, that value was substituted back into equation 17, and the linear regression was recomputed. The moisture values for the wide temperature range samples were recomputed with equation 18 to confirm the temperature correction value. K_{TC} was adjusted iteratively as needed to converge on the final value. The optimum temperature coefficients listed in table 1 were applied (equation 17) to the samples in each grain group prior to the 4th-order polynomial regression that produced the results in figure 43.

Table 1. Estimated temperature coefficients (% moisture per degree Celsius).
Temperature coefficients for sorghum and oats estimated from
grain types with similar chemical composition.

Grain Group	Temperature Coefficient
Soybeans	0.112
Sorghum	0.108
Sunflower Seeds	0.056
Yellow-dent corn	0.108
Oats	0.108
Wheat	0.112
Barley	0.108
Rough Rice	0.077

**Interpretation of Temperature Dependence
of Dielectric Constant in Grain**

A second temperature correction formula was evaluated as a possible alternative.

$$M = (A + B\varepsilon'_{DC})(1 - K_{TC}(T - T_0)) \qquad (19)$$

Equation 19 applied a correction for temperature that was proportional to the predicted

moisture level as well as the difference between the sample and reference temperatures.

Equation 18 applied a correction that was proportional to the temperature difference but

independent of moisture level. It was expected that equation 19 should provide a more

precise temperature correction than equation 18. If more moisture were present in a

sample and the variation in the dielectric characteristics with temperature were due to the

temperature characteristics of the water present, it seemed logical that the magnitude of the

temperature correction needed would have been proportional to the moisture content.

The limited temperature test data available did not confirm this hypothesis. Equation 18 provided a more precise correction for temperature differences than did equation 19. That is, a constant temperature correction (% moisture/°C) gave better consistency among moisture predictions at different sample temperatures than a moisture-dependent temperature correction did.

Apparently the magnitude of the temperature effect is not proportional to the amount of water present in the sample. A hypothesis was developed to explain this observation. The changes in slopes in figure 41 suggested the existence of two major categories of water in grain—monolayer (tightly bound) water and other water. Comparison of the (normalized) slopes of the two regions (10 versus 6) implied that the two categories of water contributed differently to the dielectric constant of the grain. The effect of temperature on dielectric characteristics may be the thermally activated promotion of monolayer water (breaking of one or more hydrogen bonds) with a concurrent increase in the dielectric contribution from that water. Since only the monolayer water would be available for promotion to a less tightly bound state, the effect of temperature on dielectric constant would be independent of moisture content at moisture levels above the monolayer limit. This interpretation is consistent with the results of the present research and could explain Trabelsi's observation at microwave frequencies that the effects of moisture level and temperature appear to be completely interchangeable.[17] Further research is needed to test the hypothesis.

Attempts to simulate the temperature dependence of the dielectric characteristics of grain at 149 MHz were unsuccessful. The strong negative temperature coefficient for the low-frequency dielectric constant of free water (figure 3) overwhelmed any positive temperature coefficient that could be explained by promotion of monolayer water. Apparently the broad bound water relaxation suggested by figure 14 is contributing to grain temperature characteristics in a more complex way than can be explained by the simulation models.

<div align="center">

Performance of Unified Moisture
Measurement Algorithm

</div>

Table 2 compares standard deviations of differences between predicted moisture results and air oven moisture results for separate calibration equations for each grain group, the Unified Moisture Algorithm for all grain groups together (4th-order polynomial regression), and the official grain moisture meter model (with individual calibrations for each grain type). All results are for the combination of data for the 1998, 1999, and 2000 crop years. This research did not include quite all of the samples that were tested with the official moisture meter, so the results are not exactly comparable.

Table 2. Comparison of moisture measurement accuracy for separate moisture calibrations (various polynomial regression orders), the Unified Moisture Algorithm, and GIPSA's official moisture meter for data from three crop years.

Grain Type	Separate Moisture Calibrations	Poly. Regr.	Unified Moisture Algorithm	Official Moisture Meter
	SDD	Order	SDD	SDD
Six-Rowed barley				0.35
Two-Rowed barley				0.46
Combined barley	0.21	3	0.23	
Low-moisture corn (< 20%)				0.38
High-moisture corn (> 19 %)				0.90
Combined corn	0.33	4	0.36	0.60
Oats	0.23	1	0.25	0.34
Long Grain Rough rice				0.34
Medium Grain Rough rice				0.45
Combined rice	0.34	3	0.38	
Sorghum	0.13	3	0.15	0.38
Soybeans	0.16	3	0.23	0.43
Sunflower seeds	0.32	3	0.35	0.67
Durum wheat				0.32
Hard Red Spring wheat				0.35
Hard Red Winter wheat				0.39
Hard White wheat				0.28
Soft Red Winter wheat				0.35
Soft White wheat				0.28
Combined wheat	0.23	3	0.23	
Combined all grains			0.29	

As shown in table 2, the Unified Moisture Algorithm's performance (with a single calibration equation) compares very favorably for every grain tested with the official moisture meter's performance (whose performance is typical of commercial RF dielectric-type grain moisture meters). The official meter uses separate calibration equations for each grain type. The overall performance (SDD = 0.29) is better than the official meter's

performance on all individual grains except for two classes of wheat. For the most difficult grain types (high-moisture corn and sunflower seeds) the Unified Moisture Algorithm improves performance by about a factor of two. This algorithm shows tremendous promise as the basis for a new generation of RF dielectric-type grain moisture meters.

Separate calibrations for individual grain types with this new algorithm yielded somewhat better accuracy statistics than those achievable with the combined calibration. The combined calibration performance could be further optimized by (1) more careful modeling of the dielectric test cell, (2) excluding the monolayer water sections of the curves from the regressions used to optimize the target weights for each grain type, and (3) selecting a function that is more suitable than a 4th-order polynomial for fitting two straight line segments that merge at the monolayer moisture threshold.

CHAPTER 5

CONCLUSIONS

This chapter summarizes the questions addressed by the research, the answers to those questions, and their implications for the future of grain moisture measurement using the RF dielectric method.

The Nature of the Dielectric Response in Grain

Discerning the nature of the dielectric response in grain is important for grain moisture measurement so that a measurement algorithm can be made optimally sensitive to all of the moisture present in grain and minimally sensitive to interfering factors that do not carry reliable information about the amount of moisture in grain. This research has shown that none of the water in grain (at least up to the moisture levels tested) is "free" water that can freeze at 0 °C. The hydrogen bonding energies for all water molecules are altered by the presence of the tightly bound layer (monolayer) of water hydrogen-bonded directly to polar sites on proteins, carbohydrates, and other grain constituents.

The two major implications of this finding are: (1) The RF dielectric method is not inherently blind to water below 0 °C. (2) Ionic conductivity (which presumably requires the presence of free water to dissolve salts) is not a viable explanation for conductivity effects in cereal grains and oilseeds.

Review of the literature revealed an alternative explanation for conductivity effects in grain—percolating protonic conductivity. Mathematical models (based on the reported characteristics of matrices exhibiting percolating protonic conductivity) showed good qualitative agreement with experimental results. This research did not prove that percolating protonic conductivity is the source of conductivity effects in grain but did establish its plausibility as an explanation that warrants further research.

Review of experimental results over a wide frequency range (from 100 Hz to 250 MHz) quantified the extent of conductivity effects (electrode polarization and Maxwell-Wagner) on dielectric measurements throughout the frequency range. Comparison of simulations to experimental results indicated that conductivity dramatically affects complex dielectric constant measurements in the kilohertz region and significantly (though subtly) influences dielectric measurements throughout the frequency range commonly used for grain moisture measurement (1 to 20 MHz).

Conductivity effects are very sensitive to grain moisture and temperature and the distribution of water within the grain kernels. At different moisture levels and temperatures, the shape of the loss peaks and the slope of the dielectric constant curves (versus frequency) vary dramatically. Features that might appear useful for predicting moisture in grain that is at equilibrium (uniform moisture distribution within the kernel) and at room temperature change radically and virtually unpredictably for grain that has been recently wetted or dried or is measured at temperature extremes.

Conductivity effects were shown to be responsible for large moisture meter errors in the case of "moisture rebound" in sunflower seeds and "location effects" in Medium

110

Grain Rough rice. The conductivity effects visible in the dielectric spectra for all grains

tested are very likely responsible for the observed instability (over time and growing

locations) in grain moisture meter calibrations. Creating grain moisture calibrations based

on dielectric measurements at a frequency where conductivity effects are present can be

likened to making topographical maps of sand dunes in a desert—instability is inevitable.

Experimental results showed that conductivity effects and overall dielectric loss are

drastically reduced by changing measurement frequencies from the 1 to 20 MHz range to

the 100 to 200 MHz range. This is particularly important for achieving high accuracy for

high-moisture samples, which have always been the greatest challenge for grain moisture

measurement. This research demonstrated that it is not necessary to move all the way to

microwave frequencies to avoid conductivity effects.

Experimental results and comparisons with mathematical simulations demonstrated

two bound water phases—a tightly bound monolayer phase and an "other water" phase.

The monolayer phase appears to have a lower static dielectric constant (approximately 40

percent less) than the other water phase, whose static dielectric constant seems to be

approximately that of pure water (78.5 at 25 °C). At frequencies above those where

conductivity effects dominate the dielectric spectrum, the presence of two bound water

phases results in a slope change in the dielectric constant versus moisture relationship.

The moisture level where the slope changes is related to the threshold moisture level for

conductivity effects at low measurement frequencies. Different grain types with different

compositions (oil content, especially) exhibit the slope change at different moisture levels.

This is consistent with differences between monolayer moisture values for cereal grains

and oilseeds given in the literature. The ratio of the two slopes appears similar for all grain types tested. Further research with very low moisture grain is needed to verify this observation.

The dielectric loss associated with bound water relaxation is visible above about 1 MHz and causes a very gradual decline in the dielectric constant through the 100 MHz to 250 MHz frequency range. Contrary to prior expectations, the monolayer water does not exhibit a much different distribution of relaxation frequencies than the other water. (Simulations showed that different relaxation frequencies for the monolayer and other water phases should have caused the shape of the dielectric constant versus moisture curve to change at different measurement frequencies. This was not observed.) Rather, the best-fit curves of the relationship between dielectric constant and moisture content were very nearly parallel for different measurement frequencies over the range from 100 MHz to 250 MHz. (Below 100 MHz, the slope changes were attributable to conductivity effects.) Therefore, moving the measurement frequency above 100 MHz does not sacrifice sensitivity to all of the water in grain.

Analysis of dielectric response versus temperature for a limited number of samples suggested that the temperature dependence of the dielectric constant is essentially independent of moisture level. A possible explanation for this behavior is that water molecules that are firmly hydrogen-bonded to grain constituents (monolayer water) at low temperatures could be "promoted" to the "other water" phase by thermal activation at higher temperatures. Further research is needed to test this explanation of the observed

temperature effect and to characterize the temperature dependence of many grain types over the full moisture range.

Optimized Density Correction Equation

Equation 10 (see page 23) was found effective in normalizing the dielectric characteristics of grain at different densities to a common target density for purposes of predicting moisture content by weight. This equation was applicable to all grain types tested, and it corrected density differences due to moisture level, test cell filling method, and kernel density. This density correction dramatically reduced the scatter in the relationship between dielectric constant and moisture content, and it significantly improved the linearity of the relationship. Density-corrected dielectric constant at a single frequency between 100 and 200 MHz was shown to be an excellent choice of dielectric parameter for moisture measurement.

Varying the target density used in the density correction equation for a grain type did not affect the achievable moisture calibration accuracy but did change the slope of the density-corrected dielectric constant versus moisture content curve. Adjusting the target densities for different grain types permitted a common slope (% moisture per unit of density-corrected dielectric constant) to be achieved for all grain types tested.

Unified Moisture Measurement Algorithm

Moving the measurement frequency from the 1 to 20 MHz range to the 100 to 200 MHz range virtually eliminated the influence of grain conductivity on the dielectric

constant measurements. A test frequency of 149 MHz was arbitrarily chosen from the center of that range for development of a unified moisture measurement equation for fifteen of the most significant grain types in the United States.

The density correction algorithm (with an adjusted target density for each grain type) minimized the scatter within each grain type and caused each grain type to have a common slope (6.000 % moisture per unit of density-corrected dielectric constant). After achieving a common slope, the fifteen grain types fell into two fairly tight groups—cereal grains in one group and oilseeds in the other group. A bias was added to the density-corrected dielectric constants for each grain type to align the density-corrected dielectric constant versus moisture curves for all grain types. The biases were very similar for all cereal grains and for all oilseeds. Therefore, normal variations in grain characteristics within a grain type would be expected to cause very small errors.

The shapes of the density-corrected dielectric constant versus moisture curves were observed to be very similar for all grain types, with a slope change apparent in the 7 to 10 % moisture range. The position of the slope change was related to the typical oil content of the grain type. The density-corrected dielectric constant versus moisture curves for sunflower seeds and soybeans were translated by 3.0 and 1.5 % moisture and 0.5 and 0.25 units of density-corrected dielectric constant, respectively, to align the slope change positions for the oilseeds with those for the cereal grains.

With the adjustments described above, a single 4th-order polynomial regression yielded an overall standard error of calibration of 0.29 % moisture for a unified calibration for fifteen grain types.   This accuracy, for all grain types together, compared very

114

favorably with the accuracy achievable for any single grain type with GIPSA's official moisture meter. The standard deviations of differences for the unified calibration were reduced by nearly half relative to the performance of existing commercial grain moisture meters. Performance statistics for individual grain types were most improved for the most difficult grain types—high-moisture corn and sunflower seeds.

Separate calibrations developed for individual grain types with the above algorithm yielded slightly better performance than the unified calibration, indicating that the unified calibration might be further improved by adjusting the unifying parameters more carefully.

Answers to Questions Addressed by the Research

This research has substantially answered the following questions that were originally posed in chapter 1.

What causes the observed instability in grain moisture meter calibrations? The instability in moisture meter calibrations is primarily due to conductivity effects, not the varying distribution of bound and free water.

What measurement frequency or combination of frequencies within the RF range is the optimum for moisture measurement? A single frequency in the range from 100 to 200 MHz appears to be the optimum. A test frequency of 149 MHz was arbitrarily chosen, but the same information is available at any frequency near 149 MHz.

What dielectric parameter is most advantageous for predicting moisture content? The dielectric constant (real part of the complex dielectric constant) is a very good choice for measuring moisture in grain. The use of the dielectric constant as a basic measurement

parameter should permit multiple instruments to use common calibrations with minimal adjustments. Avoiding the dielectric loss minimizes ambiguity due to residual conductivity effects.

What is the optimum function for minimizing the effects of sample density differences? The cube-root density correction function (equation 10) is very effective in normalizing the density of grain samples regardless of whether the density differences are due to moisture level, filling rate, or kernel density.

What type of test cell filling process should be used? It really doesn't matter whether the filling method is fast or slow if an effective density correction such as equation 10 is used. However, the filling method should provide a consistent filling action. The filling method must determine a fixed volume of grain to be weighed. Errors due to under-filling or over-filling the test cell will not be corrected precisely.

How should temperature corrections be implemented in the algorithm? A moisture-independent temperature correction (% moisture per degree Celsius) seems to be the optimal function, but more research is needed to confirm this.

Can optimization of these parameters yield improvements that are significant enough to warrant development of a new generation of moisture meters? Yes, the improved accuracy within grain types, the potential stability of moisture meter calibrations over time, the potential for using the same calibration equations with many different instruments built around the algorithm, and the potential for unified calibrations that obviate the need for separate calibrations for each and every grain type should justify development of a new generation of grain moisture meters.

APPENDIX A

GRAINS TESTED WITH HP-4291A IMPEDANCE ANALYZER

GRAINS TESTED WITH HP-4291A IMPEDANCE ANALYZER

Grain Name	1997 Crop	1998 Crop	1999 Crop**	2000 Crop	Temp. Studies	TOTALS
Black Eye Beans				17		17
Baby Lima Beans				14		14
Brewers' Milled Rice			12			12
Long Grain Brown Rice-Parboiled			10			10
Black Beans		7				7
Canola		16				16
Corn	123	125	219	186	12	665
Cranberry Beans				11		11
Sunflower Seeds (Confectionery)			49			49
Dark Red Kidney Beans			13	30		43
Smooth Dry Peas			42			42
Durum Wheat	32	4	50	40	8	134
Flaxseed			28			28
Great Northern Beans		10				10
High-Oil Corn		19	16	22		57
Hard White Wheat	14	11	1	10		36
Hard Red Spring Wheat	48	40	53	55		196
Hard Red Winter Wheat	2	25	67	57		151
Long Grain Brown Rice		10	16			26
Long Grain Rough Rice	27	43	33	46	2	151
Light Red Kidney Beans			11	21		32
Long Grain Milled Rice		10	20			30
Long Grain Milled Rice--Parboiled			6			6
Lentils			17			17
Medium Grain Brown Rice			13			13
Medium Grain Rough Rice	8	48	50	38	8	152
Medium Grain Milled Rice			21			21
Oats	6	25	19	27		77
Pea Beans		11				11
Pinto Beans		20				20
Rye		1				1
Safflower Seed			13			13
Six-Rowed Barley	19	31	25	41		116
Sunflower Seeds (Oil Type)	92	66	145	84	4	391
Sorghum (Milo)	34	11	44	38		127
Soft Red Winter Wheat	4	15	55	56		130
Short Grain Rough Rice			25			25
Soft White Wheat	11	28	53	53		145
Soybeans	125	143	139	148	9	564
Two-Rowed Barley	29	11	29	33	8	110
Waxy Corn			55			55
Total Samples Tested	574	730	1349	1027	51	3731
Total Grain Types Tested	15	24	32	21	7	41

** Also analyzed with HP-4285A system over 0.1 to 18.5 MHz frequency range

APPENDIX B

CONVERTING COMPLEX REFLECTION COEFFICIENTS

TO COMPLEX DIELECTRIC CONSTANTS

CONVERTING COMPLEX REFLECTION COEFFICIENTS TO COMPLEX DIELECTRIC CONSTANTS

David B. Funk March 26, 2001

This model is based on the signal flow graphs and calculations provided by Dr.Kurt Lawrence, ARS, Athens, GA.

The following diagram shows the signal flow graph model for the test cell between the two N-type connectors.

| Air line section | Air-grain interface | Grain-filled section | Air-grain interface | Air line section |
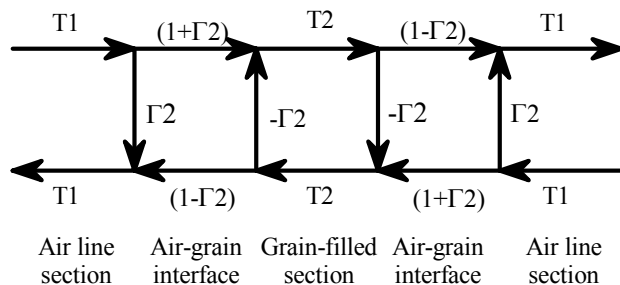
T_1 is the complex (assumed loss-free) transmission factor associated with each of the two (symmetrical) air-filled transmission line sections.

T_2 is the complex transmission factor associated with the grain-filled section.

Γ_2 is the complex reflection coefficient at each of the air-grain interfaces.

This can be simplified by combining sections to yield the following diagram.
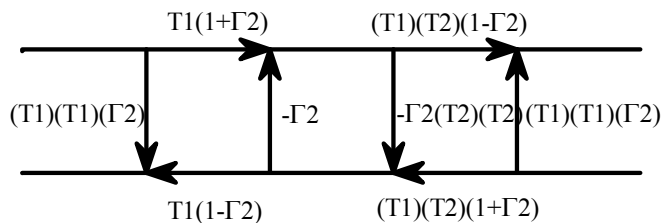
With a vector network analyzer, one inserts the two port device (the test cell) into a calibrated 50-ohm transmission line and measures the forward transmission (G21), the reverse transmission (G12), the forward reflection (G11) and the reverse reflection (G22). Because of the symmetry of this test cell, G12 = G21 and G22 = G11.

With a vector impedance analyzer such as the HP-4291A, the "far end" of the test cell is terminated with a load equal to the characteristic impedance of the air-filled transmission line (50-phm). The 50-ohm termination (theoretically, at least) absorbs all incident power, so the instrument "sees" only the forward reflection coefficient G11 = Γ.
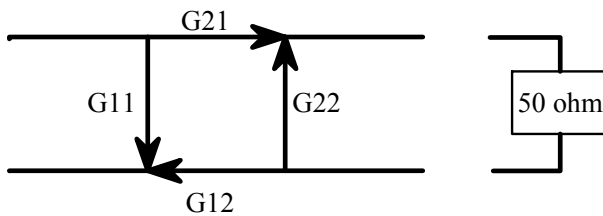
Based on this signal flow graph, the complex reflection coefficient (as measured at the connector plane of the test cell can be expressed mathematically as

$$G_{11} = T_1{}^2 \cdot \Gamma_2 + \frac{T_1 \cdot \left(1 + \Gamma_2\right)\left(-T_2{}^2 \cdot \Gamma_2\right) \cdot T_1 \cdot \left(1 - \Gamma_2\right)}{1 - \left(-\Gamma_2\right) \cdot \left(-T_2{}^2 \cdot \Gamma_2\right)}$$

The complex transmission coefficient that would be measured by a vector network analyzer is

$$G_{21} = \frac{T_1 \cdot \left(1 + \Gamma_2\right) \cdot T_1 \cdot T_2 \cdot \left(1 - \Gamma_2\right)}{1 - \left(-\Gamma_2\right) \cdot \left(-T_2{}^2 \cdot \Gamma_2\right)}$$

or, combining terms

$$G21 = \frac{T_1{}^2 \cdot T_2 \cdot \left(1 - \Gamma_2{}^2\right)}{1 - \Gamma_2{}^2 \cdot T_2{}^2}$$

The transmission factor for the air-spaced tranmission line sections T1 and the transmission factor for the grain-filled transmission line section T2 at the measurement radian frequency ω can be calculated as

$$T1 = e^{-1j \cdot \omega \sqrt{\mu \cdot \varepsilon_i} \frac{d_i}{c}}$$

$$T2 = e^{-1j \cdot \omega \sqrt{\mu \cdot \varepsilon_2} \frac{d_2}{c}}$$

d_1 is the length of the air-filled transmission line sections (50 ohm) from the connector planes to the grain filled section

d_2 is the length of the grain-filled section

the relative dielectric constant of air is $\varepsilon_1 = 1$

the relative complex dielectric constant of grain is ε_2

the relative complex permeability of air and grain is $\mu = 1$

and c is the speed of light

The complex reflection coefficient at the air-grain interface is

$$\Gamma_2 = \frac{\sqrt{\dfrac{\mu}{\varepsilon_2}} - 1}{\sqrt{\dfrac{\mu}{\varepsilon_2}} + 1}$$

Since: $\varepsilon_1 := 1$

$\mu := 1$

T_1, T_2, and Γ_2 can be simplified to:

$$T_1 = e^{-j \cdot \omega \frac{d_1}{c}}$$

$$T_2 = e^{-j \cdot \omega \sqrt{\varepsilon_2} \frac{d_2}{c}}$$

$$\Gamma_2 = \frac{1 - \sqrt{\varepsilon_2}}{1 + \sqrt{\varepsilon_2}}$$

122

Substituting terms, G_{11} and G_{21} can be written:

$$G_{11} = e^{-2j \cdot \omega \frac{d_1}{c}} \cdot \frac{1 - \sqrt{\varepsilon_2}}{1 + \sqrt{\varepsilon_2}} \cdot \frac{1 - e^{-2j \cdot \omega \sqrt{\varepsilon_2} \frac{d_2}{c}}}{1 - \left(\frac{1 - \sqrt{\varepsilon_2}}{1 + \sqrt{\varepsilon_2}}\right)^2 \cdot e^{-2j \cdot \omega \sqrt{\varepsilon_2} \frac{d_2}{c}}}$$

$$G_{21} = \frac{e^{-2j \cdot \omega \frac{d_1}{c}} \cdot e^{-j \cdot \omega \sqrt{\varepsilon_2} \frac{d_2}{c}} \cdot \left[1 - \left(\frac{1 - \sqrt{\varepsilon_2}}{1 + \sqrt{\varepsilon_2}}\right)^2\right]}{1 - \left(\frac{1 - \sqrt{\varepsilon_2}}{1 + \sqrt{\varepsilon_2}}\right)^2 \cdot e^{-2j \cdot \omega \sqrt{\varepsilon_2} \frac{d_2}{c}}}$$

The above equations relate the complex reflection coefficient G_{11} and transmission coefficient G_{21} to the complex dielectric constant ε_2 of the grain, which is desired parameter. The equations are not invertable to yield closed form solutions. Iterative processes can, however, yield precise values for the complex dielectric constant. The following Mathcad worksheet section calculates the complex dielectric constant from the complex reflection coefficient.

$c := 299792458$ Speed of light

$d_1 := 0.332$ Length of air-filled parallel plate line on either side of grain-filled section.

$d_2 := 0.1524$ Length of grain-filled section

$\varepsilon_0 := 1$

$\mu_0 := 1$ Relative permittivity and permeability of air.

$t := 0..\,140$ Frequency index

$f_t := (2 \cdot t + 1) \cdot 10^6$ Set up list of test frequencies.

$\omega_t := f_t \cdot 2 \cdot \pi$

$T1sq_t := e^{-j \cdot 2 \cdot \omega_t \frac{d_1}{c}}$ Calculate the transmission factor squared for each frequency for the air-filled sections. This can be done outside the solve block since it doesn't involve ε_2.

$\varepsilon c := 6 - 2j$

Establish initial guess values for real and imaginary parts of the complex dielectric constant.

This is the solve block (set up as a function) to compute dielectric constant from measured reflection coefficient at a single frequency.

Given

$$G11_t = T1sq_t \cdot \frac{1 - \sqrt{\varepsilon c}}{1 + \sqrt{\varepsilon c}} \cdot \frac{\left[1 - e^{-j \cdot 2 \cdot \omega_t \cdot \frac{d_2}{c} \cdot (\varepsilon c)^{\frac{1}{2}}} \right]}{1 - \left(\frac{1 - \sqrt{\varepsilon c}}{1 + \sqrt{\varepsilon c}} \right)^2 \cdot e^{-j \cdot 2 \cdot \omega_t \cdot \frac{d_2}{c} \cdot (\varepsilon c)^{\frac{1}{2}}}}$$

$DCCalc(G11, t, \omega) := (Find(\varepsilon c) - 1) \cdot 1.3 + 1$

This statement makes the solve block a function that can be called to act on a range variable (frequency and/or sample). Note the multiplicative factor of 1.3 that is needed (for mode correction?) to obtain correct dielectric constant values.

$\varepsilon hat_t := DCCalc(G11, t, \omega)^{\blacksquare}$

Call the conversion function to process reflection coefficients at all frequencies. The results are complex dielectric constants for each of the measurement frequencies.

Substituting the expression for G21 in the solve block above would yield complex dielectric contant values from complex transmission coefficient measurements.

APPENDIX C

CONVERTING HP-4291A REFLECTION COEFFICIENTS TO

DIELECTRIC CONSTANTS—ALCOHOL CALIBRATION

CONVERTING HP-4291A REFLECTION COEFFICIENTS TO DIELECTRIC CONSTANTS--ALCOHOL CALIBRATION

David B. Funk March 26, 2001

This model is based on the signal flow graphs and calculations provided to me by Dr.Kurt Lawrence, ARS, Athens, GA.

Kurt's signal flow graph model is as follows:

$$G_{11} = T_1{}^2 \cdot \Gamma_2 + \frac{T_1 \cdot \left(1 + \Gamma_2\right)\left(-T_2{}^2 \cdot \Gamma_2\right) \cdot T_1 \cdot \left(1 - \Gamma_2\right)}{1 - \left(-\Gamma_2\right) \cdot \left(-T_2{}^2 \cdot \Gamma_2\right)}$$

where:

$$T_i = e^{-1j \cdot \omega \sqrt{\mu \cdot \varepsilon_i} \frac{d_i}{c}} \qquad \Gamma_2 = \frac{\sqrt{\frac{\mu}{\varepsilon_2}} - 1}{\sqrt{\frac{\mu}{\varepsilon_2}} + 1}$$

G_{11} is the complex reflection coefficient measured by the HP4291A.

ω is the radian frequency of measurement.

d_1 is the length of the air-spaced transmission line (assumed 50 Ω) from the measurement plane to the grain-filled section.

d_2 is the length of the grain-filled section.

ε_2 is the complex relative dielectric constant of the grain.

T_1 is the complex (loss-free) transmission factor associated with each of the two air-spaced transmission line sections.

T_2 is the complex transmission factor associated with the grain-filled section.

Γ_2 is the complex reflection coefficient at the air-grain interface.

Since: $\quad \varepsilon_1 := 1 \qquad \mu_1 := 1 \qquad \mu_2 := 1$

T_1, T_2, and Γ_2 can be simplified to:

$$T_1 = e^{-j \cdot \omega \frac{d_1}{c}} \qquad T_2 = e^{-j \cdot \omega \sqrt{\varepsilon_2} \frac{d_2}{c}} \qquad \Gamma_2 = \frac{1 - \sqrt{\varepsilon_2}}{1 + \sqrt{\varepsilon_2}}$$

And G_{11} can be written:

$$G_{11} = e^{-2j \cdot \omega \frac{d_1}{c}} \cdot \frac{1 - \sqrt{\varepsilon_2}}{1 + \sqrt{\varepsilon_2}} \cdot \frac{1 - e^{-2j \cdot \omega \sqrt{\varepsilon_2} \frac{d_2}{c}}}{1 - \left(\frac{1 - \sqrt{\varepsilon_2}}{1 + \sqrt{\varepsilon_2}}\right)^2 \cdot e^{-2j \cdot \omega \sqrt{\varepsilon_2} \frac{d_2}{c}}}$$

126

$\text{DI}_0 := \text{READPRN}(\text{"xair01.txt"})$

$\text{DI}_1 := \text{READPRN}(\text{"xmeth01.txt"})$

$\text{DI}_3 := \text{READPRN}(\text{"xprop01.txt"})$

$\text{DI}_4 := \text{READPRN}(\text{"xbuta01.txt"})$

$\text{DI}_5 := \text{READPRN}(\text{"xpent01.txt"})$

$\text{DI}_6 := \text{READPRN}(\text{"xhexa01.txt"})$

$\text{DI}_{10} := \text{READPRN}(\text{"xdeca01.txt"})$

Input data for each test run. These data were supplied by Dr. Kurt Lawrence.

$D := \text{DI}_{cc}$

Specify which set to use for calculation and plotting. cc specifies the "Carbon Count" of the alcohols. Zero is for air.

$i := 0.. 125$

$\varepsilon d_i := D_{i,9} - j \cdot D_{i,10}$

Pick off Debye values from input data file.

$\Gamma m_i := D_{i,1} + j \cdot D_{i,2}$

Reassemble complex reflection coefficents from the Vector Network Analyzer data supplied by Kurt Lawrence.

$c := 299792458$

$d_1 := 0.345^{\blacksquare}$

Length of air-filled parallel plate line on either side of grain-filled section.

$d_2 := 0.1524^{\blacksquare}$

Length of grain-filled section

$\varepsilon_0 := 1$

$\mu_0 := 1$

$f_i := (2 \cdot i + 1) \cdot 10^6$

Set up list of test frequencies.

$\omega_i := f_i \cdot 2 \cdot \pi$

$T1sq_i := e^{-j \cdot 2 \cdot \omega_i \cdot \frac{d_1}{c}}$

Calculate the transmission factor squared for each frequency for the air-filled sections. This can be done outside the solve block since it doesn't involve ε_2.

$\Gamma 2(\varepsilon) := \dfrac{1 - \sqrt{\varepsilon}}{1 + \sqrt{\varepsilon}}$

Formula for reflection coefficient at air-grain interface.

$$T2sq(\varepsilon, i) := e^{-j\cdot2\cdot\omega_i\cdot\frac{d_2}{c}\cdot(\varepsilon)^{\frac{1}{2}}}$$

Formula for transmission factor through the grain-filled section.

$$G11(\varepsilon, i) := T1sq_i\cdot\Gamma2(\varepsilon)\cdot\left(\frac{1 - T2sq(\varepsilon, i)}{1 - \Gamma2(\varepsilon)^2\cdot T2sq(\varepsilon, i)}\right)$$

Function for calculating input reflection coefficient from grain dielectric constant and frequency.

$$G11Hat_i := G11(\varepsilon d_i, i)$$

Calculate reflection coefficients from the Debye dielectric constant and loss factor values.

$$\varepsilon c := 5 - j$$

Establish guess values for real and imaginary parts of the dielectric constant.

This is the solve block (set up as a function) to compute dielectric constant from reflection coefficient and frequency.

Given

$$\Gamma m_t = T1sq_t\cdot\frac{1 - \sqrt{\varepsilon c}}{1 + \sqrt{\varepsilon c}}\cdot\frac{\left[1 - e^{-j\cdot2\cdot\omega_t\cdot\frac{d_2}{c}\cdot(\varepsilon c)^{\frac{1}{2}}}\right]}{1 - \left(\frac{1 - \sqrt{\varepsilon c}}{1 + \sqrt{\varepsilon c}}\right)^2\cdot e^{-j\cdot2\cdot\omega_t\cdot\frac{d_2}{c}\cdot(\varepsilon c)^{\frac{1}{2}}}}$$

$$DCCalc(\Gamma m, t, \omega) := Find(\varepsilon c)$$

This statement makes the solve block a function that can be called to act on a range variable.

$$\varepsilon hat_i := (DCCalc(\Gamma m, i, \omega))$$

Call the conversion function to process reflection coefficients at all frequencies.

Raw values

Apply ε multiplier to correct for non-TEM mode and/or fringing fields.

$$dc_i := Re(\varepsilon hat_i)$$

$$dc2_i := (dc_i - 1)\cdot\varepsilon m + 1$$

$$lf_i := -Im(\varepsilon hat_i)$$

$$lf2_i := lf_i\cdot\varepsilon m$$

$$dcerr_i := \frac{dc2_i - Re(\varepsilon d_i)}{Re(\varepsilon d_i)}\cdot100$$

Calculate the percentage discrepancy between the measured dielectric values (converted from complex reflection coefficients) and those predicted from the published Debye coefficients for those alcohols.

$$lferr_i := \frac{lf2_i + Im(\varepsilon d_i)}{-Im(\varepsilon d_i)}\cdot100$$

$cc \equiv 10$ Carbon Count

n-decanol

$d_1 \equiv 0.332$ Length of air-filled section

$d_2 \equiv 0.1524$ Length of grain-filled section

$\epsilon m \equiv 1.30$ Mode correction factor

Comparison of Calc. and Debye DC & LF

Frequency (MHz)

——— Calc. DC w/ em
– – – Calc. LF w/ em
–·–·– Debye DC
······ Debye LF

Meas. Discrepancy (% of Debye Value)

Frequency (Hz)

——— Dielectric Constant
······ Dielectric Loss

129

$cc \equiv 6$ Carbon Count $d_1 \equiv 0.332$ Length of air-filled section

n-hexanol $d_2 \equiv 0.1524$ Length of grain-filled section

$\varepsilon m \equiv 1.30$ Mode correction factor

Comparison of Calc. and Debye DC & LF

Dielectric Constant and Loss Factor

Frequency (MHz)

——— Calc. DC w/ em
– – – Calc. LF w/ em
–·–· Debye DC
······ Debye LF

Meas. Discrepancy (% of Debye Value)

Error in dielectric const. and loss (%)

Frequency (Hz)

——— Dielectric Constant
······ Dielectric Loss

130

$cc \equiv 5$ Carbon Count $d_1 \equiv 0.332$ Length of air-filled section
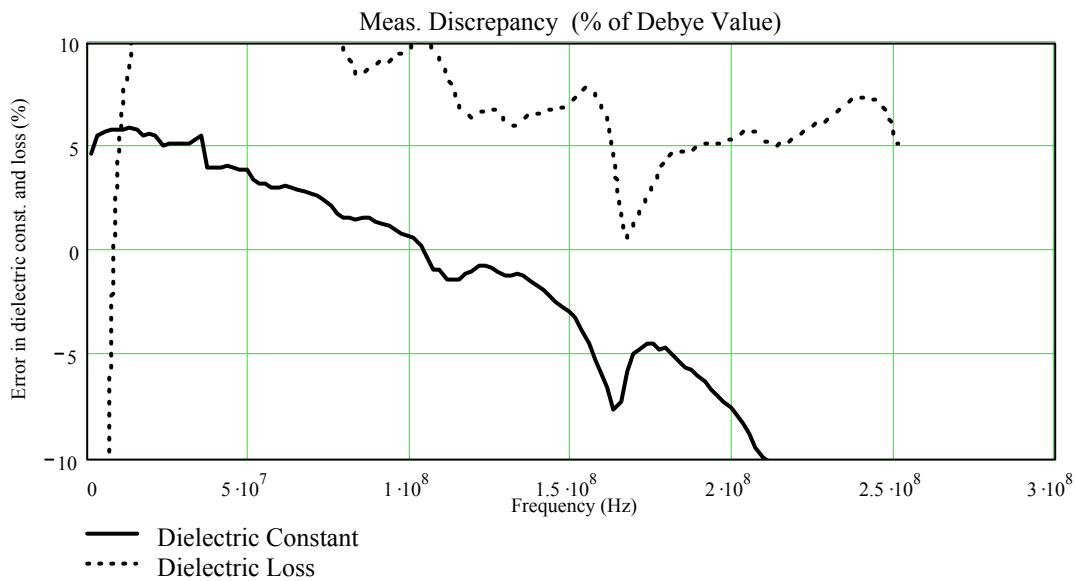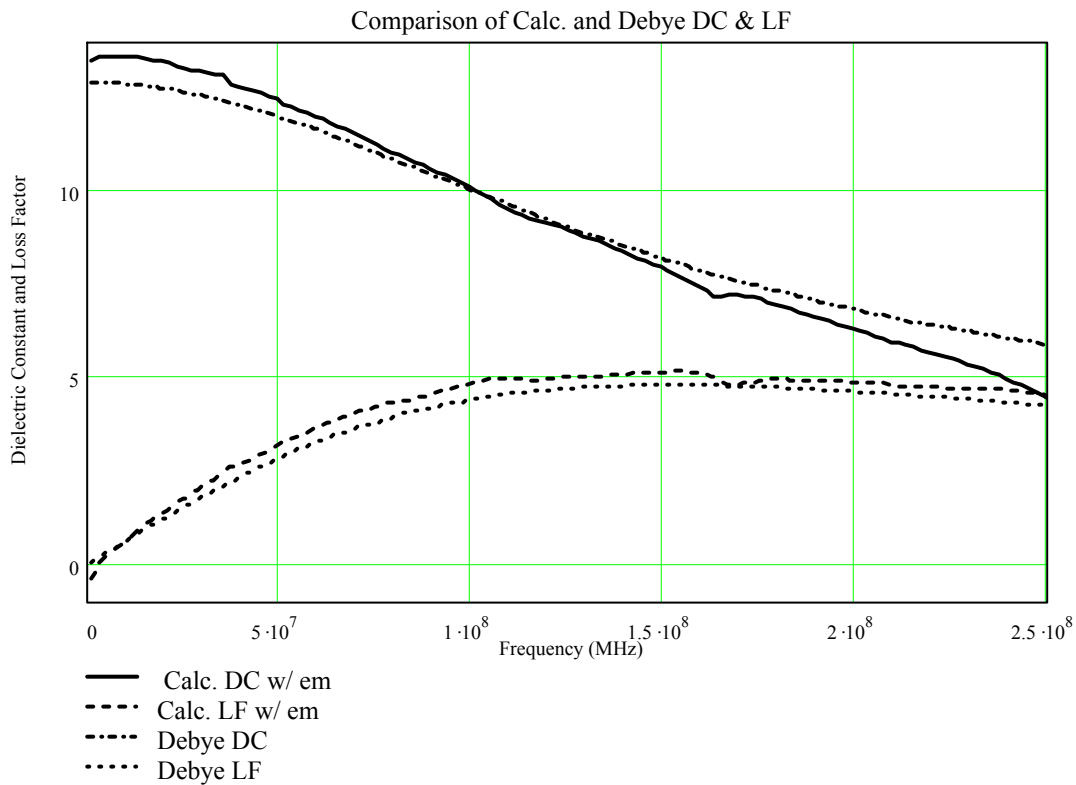
                                        $d_2 \equiv 0.1524$ Length of grain-filled section

n-pentanol $\varepsilon m \equiv 1.30$ Mode correction factor

Comparison of Calc. and Debye DC & LF

Dielectric Constant and Loss Factor

Frequency (MHz)

—— Calc. DC w/ em
- - - Calc. LF w/ em
-·-·- Debye DC
······ Debye LF

Meas. Discrepancy (% of Debye Value)

Error in dielectric const. and loss (%)

Frequency (Hz)

—— Dielectric Constant
······ Dielectric Loss

131

$cc \equiv 4$ Carbon Count

n-butanol

$d_1 \equiv 0.332$ Length of air-filled section

$d_2 \equiv 0.1524$ Length of grain-filled section

$\varepsilon m \equiv 1.30$ Mode correction factor

Comparison of Calc. and Debye DC & LF

Dielectric Constant and Loss Factor

Frequency (MHz)

——— Calc. DC w/ em
– – – Calc. LF w/ em
–·–·– Debye DC
······ Debye LF

Meas. Discrepancy (% of Debye Value)

Error in dielectric const. and loss (%)

Frequency (Hz)

——— Dielectric Constant
······ Dielectric Loss

132

$cc \equiv 3$ Carbon Count

propanol

$d_1 \equiv 0.332$ Length of air-filled section

$d_2 \equiv 0.1524$ Length of grain-filled section

$\varepsilon m \equiv 1.30$ Mode correction factor

Comparison of Calc. and Debye DC & LF

Dielectric Constant and Loss Factor

Frequency (MHz)

——— Calc. DC w/ em
- - - Calc. LF w/ em
-·-·- Debye DC
······ Debye LF

Meas. Discrepancy (% of Debye Value)

Error in dielectric const. and loss (%)

Frequency (Hz)

——— Dielectric Constant
······ Dielectric Loss

$cc \equiv 1$ Carbon Count $d_1 \equiv 0.332$ Length of air-filled section

methanol

$d_2 \equiv 0.1524$ Length of grain-filled section

$\varepsilon m \equiv 1.30$ Mode correction factor

Comparison of Calc. and Debye DC & LF

Frequency (MHz)

——— Calc. DC w/ em
– – – Calc. LF w/ em
–·–· Debye DC
····· Debye LF

Meas. Discrepancy (% of Debye Value)

Frequency (Hz)
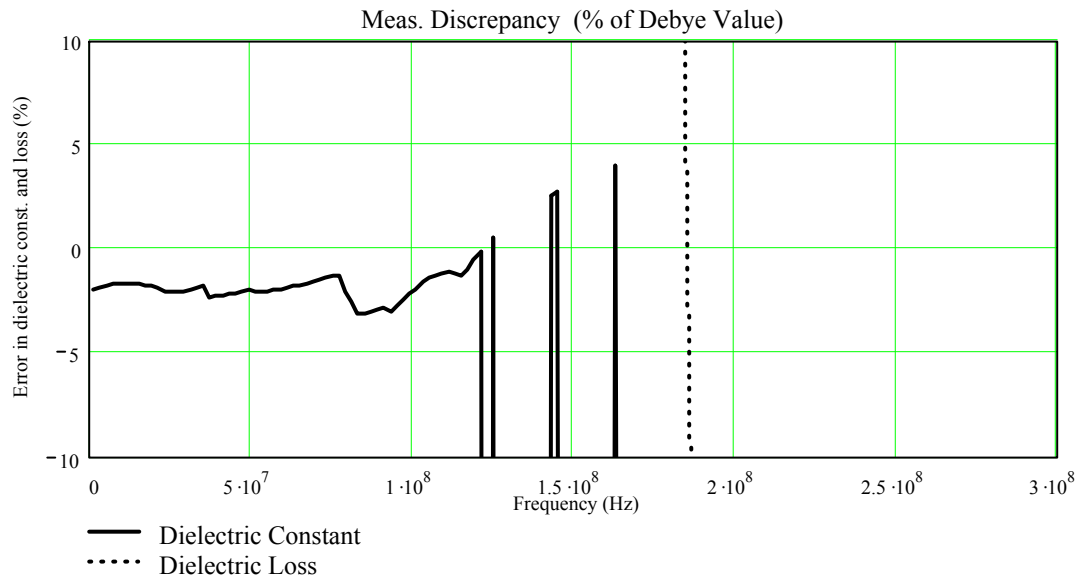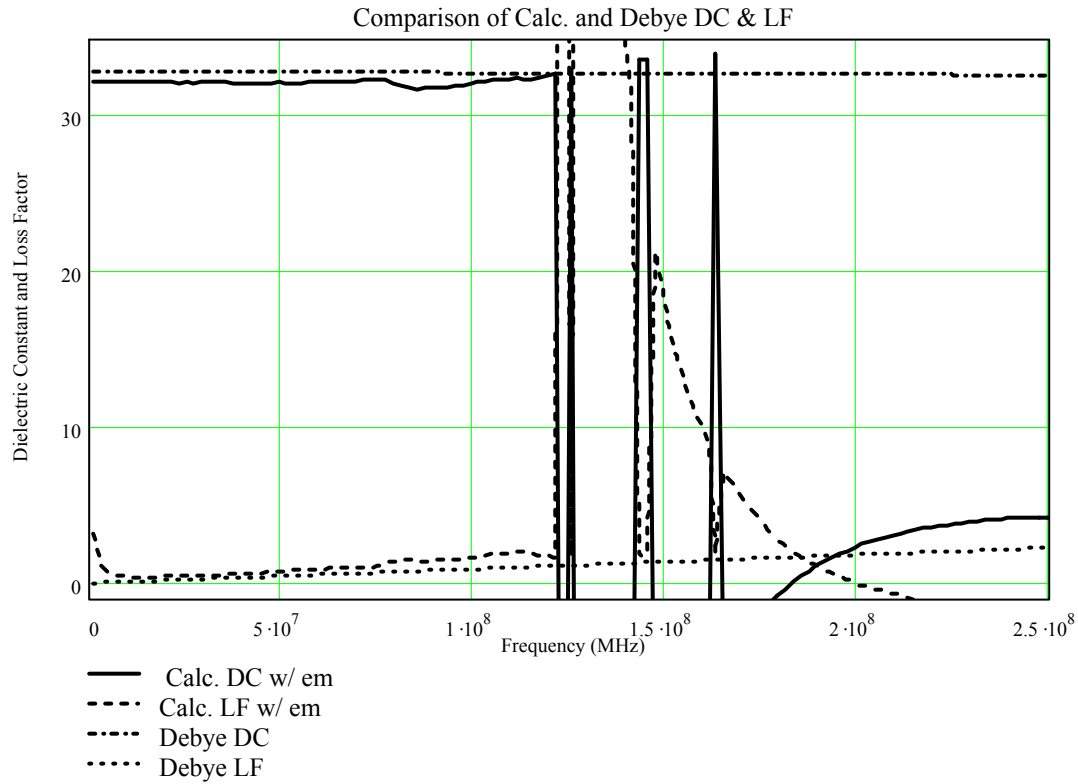
——— Dielectric Constant
····· Dielectric Loss

air (with gate installed)
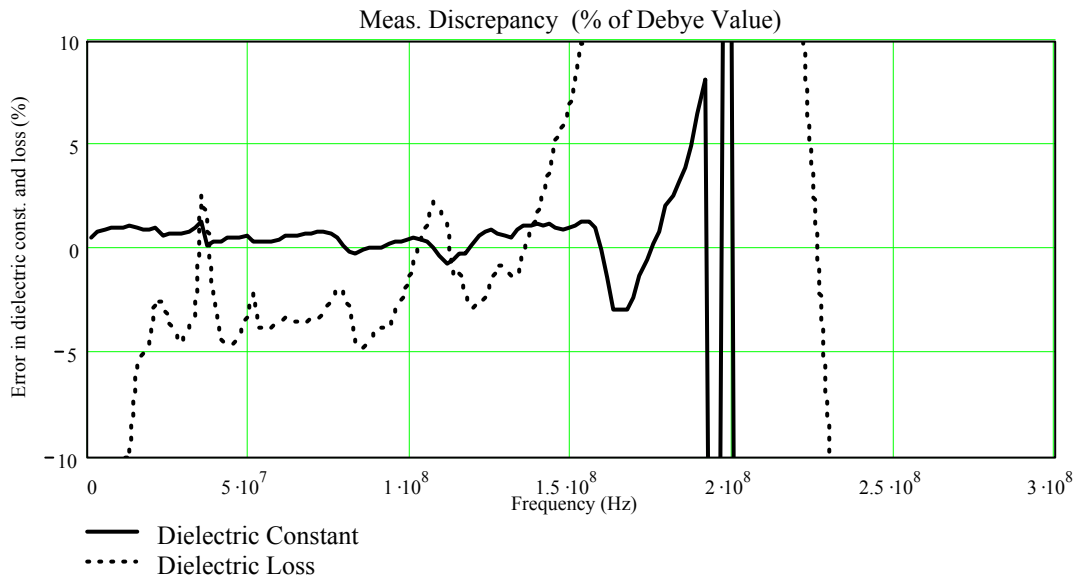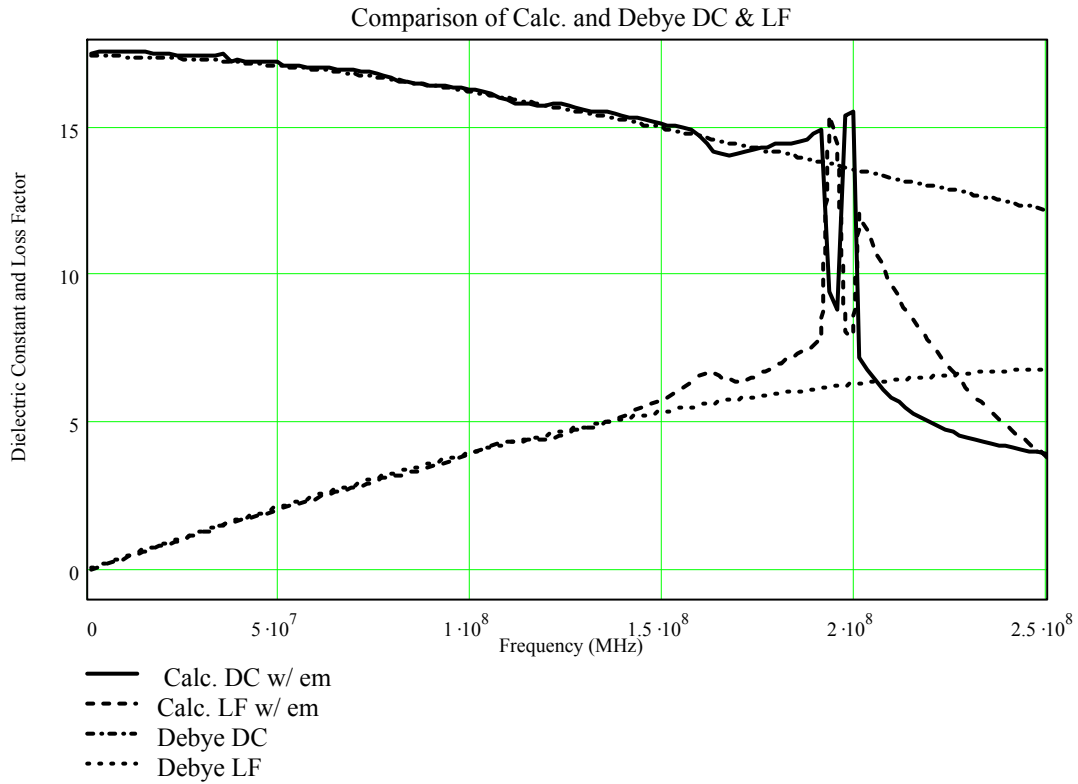
$d_1 \equiv 0.332$ Length of air-filled section

$d_2 \equiv 0.1524$ Length of grain-filled section

$\varepsilon m \equiv 1.30$ Mode correction factor

Comparison of Calc. and Debye DC & LF

Frequency (MHz)

Dielectric Constant and Loss Factor

——— Calc. DC w/ em

– – – Calc. LF w/ em

–·–·– Debye DC

····· Debye LF

Meas. Discrepancy (% of Debye Value)

Error in dielectric const. (%)

Frequency (Hz)

——— Dielectric Constant
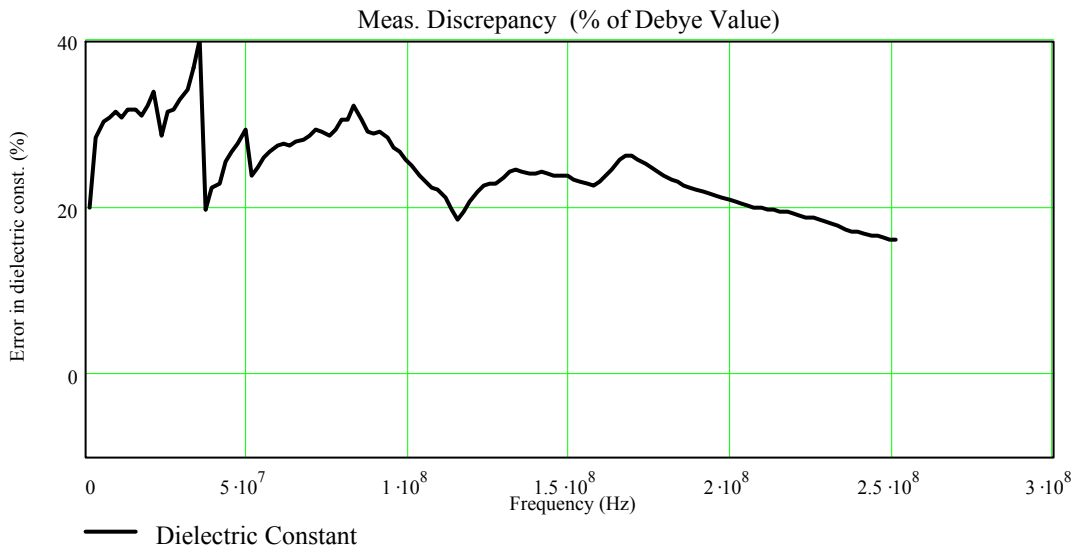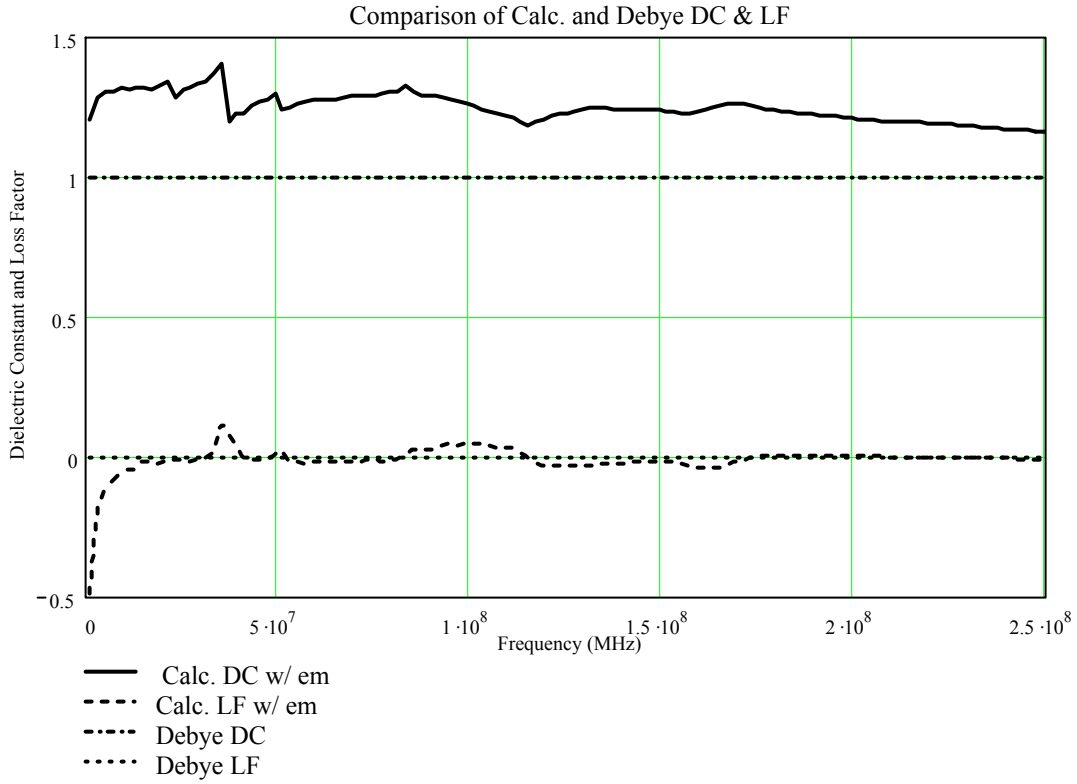
APPENDIX D

SIMULATING DIELECTRIC CHARACTERISTICS OF GRAIN

SIMULATING DIELECTRIC CHARACTERISTICS OF GRAIN

David B. Funk March 28, 2001

This worksheet permits simulation of the moisture, frequency, density, and temperature dependence of grain samples. It includes simplified simulations of electrode polarization and Maxwell-Wagner effects such as may be caused by percolating protonic conductivity.

This simulation assumes that a grain sample in a test cell can be modeled as the parallel combination of stacks of kernels between the two electrodes. Each kernel is modeled as a parallel-plate capacitor of area AK, thickness t, with a dielectric characterized by two relaxation frequencies (determined by $(Cs1*Rs1)^{-1}$ and $(Cs2*Rs2)^{-1}$ and parallel resistance Rc. Between each pair of kernels, there is a gap of thickness D with capacitance Cg and resistance Rg. At the end of each stack of kernels, there is an effective gap of thickness DE with kernel to electrode capacitance Ce and a kernel to electrode resistance Re.
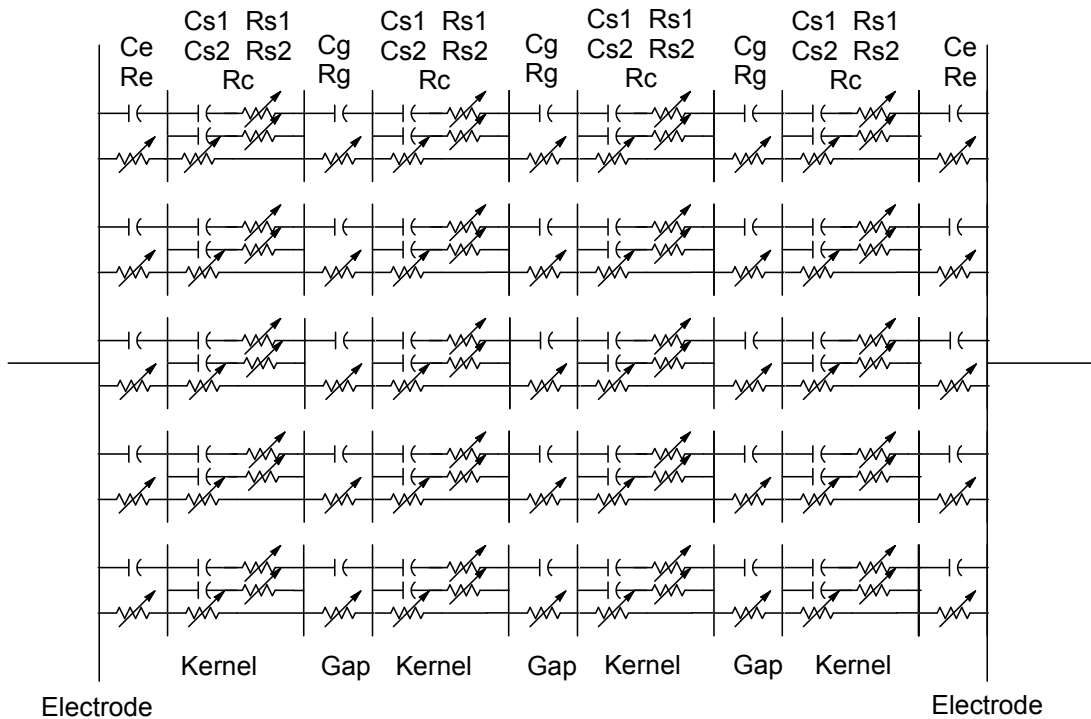
This section defines several key functions that are used later in the simulation program.

Temperature dependence of static dielectric constant of water. T in Kelvin.
From J. B. Hasted, *Aqueous Dielectrics*, pg. 37.

$$\varepsilon\text{Static}(T) := 87.740 - 0.40008(T - 273) + 9.398 \cdot 10^{-4} \cdot (T - 273)^2 - 1.410 \cdot 10^{-6} \cdot (T - 273)^3$$

Estimate εms, the dielectric constant of moist solid material by applying the cube-root density correction equation.

$$\varepsilon\text{ms}(\rho_s, M, \varepsilon_w, \varepsilon_s) := \left[\varepsilon_w^{\frac{1}{3}} \cdot \left[\frac{M \cdot \rho_s}{M \cdot (\rho_s - 1) + 1} \right] + \varepsilon_s^{\frac{1}{3}} \cdot \left[\frac{1 - M}{M \cdot (\rho_s - 1) + 1} \right] \right]^3$$

Where: ρs is density of dry material
M is moisture fraction (wet basis)
εw is dielectric constant of water
εs is dielectric constant of the dry solid material

Function to estimate relaxation frequency from binding energy
(molar activation enthalpy, kJ/mol) and temperature.

$$f_r(\Delta H, T) := f_{r0} \cdot e^{\frac{(\Delta H_0 - \Delta H) \cdot 10^3}{R \cdot T}}$$

Where:

$\Delta H_0 \equiv 20.5$ $\qquad$ $f_{r0} \equiv 17 \cdot 10^9$ $\qquad$ Enthalpy (kJ/mol) and relaxation frequency (Hz) for bulk water

$R \equiv 8.314$ $\qquad$ Gas constant

Debye equations to estimate dielectric constant of water a any frequency f as a function of static and "infinite" dielectric constants, εs and εi, and an assumed relaxation frequency fr.

$$\varepsilon\text{rr}(\varepsilon s, \varepsilon i, fr, f) := \varepsilon i + \frac{(\varepsilon s - \varepsilon i)}{1 + \left(\frac{f}{fr}\right)^2}$$
$\qquad$ Calculate relaxation of real part of complex dielectric constant.

$$\varepsilon\text{ri}(\varepsilon s, \varepsilon i, fr, f) := \frac{(\varepsilon s - \varepsilon i) \cdot \frac{f}{fr}}{1 + \left(\frac{f}{fr}\right)^2}$$
$\qquad$ Calculate imaginary part of complex dielectric constant.

The following program estimates the effective complex dielectric constant of two phases of water in grain--monolayer water and "other" water. The probability of a monolayer site being filled is based on the difference $_\Delta$H between the monolayer and upper layer binding energies.

If the total moisture content M is less than or equal to the monolayer limit MM, the monolayer moisture is the probability of filling those sites times the total moisture. The upper level moisture is the difference between the monolayer moisture and the total moisture content.

If the total moisture content M is greater than the monolayer limit MM, the monolayer moisture is the probability times the monolayer limit. The upper layer moisture is the rest of the moisture.

In either case, the composite dielectric constant is the weighted sum of the two dielectric constants.

$$\epsilon\epsilon(M, MM, T, \Delta H, \epsilon m, \epsilon u) := \begin{vmatrix} P \leftarrow 1 - e^{\dfrac{-\Delta H \cdot 10^3}{R \cdot T}} \\[6pt] \epsilon a \leftarrow P \cdot \epsilon m + (1 - P) \cdot \epsilon u \quad \text{if } M \leq MM \\[6pt] \text{otherwise} \\ \quad \begin{vmatrix} mm \leftarrow P \cdot MM \\[4pt] mu \leftarrow (1 - P) \cdot MM + (M - MM) \\[4pt] \epsilon a \leftarrow \dfrac{mm}{M} \cdot \epsilon m + \dfrac{mu}{M} \cdot \epsilon u \end{vmatrix} \\[6pt] \epsilon a \end{vmatrix}$$

$MM \equiv .10$ Specify monolayer moisture limit. The percolation threshold is specified as a fraction of the monolayer moisture limit.

$\Delta H \equiv 3$ Specify the difference in binding energy (kJ/mol) between the monolayer and upper moisture layers.

The following function (from equation 15 in text) is used to estimate the conductivity σhat of a particle due to percolating protonic conductivity.

$$\sigma hat(tt, h_c, h, E, T) := \frac{CC}{T} \cdot e^{\frac{-E}{R \cdot T}} \cdot (h - h_c)^{tt}$$

Where: $tt \equiv 1.3$ Critical exponent (assuming 2D percolation)

$h_c \equiv .45 \cdot MM$ Critical level of hydration where percolation commences

h is the dry-basis hydration weight fraction.

$CC \equiv 130$ Arbitrary constant to achieve agreement with grain measurements.

$E \equiv 2 \cdot 10^4$ Molar activation enthalpy (kJ/mol) of the proton jump. According to Colomban, this is between 0.1 eV (~10 kJ/mol) to 0.2 eV (~20 kJ/mol).

$$C1(\varepsilon_r, AK, t) := \frac{\varepsilon_0 \cdot \varepsilon_r \cdot AK}{t}$$ Function for calculating capacitance across a single kernel

$$C2(AK, D) := \frac{\varepsilon_0 \cdot AK}{D}$$ Function for calculating the capacitance across a single gap

$$G1(\sigma, AK, t) := \frac{\sigma \cdot AK}{t}$$ The dc conductance between the faces of a single kernel

$$G_g(R_g) := \frac{1}{R_g}$$ The conductance across a single gap

Set up indices and constants for the simulations

$i := 0.. 100$ — Set up frequency index for the worksheet.

$$f_i := 10^{\left(2+\frac{i}{10}\right)}$$

$$\omega_i := 2\cdot\pi\cdot f_i$$

$ii := 0.. 10$ — Set up temperature index for the worksheet.

$$T_{ii} := (250 + 10\cdot ii)$$

$j := 0.. 40$ — Set up moisture index for the worksheet.

$$h_j := \frac{j}{80}$$ — Moisture weight fraction (dry basis)

$$M_j := \frac{h_j}{1 + h_j}$$ — Moisture weight fraction (wet basis)

$\varepsilon i := 4.2$ — Assumed value of the "infinite" dielectric constant of pure water, from Hasted, pg. 47.

$\varepsilon ws_{ii} := \varepsilon Static(T_{ii})$ — Calculate the static dielectric constant of pure water for each test temperature.

$MLF \equiv .5$ — Specify the proportional relationship between the dielectric constants of loosely bound and monolayer water.

$\rho_s \equiv 1.3$ — Specify dry kernel density

$\varepsilon_{solid} \equiv 2.5$ — Specify dielectric constant of dry solid kernel

$HB \equiv 28$ — Activation enthalpy (kJ/mol) for "bound" water (used for calculating bound water relaxation frequency)

$FRB_{ii} := f_r(HB, T_{ii})$ — "Simulated bound water" relaxation frequencies at each test temperature

$\varepsilon wr_{i, ii} := \varepsilon rr(\varepsilon ws_{ii}, \varepsilon i, FRB_{ii}, f_i)$ — Calculate the dielectric constant of semi-bound water over specified ranges of temperature and frequency.

$\varepsilon wi_{i, ii} := \varepsilon ri(\varepsilon ws_{ii}, \varepsilon i, FRB_{ii}, f_i)$

$\varepsilon w_{i, ii} := \varepsilon wr_{i, ii} - j\cdot \varepsilon wi_{i, ii}$ — Combine the real and imaginary parts.

$NK \equiv 12$ Number of kernels per stack

$\varepsilon_0 \equiv 8.85 \cdot 10^{-12}$ Permittivity of free space

$AK \equiv 5 \cdot 10^{-5}$ Kernel area

$t \equiv .002$ Kernel thickness

$D \equiv .0001$ Inter-kernel gap thickness

$R_g \equiv 1 \cdot 10^{8}$ Inter-kernel gap resistance

$R_e \equiv 1 \cdot 10^{12}$ Electrode gap resistance

$DE \equiv 3 \cdot 10^{-4}$ Electrode gap thickness

$width := .070$ Test cell dimensions: width, height (approx.), and spacing in meters.

$ht := .08$

Estimated height is 8.7 cm, but 8.0 cm gives closer approximation to observed capacitance.

$Area_{meas} := width \cdot ht \cdot 2$

$Area_{meas} = 0.0112$

$d := (NK + 1) \cdot D + NK \cdot t$ Calculate electrode spacing given specified kernel parameters

$d = 0.0253$ Calculated electrode spacing (stack height)

$CEC := \dfrac{\varepsilon_0 \cdot Area_{meas}}{d}$ $CEC = 3.918 \times 10^{-12}$ Calculated empty cell capacitance

$J := rows(M) - 1$ $J = 40$ Number of different hydration levels

$I := rows(f) - 1$ $I = 100$ Number of different test frequencies

$II := rows(T) - 1$ $II = 10$ Number of differnet temperatures

Calculate the effective complex dielectric constant of the water in the simulated sample for each test condition of temperature, frequency, and hydration level.

$$EW_j := \begin{array}{|l} \text{for } i \in 0..I \\ \quad \text{for } ii \in 0..II \\ \quad\quad Out_{i,ii} \leftarrow \varepsilon e\left(M_j, MM, T_{ii}, \Delta H, \varepsilon w_{i,ii} \cdot MLF, \varepsilon w_{i,ii}\right) \\ Out \end{array}$$

Calculate dielectric constants for moist solid (exclusive of conductivity effects) for each temperature, frequency, and moisture level.

$$EMS_j := \begin{array}{|l} \text{for } i \in 0..I \\ \quad \text{for } ii \in 0..II \\ \qquad Out_{i,ii} \leftarrow \varepsilon ms\left[\rho_s, M_j, (EW_j)_{i,ii}, \varepsilon_{solid}\right] \\ Out \end{array}$$

$$\sigma 1 := \begin{array}{|l} \text{for } ii \in 0..II \\ \quad \text{for } j \in 0..J \\ \qquad \begin{array}{|l} \sigma_{ii,j} \leftarrow \sigma hat\left(tt, h_c, h_j, 2\cdot10^4, T_{ii}\right) \\ \sigma_{ii,j} \leftarrow 0 \text{ if } h_j < h_c \end{array} \\ \sigma \end{array}$$

Calculate percolating conductivity assuming jump activation energy of 0.2 eV (~20 kJ/mol) for all combinations of temperature and hydration level.

$$GK_{ii,j} := G1\left(\sigma 1_{ii,j}, AK, t\right)$$

Calculate conductance across a single kernel

Calculate total impedance across a single kernel--including capacitance, relaxation loss, and conductivity loss.

$$ZK_j := \begin{array}{|l} \text{for } i \in 0..I \\ \quad \text{for } ii \in 0..II \\ \qquad \begin{array}{|l} B_{i,ii} \leftarrow C1\left[Re\left[(EMS_j)_{i,ii}\right], AK, t\right]\cdot j\cdot\omega_i \\ Gs_{i,ii} \leftarrow G1\left[\left[-Im\left[(EMS_j)_{i,ii}\right]\cdot\omega_i\cdot\varepsilon_0\right], AK, t\right] \\ Y_{i,ii} \leftarrow GK_{ii,j} + Gs_{i,ii} + B_{i,ii} \\ Z_{i,ii} \leftarrow (Y_{i,ii})^{-1} \end{array} \\ Z \end{array}$$

$CG := C2(AK, D)$ $CG = 4.425\times 10^{-12}$ Calculate capacitance of inter-kernel gap

$CE := C2(AK, DE)$ $CE = 1.475\times 10^{-12}$ Calculate capacitance of the electrode gap

$GG := (R_g)^{-1}$ $GG = 1\times 10^{-8}$ Calculate gap conductance

$GE := \dfrac{1}{R_e}$ $GE = 1\times 10^{-12}$ Calculate electrode conductance

$YG_i := GG + j \cdot 2 \cdot \pi \cdot f_i \cdot CG$ 　　　Admittance across one gap

$ZG_i := \dfrac{1}{YG_i}$ 　　　Impedance across one gap

$ZE_i := \left(GE + j \cdot 2 \cdot \pi \, f_i \cdot CE \right)^{-1}$ 　　　Impedance across one electrode gap.

Calulate effective capacitance for the entire test cell--with multiplier for 175 parallel stacks of kernels.

$$CEFF_j := \left| \begin{array}{l} \text{for } i \in 0..\,I \\ \quad \text{for } ii \in 0..\,II \\ \qquad C_{i,\,ii} \leftarrow \dfrac{\text{Im}\left[\left[(NK-1) \cdot ZG_i + NK \cdot \left(ZK_j\right)_{i,\,ii} + 2 \cdot ZE_i \right]^{-1} \right]}{2 \cdot \pi \cdot f_i} \\ C \leftarrow C \cdot 175 \\ C \end{array} \right.$$

　　　Calculate the effective conductance (loss) for the entire test cell.

$$GEFF_j := \left| \begin{array}{l} \text{for } i \in 0..\,I \\ \quad \text{for } ii \in 0..\,II \\ \qquad G_{i,\,ii} \leftarrow \text{Re}\left[\left[(NK-1) \cdot ZG_i + NK \cdot \left(ZK_j\right)_{i,\,ii} + 2 \cdot ZE_i \right]^{-1} \right] \\ G \leftarrow G \cdot 175 \\ G \end{array} \right.$$

$\varepsilon'_j := \dfrac{\overrightarrow{CEFF_j}}{CEC}$ 　　　Calculate a nested matrix of dielectric constant values at each temperature ii and frequency i for each hydration level j.

$$\varepsilon''_j := \left| \begin{array}{l} \text{for } i \in 0..\,I \\ \quad \text{for } ii \in 0..\,II \\ \qquad Out_{i,\,ii} \leftarrow \dfrac{\left(GEFF_j\right)_{i,\,ii}}{CEC\,\omega_i} \\ Out \end{array} \right.$$ 　　　Similarly calculate dielectric loss values.

At this point in the program, the all the simulation results (for the specified kernel parameters) exist in matrices and can be plotted as desired to show relationships between moisture, temperature, and frequency. Figures 28, 29, 31, and 32 in the text are examples.

144

APPENDIX E

UNIFIED MOISTURE ALGORITHM

Unified Moisture Algorithm

David B. Funk March 20, 2001

This worksheet shows the mathematics required to generate a single calibration equation for 15 grain types with the Unified Moisture Algorithm.

$i := 0.. 125$

$f_i := (1 + 2 \cdot i) \cdot 10^6$

Establish the frequency index for the data. Complex dielectric constant data were computed from complex reflection coefficients at intervals of 2 MHz from 1 MHz to 251 MHz.

$\epsilon 0 \equiv 1.26$ Specify the equivalent empty cell dielectric constant for the dielectric test cell. This was larger than 1.000 (air) because of the sample "gate" and supports below the test cell.

$$CubicDC(\epsilon, Wt, \rho bar) := \left[\left[(\epsilon)^{\frac{1}{3}} - \epsilon 0^{\frac{1}{3}} \right] \cdot \frac{\rho bar}{Wt} + \epsilon 0^{\frac{1}{3}} \right]^3$$

Define the cube-root density correction function. (Landau & Lifschitz, Looyenga equation)

$DPath := \text{"d:\hp4291a\combdata\"}$

Establish path for data files

Build vectors of data file names for each grain types so that all data can be read and combined in one matrix.

$$FListSoy := \begin{pmatrix} \text{"sye98aa.prn"} \\ \text{"sye99aa.prn"} \\ \text{"syes00aa.prn"} \end{pmatrix}$$

Soybean data files for 1998, 1999, and 2000

$$FListRice := \begin{pmatrix} \text{"LGE98AA.prn"} \\ \text{"LGE99AA.prn"} \\ \text{"LGes00a.prn"} \\ \text{"MGe98aa.prn"} \\ \text{"MGe99a.prn"} \\ \text{"MGes00a.prn"} \end{pmatrix}$$

Long Grain Rough and Medium Grain Rough rice data files for 1998, 1999, and 2000.

$$
\text{FListWht} := \begin{pmatrix}
\text{"hwe98a.prn"} \\
\text{"hwe99a.prn"} \\
\text{"hwes00a.prn"} \\
\text{"hse98a.prn"} \\
\text{"hse99a.prn"} \\
\text{"hses00a.prn"} \\
\text{"sre98a.prn"} \\
\text{"sre99a.prn"} \\
\text{"sres00a.prn"} \\
\text{"due98a.prn"} \\
\text{"due99a.prn"} \\
\text{"dues00a.prn"} \\
\text{"swe98a.prn"} \\
\text{"swe99a.prn"} \\
\text{"swes00a.prn"} \\
\text{"hde98a.prn"} \\
\text{"hde99a.prn"} \\
\text{"hdes00a.prn"}
\end{pmatrix}
$$

Data files for 1998, 1999, and 2000 for Hard Red Winter, Hard Red Spring, Soft Red Winter, Durum, Soft White, and Hard White wheat classes.

$$
\text{FListBarley} := \begin{pmatrix}
\text{"TBE98A.prn"} \\
\text{"TBE99A.prn"} \\
\text{"tbes00a.prn"} \\
\text{"sbe98aa.prn"} \\
\text{"sbe99a.prn"} \\
\text{"sbes00a.prn"}
\end{pmatrix}
$$

Data files for 1998, 1999, and 2000 for Two-rowed and Six-rowed barley.

$$
\text{FListCorn} := \begin{pmatrix}
\text{"cne98a.prn"} \\
\text{"cne99a.prn"} \\
\text{"cnes00a.prn"}
\end{pmatrix}
$$

Data files for 1998, 1999, and 2000 for yellow-dent corn.

$$
\text{FListOats} := \begin{pmatrix}
\text{"oae98a.prn"} \\
\text{"oae99a.prn"} \\
\text{"oaes00a.prn"}
\end{pmatrix}
$$

Data files for 1998, 1999, and 2000 for oats.

$$
\text{FListSFS} := \begin{pmatrix}
\text{"sfe98a.prn"} \\
\text{"sfe99a.prn"} \\
\text{"sfes00a.prn"}
\end{pmatrix}
$$

Data files for 1998, 1999, and 2000 for oil-type sunflower seeds

147

$$\text{FListSorg} := \begin{pmatrix} \text{"sge98a.prn"} \\ \text{"sge99aa.prn"} \\ \text{"sges00a.prn"} \end{pmatrix}$$ Data files for 1998, 1999, and 2000 for sorghum.

Stack the file names for all grains to form a master list of data file names.

$$\text{FList} := \text{stack}(\text{FListSoy}, \text{FListSorg}, \text{FListSFS}, \text{FListCorn}, \text{FListOats}, \text{FListWht}, \text{FListBarley}, \text{FListRice})$$

$$J := \text{rows}(\text{FList}) - 1$$ Create index for data file names

$$j := 0..J$$

$$\text{File}_j := \text{concat}(\text{DPath}, \text{FList}_j)$$ Attach the path to each file name.

$$\text{Data}_j := \text{READPRN}(\text{File}_j)$$ Read data from all data files into a nested array

$$\text{DA}_j := \text{csort}(\text{Data}_j, 2)$$ Sort the data from each file according to increasing air oven moisture values

$$\text{DA}_7 := \text{submatrix}(\text{DA}_7, 0, \text{rows}(\text{DA}_7) - 3, 0, \text{cols}(\text{DA}_7) - 1)$$ Delete two extremely high moisture sunflower samples.

$$\text{NR}_j := \text{rows}(\text{DA}_j)$$ Count the number of rows (observations) in each of the data files

$$jj := 1..J$$

$$\text{fr}_0 := 0$$

$$\text{fr}_{jj} := \sum_{r=0}^{jj-1} \text{NR}_r$$ Calculate the first and last rows in the combined data matrix that delimit the observations in each of the original data fles.

$$\text{lr}_j := \sum_{r=0}^{j} (\text{NR}_r) - 1$$

$$\rho t := \begin{pmatrix} 557.6 \\ 625.65 \\ 440.95 \\ 607.95 \\ 627.3 \\ 644.45 \\ 662.85 \\ 631.3 \end{pmatrix} \begin{matrix} \text{Soy} \\ \text{Sorg} \\ \text{SFS} \\ \text{Corn} \\ \text{Oats} \\ \text{Wheat} \\ \text{Barley} \\ \text{Rice} \end{matrix}$$

Target cell weights for each grain group. The cell weights were adjusted to give linear regression coefficients of 6.000 percent moisture per unit of density-corrected dielectric constant for all eight grain groups at 149 MHz.

$d0 := fr_0 .. lr_2$ Soy

Establish indices for each type of grain.

$d1 := fr_3 .. lr_5$ Sorg

$d2 := fr_6 .. lr_8$ SFS

$d3 := fr_9 .. lr_{11}$ Corn

$d4 := fr_{12} .. lr_{14}$ Oats

$d5 := fr_{15} .. lr_{32}$ Wheat

$d6 := fr_{33} .. lr_{38}$ Barley

$d7 := fr_{39} .. lr_{44}$ Rice

$dd := fr_{24} .. lr_{26}$ Durum

Durum wheat is separately indexed because an air oven correction is required.

$$\text{Din} := \begin{vmatrix} D \leftarrow DA_0 \\ \text{for } kk \in 1 .. J \\ \quad D \leftarrow \text{stack}(D, DA_{kk}) \\ D \end{vmatrix}$$

Assemble the data for all grain samples into one large matrix.

Calculate average cell weight for each grain group for comparison to target values.

	Calculated mean sample weight	Target sample weight	
$\rho ts := \begin{pmatrix} \text{mean(submatrix(Din, fr}_0, \text{lr}_2, 3, 3)) \\ \text{mean(submatrix(Din, fr}_3, \text{lr}_5, 3, 3)) \\ \text{mean(submatrix(Din, fr}_6, \text{lr}_8, 3, 3)) \\ \text{mean(submatrix(Din, fr}_9, \text{lr}_{11}, 3, 3)) \\ \text{mean(submatrix(Din, fr}_{12}, \text{lr}_{14}, 3, 3)) \\ \text{mean(submatrix(Din, fr}_{15}, \text{lr}_{32}, 3, 3)) \\ \text{mean(submatrix(Din, fr}_{33}, \text{lr}_{38}, 3, 3)) \\ \text{mean(submatrix(Din, fr}_{39}, \text{lr}_{44}, 3, 3)) \end{pmatrix}$	$\rho ts = \begin{pmatrix} 613.037 \\ 665.979 \\ 328.153 \\ 609.603 \\ 424.879 \\ 667.081 \\ 541.632 \\ 515.927 \end{pmatrix}$	$\rho t = \begin{pmatrix} 557.6 \\ 625.65 \\ 440.95 \\ 607.95 \\ 627.3 \\ 644.45 \\ 662.85 \\ 631.3 \end{pmatrix}$	Soy Sorg SFS Corn Oats Wheat Barley Rice

$lr_2 - fr_0 = 370$ Soy   Calculate the number of observations in each grain group.

$lr_5 - fr_3 = 91$ Sorg

$lr_8 - fr_6 = 282$ SFS

$lr_{11} - fr_9 = 474$ Corn

$lr_{14} - fr_{12} = 56$ Oats

$lr_{32} - fr_{15} = 638$ Wheat

$lr_{38} - fr_{33} = 163$ Barley

$lr_{44} - fr_{38} = 288$ Rice

$rows(Din) = 2.331 \times 10^3$ Calculate the total number of observation (grain samples)

$n := 0 .. rows(Din) - 1$

$AOM := Din^{\langle 2 \rangle}$ Put the air oven moisture values in a separate vector.

$\varepsilon hat_{n,i} := Din_{n,6+2 \cdot i} - j \cdot Din_{n,7+2 \cdot i}$ Assemble complex dielectric constant values at the ith frequency for the nth observation from data files.

$\varepsilon c_{d0,i} := CubicDC(\varepsilon hat_{d0,i}, Din_{d0,3}, \rho t_0)$ Apply the cube-root density correction function to density-correct all complex dielectric constant data to the selected target weights for each grain.

$\varepsilon c_{d1,i} := CubicDC(\varepsilon hat_{d1,i}, Din_{d1,3}, \rho t_1)$

$\varepsilon c_{d2,i} := CubicDC(\varepsilon hat_{d2,i}, Din_{d2,3}, \rho t_2)$

$\varepsilon c_{d3,i} := CubicDC(\varepsilon hat_{d3,i}, Din_{d3,3}, \rho t_3)$

$\varepsilon c_{d4,i} := CubicDC(\varepsilon hat_{d4,i}, Din_{d4,3}, \rho t_4)$

$\varepsilon c_{d5,i} := CubicDC(\varepsilon hat_{d5,i}, Din_{d5,3}, \rho t_5)$

$\varepsilon c_{d6,i} := CubicDC(\varepsilon hat_{d6,i}, Din_{d6,3}, \rho t_6)$

$\varepsilon c_{d7,i} := CubicDC(\varepsilon hat_{d7,i}, Din_{d7,3}, \rho t_7)$

Dielectric bias adjustments to get vertical alignment
among grain groups. These came from linear regression
of each grain group separately.

$$IM := \begin{pmatrix} 0.28 \\ -0.099 \\ 0.229 \\ -0.212 \\ 0.041 \\ -0.095 \\ -0.093 \\ -0.052 \end{pmatrix} \begin{matrix} \text{Soy} \\ \text{Sorg} \\ \text{SFS} \\ \text{Corn} \\ \text{Oats} \\ \text{Wheat} \\ \text{Barley} \\ \text{Rice} \end{matrix}$$

$\varepsilon"dc_{n,i} := -Im(\varepsilon c_{n,i})\,\blacksquare$

Pick off the density-corrected dielectric loss values. This
equation is disabled because the dielectric loss is not
needed in the moisture measurement algorithm.

$$RB \equiv \begin{pmatrix} .25 & 1.5 \\ 0 & 0 \\ .5 & 3.0 \\ 0 & 0 \\ 0 & 0 \\ 0 & 0 \\ 0 & 0 \\ 0 & 0 \end{pmatrix} \begin{matrix} \text{Soy} \\ \text{Sorg} \\ \text{SFS} \\ \text{Corn} \\ \text{Oats} \\ \text{Wheat} \\ \text{Barley} \\ \text{Rice} \end{matrix}$$

Factors added to εrdc
(column 0) and AOM
(column 1) for soybeans
and sunflowers to "slide"
them along the curve to get
the bound-water "hooks" to
line up for all grains. The
added AOM factor needs to
be removed in the prediction
routine to get true predicted
moisture content.

Apply bias adjustments to dielectric constant values to align different grain groups.

$\varepsilon rdc_{d0,i} := Re(\varepsilon c_{d0,i} + RB_{0,0}) + IM_0$ $\varepsilon rdc_{d4,i} := Re(\varepsilon c_{d4,i} + RB_{4,0}) + IM_4$

$\varepsilon rdc_{d1,i} := Re(\varepsilon c_{d1,i} + RB_{1,0}) + IM_1$ $\varepsilon rdc_{d5,i} := Re(\varepsilon c_{d5,i} + RB_{5,0}) + IM_5$

$\varepsilon rdc_{d2,i} := Re(\varepsilon c_{d2,i} + RB_{2,0}) + IM_2$ $\varepsilon rdc_{d6,i} := Re(\varepsilon c_{d6,i} + RB_{6,0}) + IM_6$

$\varepsilon rdc_{d3,i} := Re(\varepsilon c_{d3,i} + RB_{3,0}) + IM_3$ $\varepsilon rdc_{d7,i} := Re(\varepsilon c_{d7,i} + RB_{7,0}) + IM_7$

$$KTC := \begin{pmatrix} .062 \\ .060 \\ .031 \\ .060 \\ .060 \\ .062 \\ .060 \\ .043 \end{pmatrix} \begin{matrix} \text{Soy} \\ \text{Sorg} \\ \text{SFS} \\ \text{Corn} \\ \text{Oats} \\ \text{Wheat} \\ \text{Barley} \\ \text{Rice} \end{matrix}$$

Vector of temperature correction coefficients (%moisture /degree F) for each grain type

$AO_{d0} := AOM_{d0} + RB_{0,1} + KTC_0 \cdot \left(Din_{d0,4} - 77 \right)$

Apply temperature corrections (in reverse) and bound-water "slide" to air oven values before doing the regression. The fifth column of Din is the sample temperature in degrees Fahrenheit.

$AO_{d1} := AOM_{d1} + RB_{1,1} + KTC_1 \cdot \left(Din_{d1,4} - 77 \right)$

$AO_{d2} := AOM_{d2} + RB_{2,1} + KTC_2 \cdot \left(Din_{d2,4} - 77 \right)$

$AO_{d3} := AOM_{d3} + RB_{3,1} + KTC_3 \cdot \left(Din_{d3,4} - 77 \right)$

$AO_{d4} := AOM_{d4} + RB_{4,1} + KTC_4 \cdot \left(Din_{d4,4} - 77 \right)$

$AO_{d5} := AOM_{d5} + RB_{5,1} + KTC_5 \cdot \left(Din_{d5,4} - 77 \right)$

$AO_{d6} := AOM_{d6} + RB_{6,1} + KTC_6 \cdot \left(Din_{d6,4} - 77 \right)$

$AO_{d7} := AOM_{d7} + RB_{7,1} + KTC_7 \cdot \left(Din_{d7,4} - 77 \right)$

$AO_{dd} := AOM_{dd} + 0.4\%$

Add air oven correction for durum wheat samples.

$order \equiv 4$

Specify the order of the polynomial regression to follow.

$r := 0 \,.. \, order$

$KCC^{\langle i \rangle} := regress\left(\varepsilon crdc^{\langle i \rangle}, AO, order \right)$

Generate calibration coefficients using polynomial regression of the specified order at each measurement frequency.

$KCC := submatrix(KCC, 3, rows(KCC) - 1, 0, 125)$

$$KC74 := KCC^{\langle 74 \rangle}$$

$$KC74 = \begin{pmatrix} -69.63956 \\ 57.3285 \\ -15.76267 \\ 2.07381 \\ -0.09858 \end{pmatrix}$$

The 4th order polynomial regression coefficients for all grains at 149 MHz.

$$MCHat_{n,i} := KCC_{0,i} + \sum_{r=1}^{order} KCC_{r,i} \cdot \left(\varepsilon crdc_{n,i} \right)^r$$

Calculate predicted moisture values for each sample at each measurement frequency.

$$MD_{n,i} := MCHat_{n,i} - AO_n$$

Calculate moisture residuals (predicted minus actual) for each sample at each frequency.
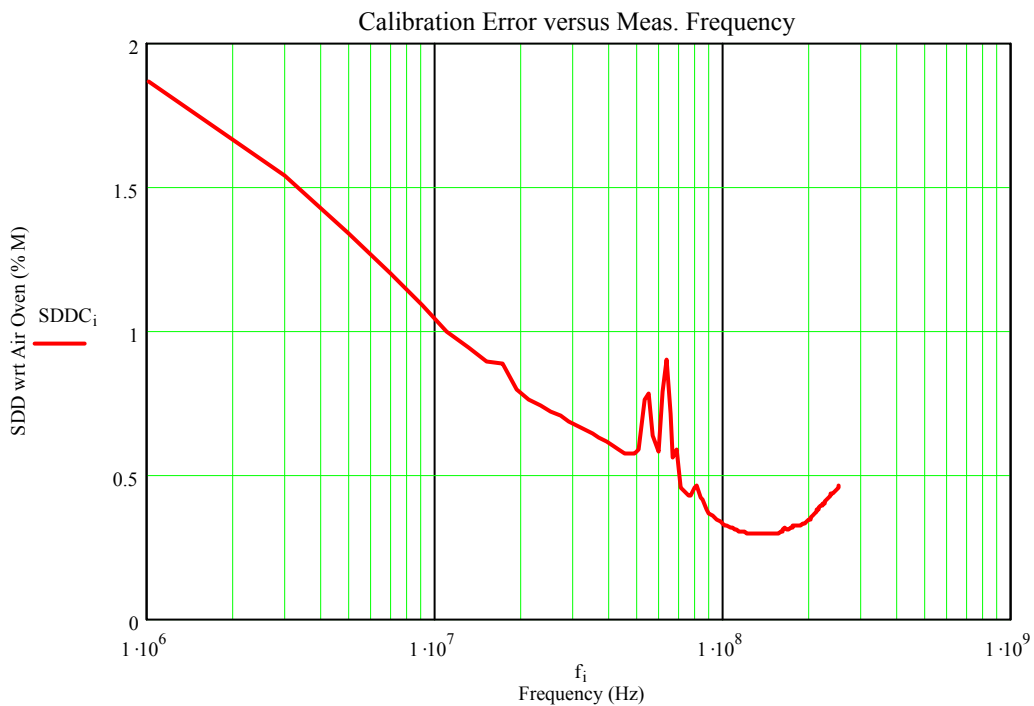
$$SDDC_i := stdev\left(MD^{\langle i \rangle} \right)$$

$$\min(SDDC) = 0.294$$

Calculate Std of error for each measurement frequency.

Find minimum standard deviation of differences across frequencies

$$polynomial\ order = 4$$

Note the broad minimum between 100 and 200 MHz in error plot below.

Calibration Error versus Meas. Frequency

REFERENCE LIST

[1]Jean Louis Multon, "Basics of Moisture Measurement in Grain," in *Uniformity by 2000--Highlights of an International Workshop on Maize and Soybean Quality*, edited by Lowell D. Hill (Scherer Communications, Champaign, Ill., 1990), pp. 69-91.

[2]ICC, "ICC - Standard Nr. 109/1 Determination of the Moisture Content of Cereals and Cereal Products (Basic Reference Method)," edited by J. L. Multon (International Association for Cereal Chemistry, Vienna, Austria, 1976).

[3]ISO, "International Standard ISO 760--Determination of Water -- Karl Fischer Method (General Method)," (International Standards Organization, Geneva, Switzerland, 1978).

[4]L.J. Briggs, "An Electrical Resistance Method for the Rapid Determination of the Moisture Content of Grain," U.S. Department of Agriculture, Bureau of Plant Industry Circular Report No. 20, 1908.

[5]W. Haward Hunt and S.W. Pixton, "Moisture--Its Significance, Behavior, and Measurement," in *Storage of Cereal Grains and Their Products*, edited by C.M. Christenson (American Association of Cereal Chemists, Minneapolis, Minn., 1972), pp. 1-55.

[6]Andrzej W. Kraszewski, Samir Trabelsi, and Stuart O. Nelson, "Comparison of Density-independent Expressions for Moisture Content Determination in Wheat at Microwave Frequencies," J. Agric. Engng Res. **71**, 227-237 (1998).

[7]Samir Trabelsi and Stuart O. Nelson, "Density-Independent Functions for On-Line Microwave Moisture Meters: A General Discussion," Meas. Sci. Technol. **9**, 570-578 (1998).

[8]Andrzej W. Kraszewski and Stuart O. Nelson, "Wheat Moisture Content and Bulk Density Determination by Microwave Parameters Measurement," Canadian Agricultural Engineering **34** (4), 327-335 (1992).

[9]Samir Trabelsi, Andrzej W. Kraszewski, and Stuart O. Nelson, "Nondestructive Microwave Characterization for Determining the Bulk Density and Moisture Content of Shelled Corn," Meas. Sci. Technol. **9**, 1548-1556 (1998).

[10]Samir Trabelsi, Andrzej Kraszewski, and Stuart O. Nelson, "A Unified Calibration Method for Moisture Sensing in Particulate Materials," presented at the Third Workshop on Electromagnetic Wave Interaction with Water and Moist Substances, Athens, Georgia, 1999.

[11]J. B. Hasted, "Dielectric Properties of Absorbed Water," in *Aqueous Dielectrics* (Chapman and Hall, London, 1973), pp. 234-255.

[12]Andrzej W. Kraszewski, "Microwave Aquametry: Introduction to the Workshop," in *Microwave Aquametry--Electromagnetic Wave Interaction with Water-Containing Materials*, edited by Andrzej W. Kraszewski (IEEE Press, New York, 1996), pp. 3-34.

[13]Frederick W. Stein, United States Patent No. 2,251,641 (5 August 1941).

[14]Claudia Waterloo, "How Farmers Lost Millions," in *Des Moines Sunday Register* (Des Moines, Iowa, 1980), pp. 8A.

[15] David B. Funk, David M. Beams, and Dennis E. Grim, U.S. Patent No. 4,584,655 (22 April 1986).

[16] Roger F. Harrington, "Fundamental Concepts," in *Time-Harmonic Electromagnetic Fields* (McGraw-Hill, New York, 1961), pp. 1-35.

[17] Samir Trabelsi, Andrzej W. Krazsewski, and Stuart O. Nelson, "New Density-Independent Calibration Function for Microwave Sensing of Moisture Content in Particulate Materials," IEEE Transactions for Instrumentation and Measurement **47** (3), 613-662 (1998).

[18] J. B. Hasted, "The Water Molecule and Dielectric Theory," in *Aqueous Dielectrics* (Chapman and Hall, London, 1973), pp. 302.

[19] Peter Debye, *Polar Molecules* (Chemical Catalog Company, New York, 1929).

[20] Arthur von Hippel, "Representation of Dielectrics by Lumped Circuit Equivalents," in *Dielectrics and Waves* (Artech House, Boston, 1995), Vol. 1, pp. 86-91.

[21] Vera V. Daniel, "Relaxation in Electrical Circuits," in *Dielectric Relaxation* (Academic Press Inc., New York, 1967), pp. 1-12.

[22] Shafiur Rahman, "Water Activity and Sorption Properties of Foods," in *Food Properties Handbook* (CRC Press, Inc., Boca Raton, Florida, 1995), pp. 1-82.

[23] S. Brunauer, P. H. Emmett, and E. Teller, "The Adsorption of Gases in Multimolecular Layers," J. Am. Chem. Soc. **60**, 309-319 (1938).

[24] Max A. Hilhorst, "Dielectric Characterisation of Soil," Doctoral Thesis, Wageningen Agricultural University, 1998.

[25] S. Glasstone, K.J. Laidler, and H. Eyring, *The Theory of Rate Processes* (McGraw-Hill, New York, 1941).

[26] Udo Kaatze, "Microwave Dielectric Properties of Water," in *Microwave Aquametry--Electromagnetic Wave Interaction with Water-Containing Materials*, edited by Andrzej W. Kraszewski (IEEE Press, New York, 1996), pp. 37-53.

[27] W. R. Tinga and Stuart O. Nelson, "Dielectric Properties of Materials for Microwave Processing--Tabulated," Journal of Microwave Power **8** (1), 23-65 (1973).

[28] Udo Kaatze and V. Uhlendorf, "The Dielectric Properties of Water at Microwave Frequencies," Zeitschrift fur Phys. Chem. Neue Folge **126**, 151-165 (1981).

[29] J. B. Hasted, "The Dielectric Properties of Ice," in *Aqueous Dielectrics* (Chapman and Hall, London, 1973), pp. 100-116.

[30] Stuart O. Nelson and Laverne E. Stetson, "Frequency and Moisture Dependence of the Dielectric Properties of Hard Red Winter Wheat," J. Agric. Engng. Res. **21**, 181-192 (1976).

[31] J. B. Hasted, "The Dielectric Properties of Heterogeneous Substances," in *Aqueous Dielectrics* (Chapman and Hall, London, 1973), pp. 117-135.

[32] Arthur von Hippel, "Interfacial and Space-Charge Polarization," in *Dielectrics and Waves* (Artech House, Boston, 1995), Vol. 1, pp. 228-234.

[33] Stuart O. Nelson, "Density Dependence of the Dielectric Properties of Particulate Materials," ASAE Paper No. 823554, St. Joseph, Michigan, 1982

[34]Stuart O. Nelson and T-S You, "Relationships Between Microwave Permittivities of Solid and Pulverized Plastics," J. Phys. D: Appl. Phys. **23**, 346-353 (1990).

[35]Stuart O. Nelson, "Correlating Dielectric Properties of Solids and Particulate Samples Through Mixture Relationships," Trans. Am. Soc. Agr. Eng. **35** (2), 625-629 (1992).

[36]Stuart O. Nelson, "Measurement and Computation of Powdered Mixture Permittivities," in *Proceedings of the 17th IEEE Instrumentation and Measurement Technology Conference*, **1** 8-11, (2000).

[37]Stuart O. Nelson, L. H. Soderholm, and F. D. Yung, "Determining the Dielectric Properties of Grain," Agr. Eng. (September), 608-610 (1953).

[38]J.L. Jorgensen, A. R. Edison, Stuart O. Nelson, and Laverne E. Stetson, "A Bridge Method for Dielectric Measurements of Grain and Seed in the 50- to 250- MHz Range," Trans. Am. Soc. Agr. Eng. **13** (1), 18-20, 24 (1970).

[39]Stuart O. Nelson, "Improved Sample Holder for Q-Meter Dielectric Measurements," Trans. Am. Soc. Agr. Eng. **22** (4), 950-954 (1979).

[40]Kurt C. Lawrence and Stuart O. Nelson, "Sensing Moisture Content of Cereal Grains with Radio-Frequency Measurements -- A Review," presented at the Third International Symposium on Humidity & Moisture, London, England, 1998.

[41]Kurt C. Lawrence, Stuart O. Nelson, and Philip G. Bartley, "Flow-Through Coaxial Sample Holder Design for Dielectric Properties Measurements from 1 to 350 MHz," IEEE Transactions on Instrumentation and Measurements **47** (2), 354-361 (1998).

[42] Kurt C. Lawrence, David B. Funk, and William R. Windham, "Parallel-Plate Moisture Sensor for Yellow-Dent Field Corn," Trans. Am. Soc. Agr. Eng. **42** (5), 1353-1357, (1999).

[43] Kurt C. Lawrence, David B. Funk, and William R. Windham, "Swept-Frequency Grain Moisture Sensor," presented at the Third Workshop on Electromagnetic Wave Interaction with Water and Moist Substances, Athens, Georgia, 1999.

[44] Samir Trabelsi and Andrzej W. Kraszewski, "Universal Microwave Moisture Sensor for Granular Materials," ASAE Paper No. 003061, St. Joseph, Michigan, 2000

[45] Andrzej Kraszewski, "Microwave Aquametry: Electromagnetic Wave Interaction with Water-Containing Materials," in *TAB-IEEE Press Book Series*, edited by Willis J. Tompkins (IEEE Press, New York, 1996), pp. 484.

[46] David M. Pozar, "Microwave Network Analysis," in *Microwave Engineering*, edited by Charity Robey (John Wiley & Sons, Inc., New York, 1998), pp. 182-250.

[47] W. Haward Hunt and M. H. Neustadt, "Factors Affecting the Precision of Moisture Measurement in Grain and Related Crops," Journal of the A.O.A.C **49** (4), 757-763 (1966).

[48] Stuart O. Nelson, "Use of Electrical Properties for Grain-Moisture Measurement," Journal of Microwave Power **12** (1), 67-72 (1977).

[49] David B. Funk, "Uniformity in Dielectric Grain Moisture Measurement," in *Uniformity by 2000--Highlights of an International Workshop on Maize and Soybean Quality*, edited by Lowell D. Hill (Scherer Communications, Champaign, Ill., 1990), pp. 69-91.

[50]David B. Funk, "The State of Grain Moisture Measurement in the United States,"
presented at the Third International Symposium on Humidity & Moisture, London,
England, 1998.

[51]David B. Funk, "Dielectric Grain Moisture Measurement--Practical, Technical, and
Regulatory Issues," presented at the Third Workshop on Electromagnetic Wave
Interaction with Water and Moist Substances, Athens, Georgia, 1999.

[52]Stuart O. Nelson, Andrzej W. Kraszewski, Kurt Lawrence, C., and Samir Trabelsi,
"Fifteen Years of Research on Moisture Content Determination in Cereal Grains,"
presented at the Third Workshop on Electromagnetic Wave Interaction with Water and
Moist Substances, Athens, Georgia, 1999.

[53]Stuart O. Nelson, Andrzej W. Kraszewski, Samir Trabelsi, and Kurt C. Lawrence,
"Using Cereal Grain Permittivity for Sensing Moisture Content," IEEE Transactions on
Instrumentation and Measurement **49** (3), 470-475 (2000).

[54]Kenneth M. Greenwood and Edward W. Mazerall, USA Patent No. 2,693,575 (2
November 1954).

[55]Dominique Le Gigan, USA Patent No. 5,253,512 (19 October 1993).

[56]Ronald F. Vogel, USA Patent No. 3,778,707 (11 December 1973).

[57]George H. Fathauer, USA Patent No. 3,761,810 (25 September 1973).

[58]David B. Funk and William E. Midden, U. S. Patent No. 4,121,151 (17 October 1978).

[59]David B. Funk, U.S. Patent No. 4193116 (11March 1980).

60J. Matthews, "The Design of an Electrical Capacitance-Type Moisture Meter for Agricultural Use," J. Agric. Engng. Res. **8** (1), 17-30 (1963).

61R. N. Jones, National Bureau of Standards NBSIR Report No. 78-897, 1978.

62Kurt C. Lawrence, William R. Windham, and Stuart O. Nelson, "Sensing Wheat Moisture Content Independent of Density," Trans. Am. Soc. Agr. Eng. **41** (3), 693-699 (1998).

63Kurt C. Lawrence, David B. Funk, and William R. Windham, "Dielectric Moisture Sensor for Cereal Grains and Soybeans," ASAE Paper No. 993176, St. Joseph, Michigan, 1999

64GIPSA-TSD, "FGIS-PN-00-4: Sample Collection Responsibilities for Verifying the Accuracy of Moisture Meter Calibrations. Crop Year 2000," (USDA-GIPSA, Washington, D.C., 2000).

65Bill Burden, "Working Instructions for Air Oven Methods," in *WI No: AO1-10* (USDA-GIPSA-TSD, Kansas City, Missouri, 1998).

66USDA-GIPSA, *Moisture Handbook* (USDA-GIPSA, Washington, D.C., 1999).

67National Institute of Standards and Technology, "Sec. 5.56a Grain Moisture Meters," in *NIST Handbook 44--Specifications, Tolerances, and Other Technical Requirements for Weighing and Measuring Devices*, edited by Tina Butcher, Terry Grimes, and Juana Williams (U.S. Government Printing Office, Washington, D.C., 2000), pp. 5.21-5.27.

68National Institute of Standards and Technology, "Section 2, Chapter 6, Checklist for Grain Moisture Meters," in *NCWM Publication 14--National Conference on Weights*

and Measures National Type Evaluation Program--Technical Policy Checklists, and Test Procedures, edited by Tina Butcher and Terry Grimes (U.S. Government Printing Office, Washington, D.C., 2000), pp. 6.1-6.50.

[69]Greg Amorese, "RF Impedance Measurement Basics," in *Back to Basics Seminar* (Hewlett-Packard Company, 1998), pp. 4.1-4.86.

[70]Kurt C. Lawrence (Personal Communication).

[71]MathSoft Inc., Mathcad 2000 Professional (MathSoft, Inc., Cambridge, Mass., 1999).

[72]David M. Pozar, "Transmission Lines and Waveguides," in *Microwave Engineering*, edited by Charity Robey (John Wiley & Sons, Inc., New York, 1998), pp. 104-181.

[73]Hewlett-Packard, *HP 4291A RF Impedance/Material Analyzer Operating Manual Set* (Hewlett-Packard, Japan, 1994).

[74]Hewlett-Packard, *HP 4285A Precision LCR Meter Operation Manual* (Hewlett-Packard, Japan, 1996).

[75]Hewlett-Packard, "Cable Correction," in *HP 4285A Precision LCR Meter Operation Manual* (Hewlett-Packard, Japan, 1996), pp. 6-15 to 6-20.

[76]Agilent Technologies, *Agilent 4294A Precision Impedance Analyzer Operation Manual* (Agilent Technologies, Japan, 1999).

[77]S. S. Stuchly, "Dielectric Properties of Some Granular Solids Containing Water," Journal of Microwave Power **5** (2), 62-68 (1970).

[78]Stuart O. Nelson, "Dielectric Properties of Grain and Seed in the 1 to 50-MC Range," Trans. Am. Soc. Agr. Eng. **8** (1), 38-48 (1965).

[79] Stuart O. Nelson, "250-Hz to 12-GHz Dielectric Properties of Grain and Seed," Trans. Am. Soc. Agr. Eng. **18** (4), 714, 715, 718 (1975).

[80] Stuart O. Nelson, "Audiofrequency Dielectric Properties of Grain and Seed," Trans. Am. Soc. Agr. Eng. **15** (1), 180-184, 188 (1972).

[81] Samir Trabelsi (Personal Communication).

[82] T. Gregory Dewey, "Percolation of Proton Transport in Hydrated Proteins," in *Fractals in Molecular Biophysics* (Oxford University Press, Oxford, 1997), pp. 232-235.

[83] G. Careri, M. Geraci, A. Giansanti, and John A. Rupley, "Protonic Conductivity of Hydrated Lysozyme Powders at Megahertz Frequencies," Proc. Natl. Acad. Sci, USA **82**, 5342-5346 (1985).

[84] G. Careri, A. Giansanti, and John A. Rupley, "Proton Percolation on Hydrated Lysozyme Powders," Proc. Natl. Acad. Sci, USA **83**, 6810-6814 (1986).

[85] John A. Rupley, Linda Siemankowski, Giorgio Careri, and Fabio Bruni, "Two-Dimensional Protonic Percolation on Lightly Hydrated Purple Membrane," Proc. Natl. Acad. Sci, USA **85**, 9022-9025 (1988).

[86] P. Pissis and A. Anagnostopoulou-Konsta, "Protonic Percolation on Hydrated Lysozyme Powders Studies by the Method of Thermally Stimulated Depolarization Currents," J. Phys. D: Appl. Phys. **23**, 932-939 (1990).

[87] Philippe Colomban, *Proton Conductors: Solids, Membrane, and Gels--Materials and Devices* (Cambridge University Press, Cambridge, 1992).

[88]J. O. Thomas, "Structural Studies of Proton Conductors," in *Proton Conductors: Solids, Membranes and Gels -- Materials and Devices*, edited by Philippe Colomban (Cambridge University Press, Cambridge, 1992), pp. 79-89.

[89]Stuart O. Nelson and Kurt C. Lawrence, "Evaluation of a Crushing-Roller Conductance Instrument for Single-Kernel Corn Moisture Measurement," Trans. Am. Soc. Agr. Eng. **32** (2), 737-743, (1989).